ASSESSMENT OF THE COEFFICIENT OF THERMAL EXPANSION OF

ALABAMA CONCRETE

Except where reference is made to the work of others, the work described in this thesis is my own or was done in collaboration with my advisory committee. This thesis does not include proprietary or classified information.

_____

Kwame Opare Sakyi-Bekoe

Certificate of Approval:

_____	_____
Robert W. Barnes James J. Mallett Associate Professor Civil Engineering	Anton K. Schindler, Chair Gottlieb Associate Professor Civil Engineering
_____	_____
Mary L. Hughes Instructor Civil Engineering	George T. Flowers Interim Dean Graduate School

ASSESSMENT OF THE COEFFICIENT OF THERMAL EXPANSION OF ALABAMA CONCRETE

Kwame Opare Sakyi-Bekoe

A Thesis

Submitted to

the Graduate Faculty of

Auburn University

in Partial Fulfillment of the

Requirements for the

Degree of

Master of Science

Auburn, Alabama
December 19, 2008

ASSESSMENT OF THE COEFFICIENT OF THERMAL EXPANSION OF

ALABAMA CONCRETE

Kwame Opare Sakyi-Bekoe

_____

Signature of Author

_____

Date of Graduation

VITA

Kwame Opare Sakyi-Bekoe, son of Dr. Kofi Sakyi-Bekoe and Madam Comfort Prempeh, was born on December 22, 1973, at Akwatia, Ghana. He is a 1992 graduate of Okuapemman Secondary School in Akropong-Akuapem, Ghana. He attended University of Science and Technology, Kumasi in Ghana where he earned a Bachelor of Science degree in Civil Engineering in February 1999. Upon completion of his undergraduate course work, he practiced as a Civil/Structural Engineer before entering graduate school at Auburn University with the intent of earning the degree of Master of Science in Civil Engineering.

THESIS ABSTRACT

ASSESSMENT OF THE COEFFICIENT OF THERMAL EXPANSION OF ALABAMA CONCRETE

Kwame Opare Sakyi-Bekoe

Master of Science, December 19, 2008
(B.Sc.Civil Engineering, University of Science and Technology 1998)

213 Typed Pages

Directed by Anton K. Schindler

The coefficient of thermal expansion (CTE) is a fundamental property of portland cement concrete. It represents the change in unit length of concrete per degree of temperature change. The CTE is a very important property in concrete pavement design and in the design of integral structures, especially bridge decks, as it can affect early-age cracking, the serviceability, and performance of these concrete structures.

The increasing recognition of the potential magnitudes of thermal movements and stresses induced in integral structures, especially bridge decks, and in pavements exposed to the daily ambient temperature, suggest the need for a realistic CTE rather than an assumed value for use in their design. The prime purpose of this research work was to

quantify the CTE for concretes made with commonly used coarse aggregate types in the Alabama concrete industry.

A total of fifty-four concrete samples were tested for their CTEs using the Association of the American State Highways and Transportation Officials (AASHTO) TP 60 (2004) test method at a concrete age of 28 days. The concrete was made of three different coarse aggregate types. The coarse aggregate types used were siliceous river gravel, granite, and dolomitic limestone. Three different sand-aggregate ratios of 0.40, 0.45, and 0.50 as well as water-cement ratios of 0.32, 0.38, and 0.44 were used. Thus for each coarse aggregate type, a total of nine concrete mixtures were made and a total of eighteen concrete samples were tested for their CTEs using concrete cylinders of size 4 in.(diameter) x 7 in.(height) (100 mm x 175 mm). The CTEs were calculated for each concrete sample in accordance with the procedure outlined in AASHTO TP 60 (2004).

The results showed that concretes made with siliceous river gravel have the highest CTEs with an average value of 6.95 x 10^{-6} /^{o}F (12.51 x 10^{-6} /^{o}C) while those made of granite have lower values, with an average of 5.60 x 10^{-6} /^{o}F (10.08 x 10^{-6} /^{o}C). The lowest CTEs were observed for concretes made with dolomitic limestone, which had an average value of 5.52 x 10^{-6} /^{o}F (9.93 x 10^{-6} /^{o}C).

It was determined for the materials tested that the sand-aggregate ratio and water-cement ratio did not have as much influence on the concrete CTE as does the coarse aggregate type. An increase in the volume of the coarse aggregate or a decrease in the sand-aggregate ratio increases the CTE for concretes made with river gravel and decreases the CTE for concretes made of granite.

ACKNOWLEDGEMENTS

I would like to thank my advisor Dr. Anton K. Schindler for his direction throughout my entire studies at Auburn University.

This project would not have been possible without the tireless efforts of the many faculty, not forgetting my committee members, graduate and undergraduate students working in the Structural Research Laboratory at Auburn University. To you all, I say thank you.

Special thanks also goes to Mr. Billy Wilson, the structural research laboratory technician at Auburn University, for his guidance, and help throughout my research work at Auburn University.

I am also grateful to all my family members who helped me in diverse ways throughout the course of my studies at Auburn University.

Finally, I would like to thank God. All things are truly possible in His name. I thank Him for staying with me throughout all of my pitfalls and for blessing me with such a wonderful life and the opportunity to bless His Holy name.

Style manual or journal used: Chicago Manual of Style, 15th Edition.

Computer software used: Microsoft® Word, and Microsoft® Excel

---

TABLE OF CONTENTS

LIST OF TABLES

LIST OF FIGURES

CHAPTER 1

INTRODUCTION

1.1 BACKGROUND

Concrete structures, upon exposure to daily temperature changes, experience thermal movements (expansion and contraction). Depending on the temperature range and the material properties of the concrete structure, large thermal stresses may develop at early ages as a result of restraint of the volume change, which could lead to cracking in the concrete structure. Cracking that develops at early ages can be detrimental to the life and durability of the concrete structure (Schindler and McCullough 2002).

An evaluation of bridge decks in the United States identified more than 100,000 bridge decks that exhibited early-age transverse cracking (Krauss and Rogalla 1996). This early-age cracking, typically caused by drying shrinkage (and often coupled with autogenous and thermal shrinkage), can have several detrimental effects on long-term behavior and durability. Darwin and Browning (2008) recently reported that "by controlling early age cracking, the amount of cracking at later ages should remain low."

In Figure 1.1, the process of concrete crack development with change in temperature of the concrete at early ages is shown. Schindler and McCullough (2002)

write that the final setting temperature $T_{final\text{-}set}$, indicated by line (A) is the temperature at which concrete begins to resist stresses induced by temperature changes.

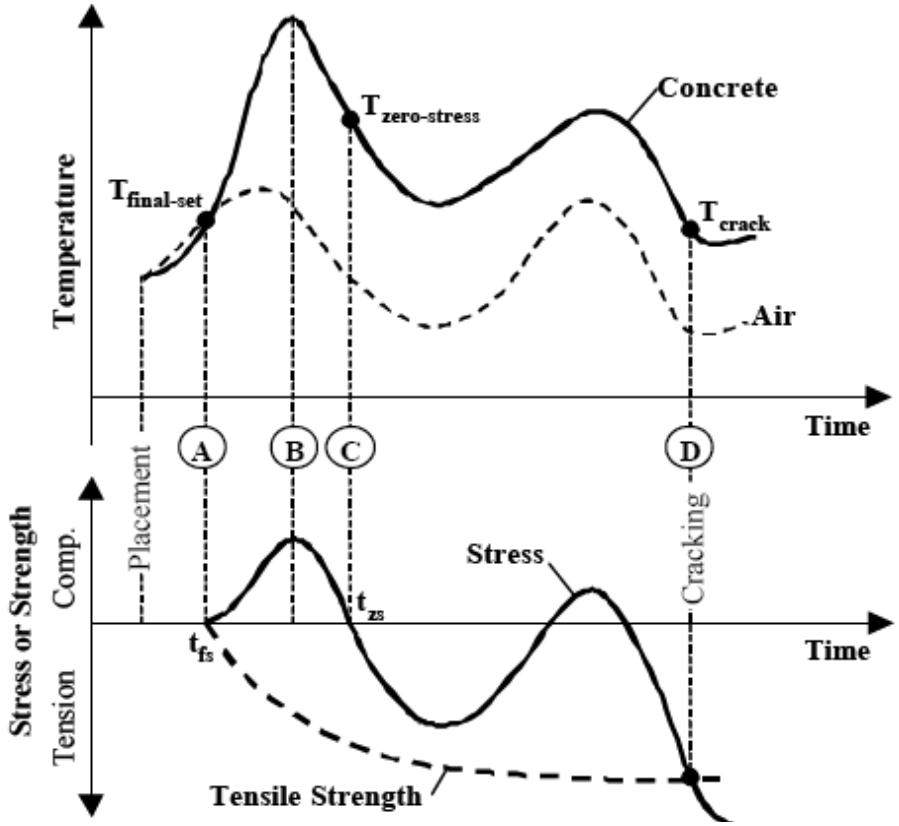

Figure1.1 A graphical representation of the development of thermal stresses in concrete at early ages (Schindler and McCullough 2002)

During high-temperature seasons (i.e. summer months), when a high peak temperature is realized due to the combined effect of heat of hydration and solar radiation as indicated by line (B), the concrete structure will be in compression when it is restrained by its surroundings. When the concrete is subjected to high compressive stresses at this very young age, high amounts of early-age relaxation may occur. When there is a decline in the concrete temperature, there is the relieving of the compressive

stress until the concrete temperature drops below the zero-stress temperature, $T_{zero\text{-}stress}$. The stress condition in the concrete beyond this point, line (C), is now tensile. Upon further cooling, tensile stresses develop, and when the tensile stress developed exceeds the concrete tensile strength, cracking occurs in the concrete as indicated by line (D). Hence, the higher the rise in early-age temperatures, the greater the possibility of cracking due to thermal effects.

Kada et al. (2002) reports that concrete cracking as a result of its volumetric changes from exposure to high temperatures at early ages is a serious issue that did not always receive the attention of engineers and researchers interested in improving the durability of concrete structures until recently. A good understanding of these volumetric changes of concrete, coupled with proper curing, should minimize the often very harmful consequences of cracking, while enhancing the durability of concrete structures (Kada et al. 2002). Kada et al. (2002) further write that a proper evaluation of the volumetric changes is of critical importance in any process aimed at estimating thermal stresses and evaluating the risk of cracking in concrete structures, and that to separate the thermal effect from autogenous shrinkage, it is necessary to know at any moment the evolution of the coefficient of thermal expansion of the concrete from its initial setting.

The coefficient of thermal expansion (CTE) of concrete is the change in unit length of concrete per degree of temperature change (Mehta and Monteiro 2006). The CTE is a very important property in concrete pavements as it can affect the curling stresses and axial stresses and as a consequence, impact the performance and the serviceability of the pavement structure (Tanesi et al. 2007). Mallela et al. (2005)

conclude from experimental works performed on hundreds of cores at the Federal Highway Administration's (FHWA) Turner-Fairbank Highway Research Laboratory (TFHRL) that the CTE can influence the early-age cracking, fatigue cracking, faulting, and joint spalling. CTE is also used in the American Association of State Highway and Transportation Officials (AASHTO) design guide to calculate the opening and closing of transverse joints when designing the proper sealant reservoir dimensions and also in the design of longitudinal reinforcement of continuously reinforced concrete pavement (Mallela et al. 2005). Tanesi et al. (2007) write that despite the importance of the concrete CTE, the AASHTO mechanistic–empirical pavement design guide (MEPDG) is believed to be the first design approach to directly incorporate the CTE as an input parameter in the design of rigid pavements. The MEPDG possesses three hierarchical levels for the input of CTE: level one from actual tests resulting in the highest accuracy; level two from less than optimal testing or by calculations considering the individual CTEs of the aggregates and the cement paste; and level three from agency databases, user–selected default values, typical averages for the region, or a default value based on the type of coarse aggregate (Hossain et al. 2006).

Several researchers (Mitchell 1953; Parsons and Johnson 1944) in the past have reported that the low durability of concrete could be caused by thermal incompatibility between the cement paste and the aggregate. They attributed this incompatibility to the wide differences in the CTE of the various materials making up the concrete. For instance, if the CTE of an aggregate differs considerably from that of the cement paste, a potential thermal incompatibility exists which may result in excessive internal stresses and hence volumetric changes or cracking if the concrete is subjected to large

temperature changes (Parsons and Johnson 1944). In line with this, Berwanger and Sarkar (1976) reported from research performed on steel-concrete composite construction for highway bridges that through the action of bond or by means of shear connectors, steel and concrete, having different CTE, are forced to deform together producing stresses when exposed to temperature changes. These stresses, depending on their magnitude and the strength of the concrete, could lead to cracking in the reinforced concrete bridge deck.

It is apparent from the foregoing paragraphs, then, that knowledge of the CTE of concrete will be an important consideration in the design of concrete structures, especially those exposed to the daily ambient temperature changes. Mallela et al. (2005) report that the CTE is an intrinsic property of a portland cement concrete mixture and that it may not be cost-effective or practical to change concrete mixture constituents to achieve a beneficial CTE for a given design situation. However, knowledge of the CTE for a given mixture and the climatic conditions under which the pavement structure will serve, will allow the designer to more easily change adjustable parameters during material selection and structural design to mitigate its impact. Mallela et al. (2005) further write that to be able to fully accommodate the impact of the CTE on the performance of concrete pavements, its interaction with other design and site factors such as cracking, faulting, and international roughness index-that affect pavement performance, should be considered. Results of the research conducted by Mallela et al. (2005) on hundreds of cores at the Federal Highway Administration's Turner-Fairbank Highway Research Laboratory lead the authors to conclude that:

- An increase in the CTE results in an increase in slab cracking and fatigue damage and that increased joint spacing also causes increased slab cracking and makes the design more sensitive to the CTE.

- Shorter joint spacing, i.e. 15 ft (4.57 m), in combination with higher flexural strength, i.e. 750 psi (5.18 MPa), makes transverse cracking practically insensitive to CTE.

- For longer slabs in excess of 20 ft (6.10 m), slab and fatigue cracking increase significantly with an increase in the CTE.

The relationship between slab cracking and concrete CTE is shown in Figure 1.2. It is observed that at CTEs of approximately 6.0 x 10^{-6} in./in./^{o}F and above, an increase in CTE significantly increases the percent of slab cracking as compared to lower values of CTE (i.e. below 5 x 10^{-6} in./in./^{o}F).

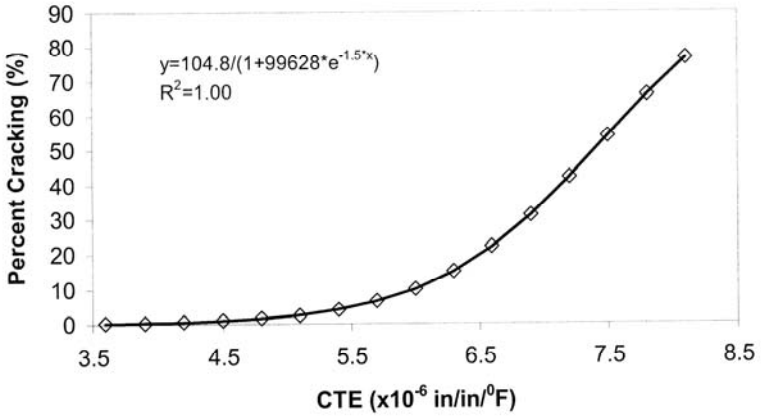

Figure 1.2: Effect of concrete CTE on the predicted percent of slabs cracked (Tanesi et al. 2007)

Mallela et al. (2005), and later on Tanesi et al. (2007) also showed that as the concrete CTE and joint spacing increase, joint opening and faulting increase. The relationship between concrete CTE and faulting is shown in Figure 1.3. It is observed that, for all values of concrete CTE, an increase in the concrete CTE significantly causes an increase in the faulting.

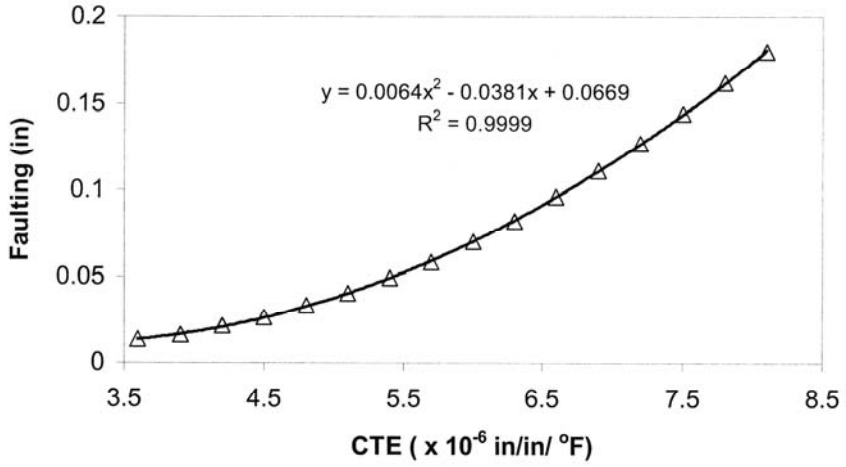

Figure 1.3: Effect of concrete CTE on the predicted faulting (Tanesi et al. 2007)

The international roughness index (IRI) is an index computed from a longitudinal profile measurement using a quarter-car simulation at a simulation speed of 50 mph (80km/h) (ASTM E867-2006). Tanesi et al. (2007) write that when predicting the IRI, the MEPDG model takes into account the effect of the initial IRI, transverse cracking, transverse joint spalling, patching and corner breaks, and that CTE of concrete is not directly considered. However, the CTE will impact the IRI indirectly, as both cracking and faulting affect the IRI. Mallela et al. (2005) report that the combined effects of slab length and concrete strength show an interaction with CTE on its effect on smoothness. Longer slab length cause higher IRI. The relationship between the IRI and the CTE is

shown in Figure 1.4. It is observed that as the CTE increases, the IRI also increases as a result of the increased cracking and faulting.

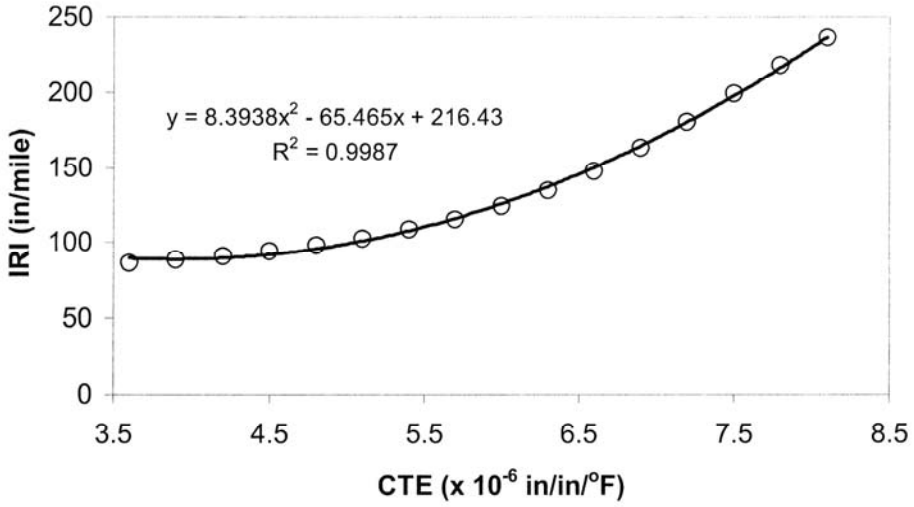

Figure 1.4: Effect of concrete CTE on the predicted IRI (Tanesi et al. 2007)

CTE also affects the thermal stresses in concrete bridge decks. The stresses that develop from a temperature change in bridge decks are linearly proportional to the concrete CTE (Krauss and Rogalla 1996). Therefore, thermal stresses and transverse cracking can be reduced by using concretes with lower CTE. Increasing the aggregate content can reduce the concrete CTE by reducing the more thermally expansive paste content and increasing the less thermally expansive aggregate (Krauss and Rogalla 1996). It can be inferred from the findings of Krauss and Rogalla (1996) that using aggregates with lower thermal expansion rates should also decrease the thermal expansion rate of the concrete. It is imperative that in the design of concrete mixtures for bridge deck construction, close attention should be given to the proportioning of the constituents of the concrete and the selection of the concrete raw material.

It is noted from the above discussions that CTE is an important concrete property that should be considered in the design of pavements and concrete bridge decks as it can affect pavement and deck performance significantly.

1.2 RESEARCH NEEDS STATEMENT

The thermal coefficient of expansion of concrete is important in numerous engineering applications. The increasing recognition of the potential magnitudes of thermal movements and stresses induced in integral or tied structures, especially bridge decks, suggest a need for a realistic thermal coefficient rather than an assumed value for use in design (Emmanuel and Hulsey 1977; Ndon and Bergeson 1995).

Many design manuals for highway construction recommend concrete CTEs for the design of highway structures. The AASHTO LRFD Bridge Design Specification (2007) gives a recommended concrete CTE of 6 x 10^{-6} in./in./^{o}F (10.8 x 10^{-6} in./in./^{o}C). The AASHTO's recommended value for the concrete CTE does not take into consideration the variations in local material properties. Concrete is a composite construction material and its coefficient of thermal expansion is dependent on material factors such as aggregate, moisture condition, cement paste etc. (Emmanuel and Hulsey 1977; Mindess, Young, and Darwin 2002; Parsons and Johnson 1944). It is thus imperative that a sound design practice will require a CTE determined from concretes made with local materials. The AASHTO TP 60 (2004) is a relatively new (provisional) test method developed to determine the CTE of concrete; it has not been evaluated for its accuracy and repeatability. Hence there is the need to evaluate this test method and to determine the CTE of concrete mixtures in Alabama.

1.3 OBJECTIVES OF STUDY

The objectives of this study are to:

- Recommend CTE values of concrete made with commonly used coarse aggregate types found in Alabama.
- Quantify the effect of coarse aggregate type and amount, water-cement ratio, and sand-aggregate ratio on the concrete CTE.
- Evaluate the experimental test setup proposed in the preliminary AASHTO TP 60 test (2004) titled: Standard Method of Test for Coefficient of Thermal Expansion of Hydraulic Cement Concrete.

1.4 SCOPE

Chapter 2 documents a review of the literature about the CTE, and further discusses all the know factors affecting the CTE. The test methods that have been used to test the CTE of concrete, including AASHTO TP 60 (2004), are also presented in this chapter.

An introduction to the geology of Alabama, and also the geological description of the coarse aggregates used in this study, their mineral content, and their locations in Alabama are presented in Chapter 3.

In Chapter 4, the CTE experimental test setup, test procedure, and the properties of the concrete raw materials used in the study are presented.

Statistical analyses performed on the CTE test results, the effects of sand-aggregate ratio, water-cement ratio, and aggregate type on the concrete CTE are presented, discussed, and documented in Chapter 5.

Chapter 6 details the conclusions and recommendations drawn from this study.

In Appendix A, all the CTE test data are presented, while Appendix B presents the statistical analysis results. Appendix C documents all the data recording and calculation sheets used in this study.

CHAPTER 2

LITERATURE REVIEW

The coefficient of thermal expansion (CTE) of concrete is an important fundamental property of concrete that is used in the analysis and design of concrete pavements and bridge decks. The CTE, as discussed in Chapter 1, can influence the early-age cracking, fatigue cracking, faulting and joint spalling that occur in concrete bridge decks and concrete pavements. The factors that affect the concrete CTE are discussed in this chapter. Also discussed here are the test methods used by various researchers in testing for the CTE.

2.1 FACTORS AFFECTING THE COEFFICIENT OF THERMAL EXPANSION OF CONCRETE

Several variables that affect the CTE of concrete have been reported. The variables that have a great influence on the CTE of concrete are the type and amount of aggregate, moisture content of the concrete, the type and amount of cement, and the concrete age (Mindess, Young and Darwin 2002; Emanuel and Hulsey 1977; Mehta and Monteiro 2006). Cylinder size, water-cement ratio, sand-aggregate ratio and temperature are reported to affect the CTE minimally (Alungbe et al. 1992; Kohler et al. 2006).

2.1.1 MOISTURE CONTENT

Investigations by Kada et al. (2002) indicate that at early ages, i.e. before initial setting, a rather important variation of the concrete CTE occurs, which then stabilizes there afterwards. They believed this early-age variation was essentially caused by the presence of water not yet bounded by hydration in the system. Kada et al. (2002) found out that at this state, i.e. 68 ^{o}F (20 ^{o}C), the water has a CTE of up to twenty times greater than the other constituents of concrete. The concrete CTE at this stage will therefore depend greatly on the CTE of the water. Similarly, Sellevold and Bjontegaard (2006) further clearly demonstrated the dominant influence of moisture content on the CTE of concrete both at the early ages and also at later ages. Investigations carried out by Sellevold and Bjontegaard (2006) indicated that before setting, concrete has a high CTE since no solid microstructure exists and the continuous water phase dominates. As solid hydration products are formed, the CTE decreases, reaching a minimum value around final set, from then on the CTE increases as self desiccation progresses, which contradicts the findings of Kada et al. (2002).

Emanuel and Hulsey (1977) report that the moisture content of hardened concrete, which is related to the ambient relative humidity, strongly affects the CTE; however, the water-cement ratio has little effect. The CTE was reported to be least for saturated concrete, and is slightly higher for oven-dry concrete, and is a maximum for some partially dry condition. The maximum value for the partially dry state of the *concrete* is approximately 15% higher than for the saturated state and is dependent upon the proportion of aggregate (Emanuel and Hulsey 1977). The maximum CTE for partially dry neat cement *paste* samples is approximately 1.8 times the average maximum value

for saturated *paste* samples (Emanuel and Hulsey 1977). This trend is shown graphically in Figure 2.1. This dependency of CTE on the moisture condition of the concrete sample has also been reported by other researchers (Neville and Brooks 1987; Mindess, Young and Darwin 2002). It may be concluded from Figure 2.1 that the CTE has a maximum value occurring between the moisture content of 50 % and 80 %, and usually, with maximum CTE around a moisture content of 70 %. This behavior of cement paste and hence concrete is summarized in Figures 2.1, 2.2, and 2.3.

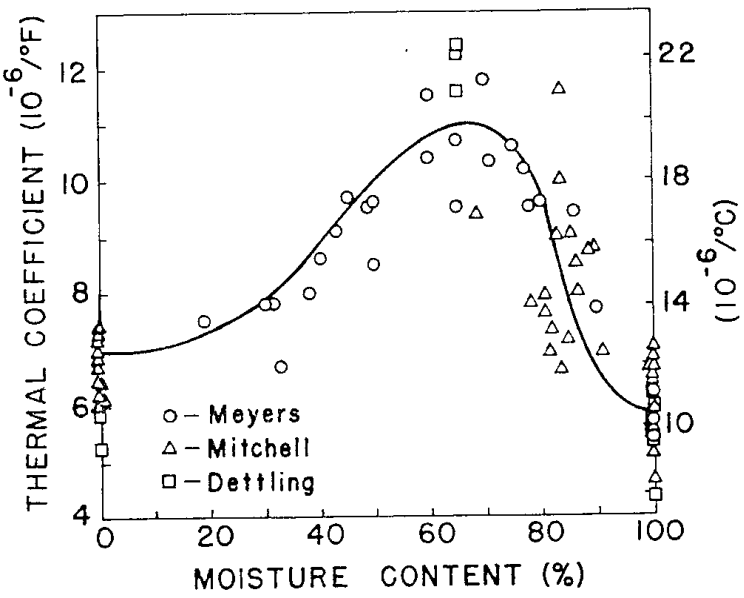

Figure 2.1: Variation of CTE of neat cement *paste* with moisture content (Emanuel and Hulsey 1977)

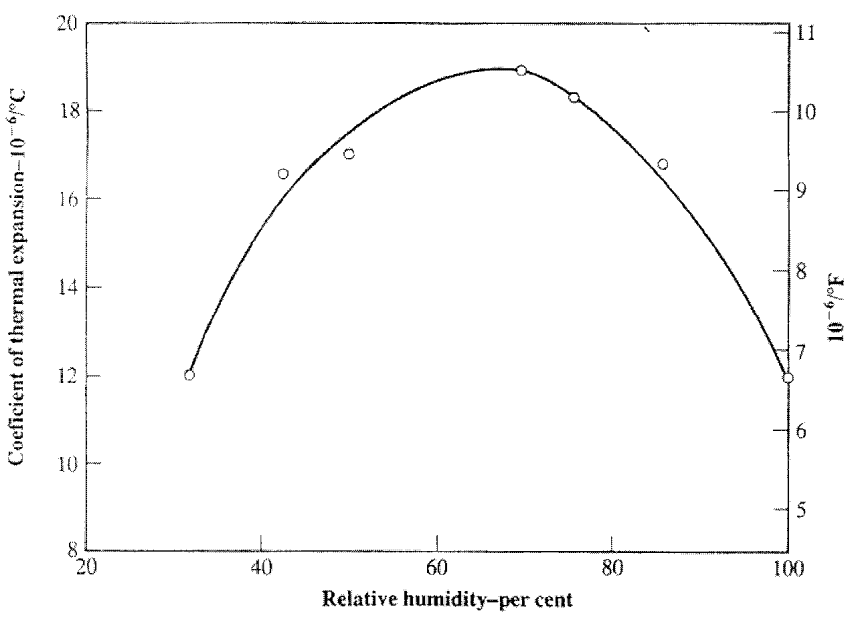

Figure 2.2: Relation between ambient relative humidity and the linear CTE of neat cement *paste* (Neville and Brooks 1987)

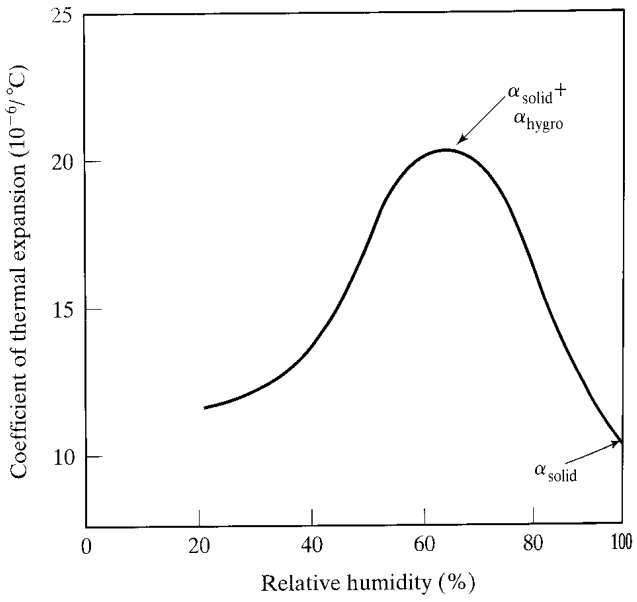

Figure 2.3: Variation of the CTE with moisture content of cement *paste* (Mindess, Young and Darwin 2002)

Neville and Brooks (1987) attempt to explain this behavior of concrete and or cement paste, shown in Figure 2.2, by considering the *so-called* two components of CTE of cement paste: the true (kinetic) thermal coefficient, which is caused by the molecular movement of the paste, and the hygrothermal expansion coefficient. The latter arises from an increase in the internal relative humidity (water vapor pressure) as the temperature increases, with a consequent expansion of the cement paste. No hygrothermal expansion is possible when the paste is totally dry or when it is saturated, since there can be no increase in the water vapor pressure. However, at intermediate moisture contents, hygrothermal expansion occurs in cement paste and hence in concretes. In concrete, the hygrothermal effect is naturally smaller. This concept is shared by Mindness, Young and Darwin (2002). They are of the view that the hygrothermal expansion is dependent on the water-cement ratio and age, and that because these factors determine the porosity characteristics of the paste, the following relationship exists:

$$\alpha_{actual} = \alpha_{solid} + \alpha_{hygro} \qquad \textit{Equation 2.1}$$

where,

α_{actual} is the measured CTE

α_{solid} is the CTE measured in the absence of hygrothermal change, depending on kinetic molecular movement, and

α_{hygro} is the coefficient of hygrothermal expansion.

Sellevold and Bjontegaard (2006) explain this CTE dependency on moisture content by discussing the mechanism in three categories:

- Pure thermal dilation,
- Thermal shrinkage or swelling, and
- Relative humidity change.

2.1.1.1 Pure Thermal Dilation

The CTE of water is much higher than the CTE of solids, and water in small pores *probably* has higher CTE than bulk water (Sellevold and Bjontegaard 2006; Kada et al. 2000). Thus a very fast temperature increase followed by an isothermal period will lead to fast expansion, followed by a time-dependent contraction as the induced excess pressure in filled pores is dissipated by flow to the outside or to partly empty pores. Sellevold and Bjontegaard (2006) and Kada et al. (2000) claim that depending on the permeability of the paste and the distance to available "sinks," the pressure relief may be fast or slow, thus it may appear as an instantaneous deformation and be counted in CTE, or as a delayed deformation. Delayed deformation is much more prevalent in saturated samples than in partly dried samples (Scherer 2000; Ai 2001). Thus for concrete in practice, where the normal moisture state is a "natural self-desiccated condition," less delayed deformation is found and any pressure relief mechanism is presumably very fast and counted as instantaneous deformation and hence part of CTE.

2.1.1.2 Thermal Shrinkage and Swelling

According to Sellevold and Bjontegaard (2006), pore water can be roughly divided into two types: gel water, a collective term for water which is strongly influenced by its proximity to solid surfaces (i.e. interlayer water, adsorbed water, etc.), and capillary water (i.e. water in larger pores). Equilibrium requires that the chemical potential of coexisting water phases is equal both before and after a temperature change.

The rate of change of the chemical potential of a water phase with respect to increasing temperature is the negative of the entropy. The entropy of the gel water is lower than the capillary water, thus a sudden increase in temperature leads to a higher chemical potential in gel water than in capillary water (Radjy, Sellevold, and Hansen 2003). This sets up a driving force for an internal redistribution of water from gel to capillary pores. This is expected to lead to shrinkage, i.e. sudden heating of a cement paste sample is expected to produce a sudden expansion followed by a time-dependent contraction and vice versa upon cooling. It is perhaps difficult to visualize how water can redistribute in a saturated sample, i.e. when there is no available space. The theory behind this, Radjy, Sellevold and Hansen (2003) claim, is that cooling will force water to the gel pores in an amount necessary to increase the local pressure (disjoining pressure) enough to establish equilibrium in chemical potential with the water in capillary pores. This pressure in the gel water will produce expansion.

In partly saturated samples, the situation is that the gel pores are full, but the capillary pores are partly empty with the water under capillary tension. The redistribution takes place in the same way as for the saturated samples; in theory, this implies the possibility of a situation after cooling when the gel water is under pressure while the capillary water is under tension.

2.1.1.3 Relative Humidity Change

A plot of vapor pressure versus temperature for a given cement paste at different moisture contents is shown in Figure 2.4. Sellevold and Bjontegaard (2006) showed that the resulting curves are nearly straight lines and that the slopes increase as the moisture

contents are reduced, i.e. the enthalpy of the pore water increases with decreasing moisture content. Sellevold and Bjontegaard (2006) explain further that, if the lines were to be parallel, then the relative humidity (RH) would be independent of temperature but when the lines are not parallel as shown, then the results of heating from T_1 to T_2 is that the RH increases, since

$$\frac{P^2}{P_s^2} > \frac{P^1}{P_s^1} \qquad \textit{Equation 2.2}$$

hence $RH_2 > RH_1$ *Equation 2.3*

where,

P_s^1 = Saturation vapor pressure at temperature T_1,

P_s^2 = Saturation vapor pressure at temperature T_2,

P^1 = Vapor pressure at temperature T_1, and

P^2 = Vapor pressure at temperature T_2.

This effect, shown in Figure 2.5, has important consequences for the CTE (Radjy, Sellevold and Hansen 2003). Sellevold and Bjontegaard (2006) further argue that the effect of the increase in relative humidity (RH) on heating for CTE may be estimated using Figure 2.5 and isothermal shrinkage data. A mature paste cured isolated may self desiccate to 85 % relative humidity. The percent relative humidity per degree Celsius factor may be about 0.2 % /^{o}C, and the slope of the shrinkage-relative humidity curve is about 60 microstrain per percent relative humidity (Sellevold and Bjontegaard 2006).

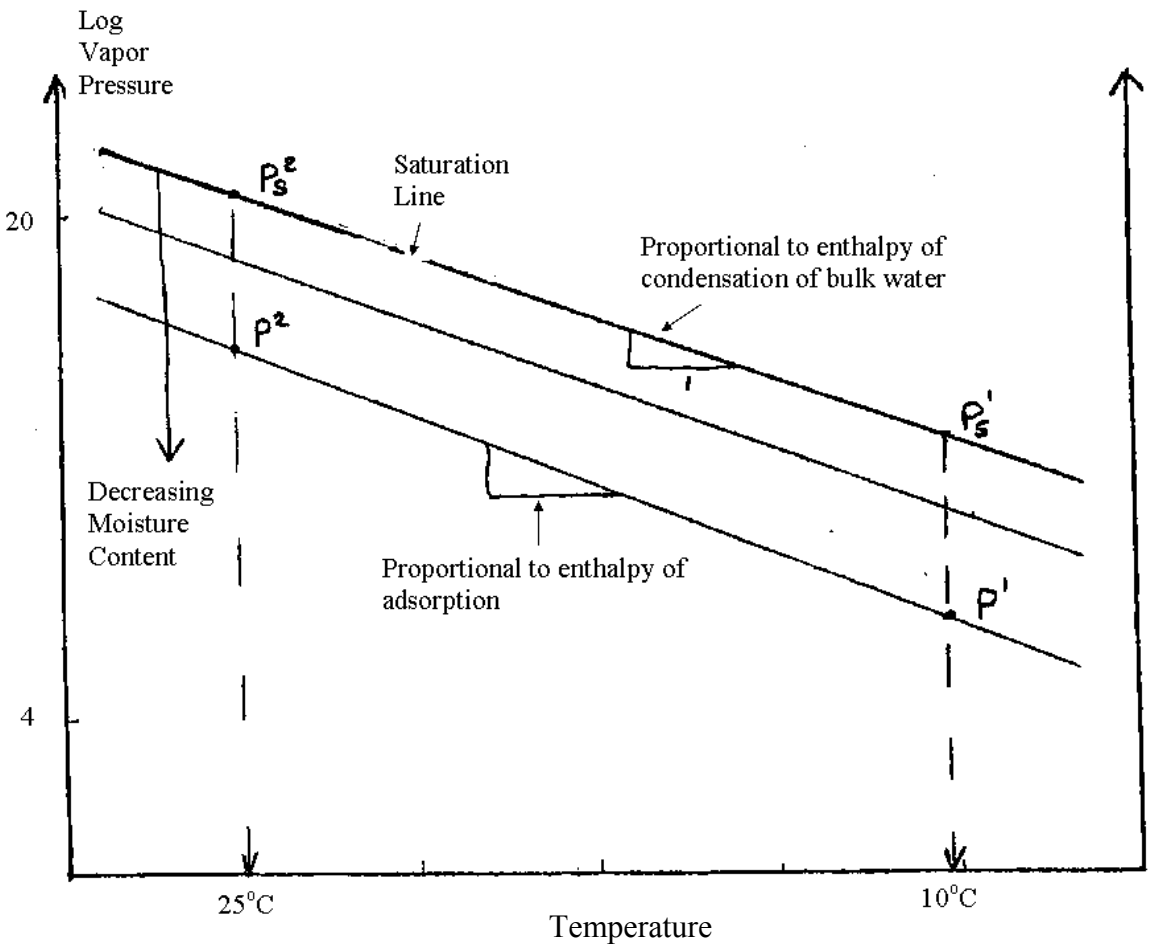

Figure 2.4: Log vapor pressure against temperature (Adapted from Sellevold and Bjontegaard 2006)

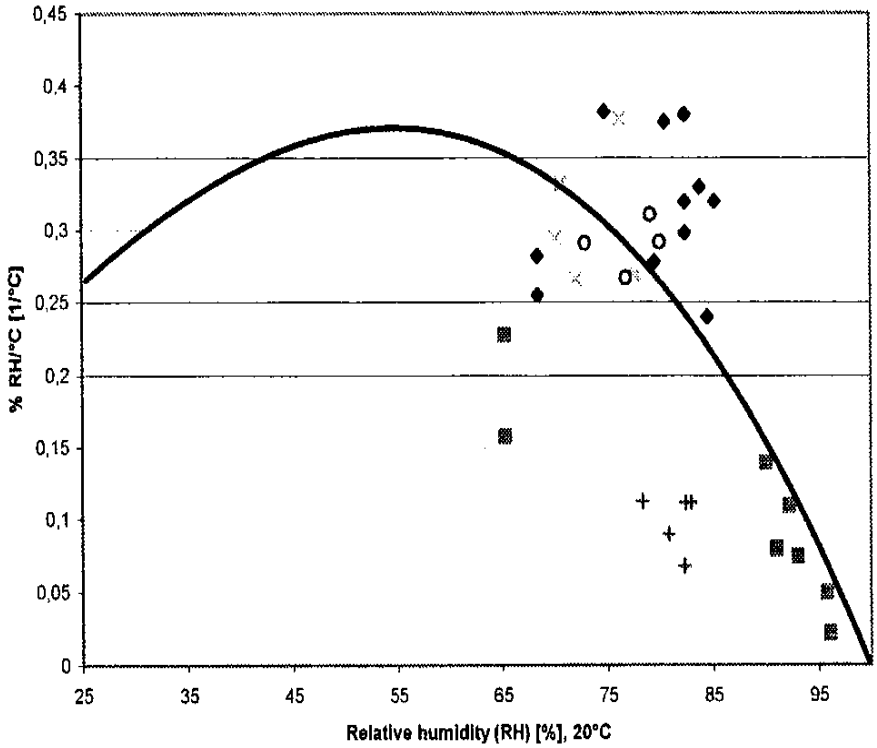

Figure 2.5: Plot of percent relative humidity/°C vs. relative humidity at 20 °C (Radjy, Sellevold and Hansen 2003)

Then the apparent CTE from this mechanism becomes 0.2 x 60 = 12 x 10^{-6} /^{o}C. From Figure 2.6, the CTE is estimated to be 22 x 10^{-6} /^{o}C for 88 % saturated paste (roughly corresponding to a RH of 85 %), of which 12 x 10^{-6} /^{o} C may be caused by the relative humidity effects.

Thus the relative humidity mechanisms alone are able to explain the effect of moisture content on CTE. It is of course implied that the relative humidity effect is fast and the resulting deformation is instantaneous deformation and hence recorded as part of the CTE.

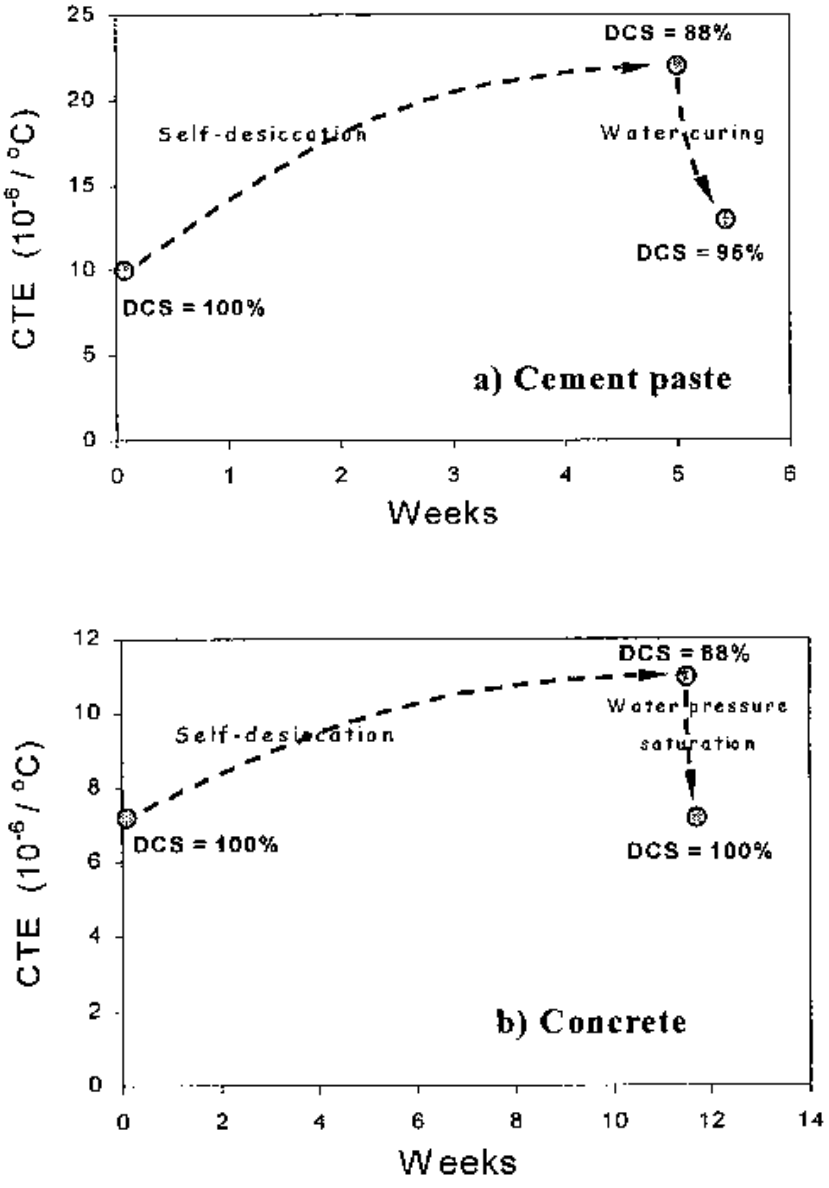

Figure 2.6: Evolution of CTE with time (Sellevold and Bjontegaard 2006)

(Where DCS = degree of capillary saturation)

2.1.2 AGGREGATES

Mehta and Monteiro (2006) report that the concrete CTE is directly related to the CTE of the aggregate present (Figure 2.7). They further comment that in mass concrete, the selection of an aggregate with a lower CTE provides another approach towards lowering the thermal strain. It is observed from Figure 2.7 that quartz with a high CTE of 6.1×10^{-6} /°F (11×10^{-6} /°C) produces a concrete of high CTE of 6.7×10^{-6} /°F (12×10^{-6} /°C), whereas limestone with a low CTE of 2.8×10^{-6}/°F (5×10^{-6} /°C) produces a corresponding concrete of CTE 3.3×10^{-6} /°F (6×10^{-6} /°C).

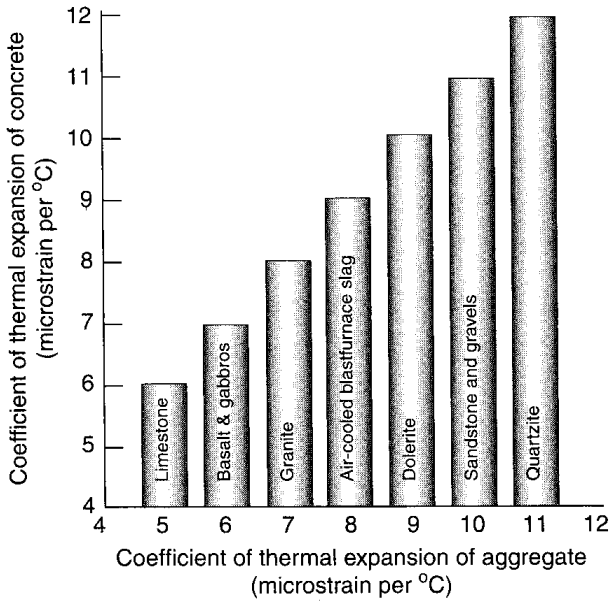

Figure 2.7: Influence of the aggregate type on the CTE of concrete (Mehta and Monteiro 2006)

Some researchers (Ziegeldorf, Kleiser and Hilsdorf 1978; Emanuel and Hulsey 1977) are of the view that, if cement paste and aggregates could expand freely in

concrete, then the concrete CTE could be computed as the volumetric average of the CTEs of its constituents. Emanuel and Hulsey (1977) provide an expression to calculate the CTE of concrete and this is presented later on in section 2.3. In reality however, a smaller value of the concrete CTE is observed than expected (Ziegeldorf, Kleiser and Hilsdorf 1978). This, they believe is due to the restraint of free deformation of the cement paste by the aggregate, resulting from the aggregates larger modulus of elasticity and smaller thermal coefficient of expansion (Ziegeldorf, Kleiser and Hilsdorf 1978). This relationship between thermal expansion of concrete and that of its components is shown in Figure 2.8. It is observed that as the aggregate content increases, correspondingly, the strain associated with it also increases, and hence the strain of the cement paste decreases. This works out such that at a 100 % aggregate content, the total strain in the system is provided by the aggregate and the total CTE is that of the aggregate. The shaded portion shows the restraint offered the cement paste by the aggregate. The CTE is reported to be affected by the type and amount of aggregates present in the mixture (Emanuel and Hulsey 1977; Alungbe et al. 1992; Mindess, Young and Darwin 2002; Dossey, McCullogh and Dumas 1994; Parsons and Johnson 1944; Hossain et al. 2006; Neville and Brooks 1987, Ziegeldorf, Kleiser and Hilsdorf 1978; Mehta and Monteiro 2006). The extent to which the concrete CTE depends on the mineralogical composition and volume is explained in the next section.

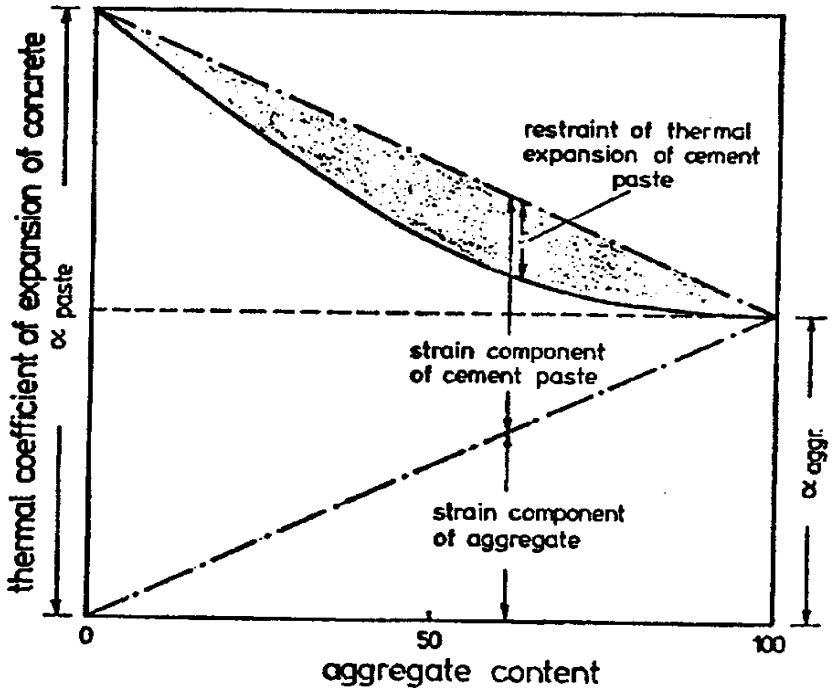

Figure 2.8: Relationship between thermal expansion of concrete and of thermal expansion of its components (Ziegeldorf, Kleiser and Hilsdorf 1978)

2.1.2.1 Aggregate Mineral Composition

Bonnel and Harper (1950) reported that siliceous rocks have the highest CTE, carbonate rocks the lowest, and igneous rocks have intermediate values. Alungbe et al. (1992) and Ziegeldorf, Kleiser and Hilsdorf (1978) similarly concluded that river gravels produced the highest CTE of concrete while limestone rocks (carbonate rocks) produced the lowest concrete CTE. Mindess, Young and Darwin (2002) also report that quartz has the highest CTE, 7 x 10^{-6} /^{o}F (12.6 x 10^{-6} /^{o}C), of any common mineral and that the CTE of various rocks are related to their quartz (silicon dioxide) content. Rocks with high quartz (quartzite, sandstone) have CTE similar to quartz; those containing no quartz

(limestone, marble) but are high in calcium oxide have CTE around 3 x 10^{-6}/°F (5.4 x 10^{-6}/°C). These views are also shared by Mehta and Monteiro (2006) as shown in Figure 2.7. The effects of silicon dioxide and calcium oxide on concrete CTE are shown in Figures 2.9 and 2.10, respectively. It is observed that as the silicon dioxide content in concrete mixture increases, the concrete CTE also increases, while the concrete CTE increases with a decrease in the calcium oxide content. It is also observed from Figure 2.9 that the slope of the graph is steep throughout, implying that the CTE of concrete is sensitive to the silicon dioxide content irrespective of the level of silicon dioxide. On the other hand, for the calcium oxide plot, the slope of the graph is not steep throughout. At higher percentages of calcium oxide, i.e. above 60 %, the change in calcium oxide content does not have much impact on the CTE; however, between 6 % and 60 % calcium oxide content, the CTE is very sensitive to the calcium oxide content and below 6 %, the sensitivity of the CTE to the calcium oxide content increases asymptotically.

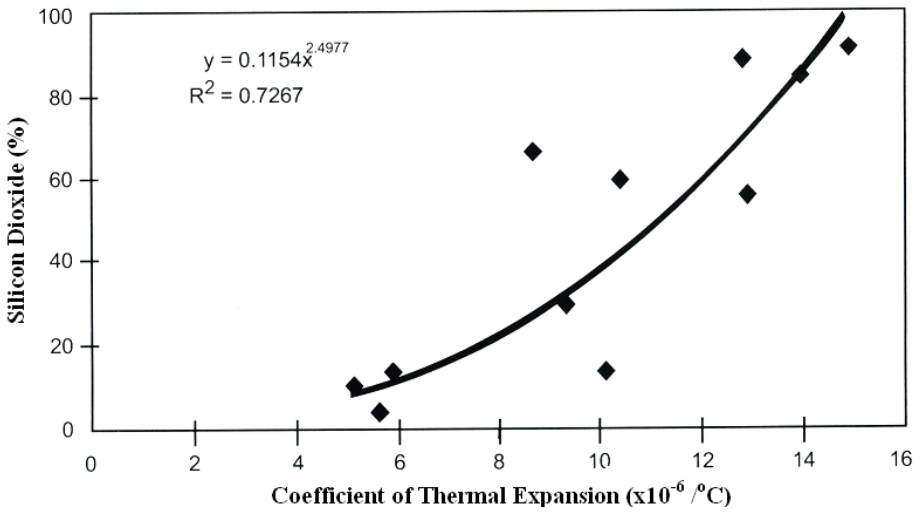

Figure 2.9: Effect of silicon dioxide content on CTE (McCullough, Zollinger, and Dossey 1999)

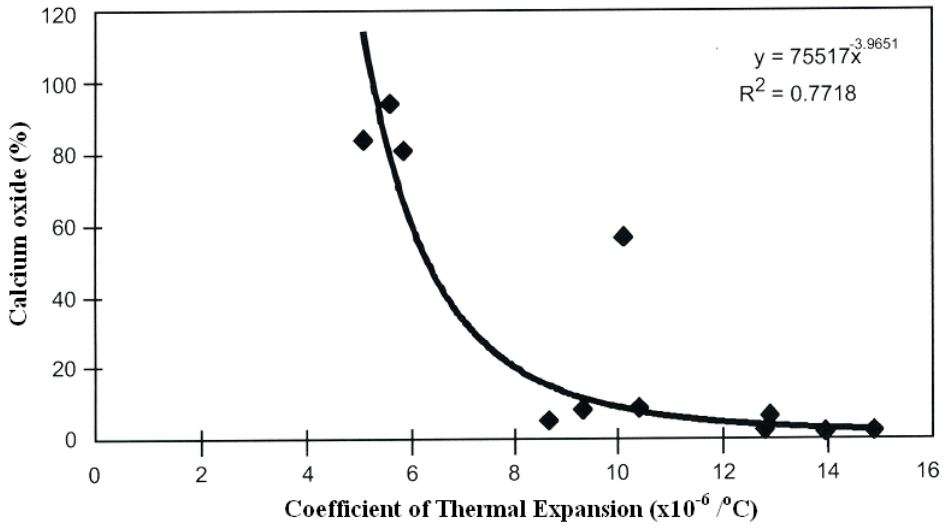

Figure 2.10: Effect of calcium oxide content on the CTE (McCullough, Zollinger and Dossey 1999)

Researchers have shown that aggregate mineralogy composition has a major effect on the material properties (i.e. CTE) of the finished concrete and ultimately on the pavement performance (Dossey, Salinas and McCullough 1992). These conclusions are also in harmony with the works of Parsons and Johnson (1944). They believe that rocks from various sources but of similar composition have approximately the same thermal expansion coefficients if orientation differences are disregarded, a fact which is also shared by Mitchell (1953). He claims that similar type aggregate from different sources may have totally dissimilar coefficients of thermal expansion. Emanuel and Hulsey (1977), in agreement with the above conclusions, wrote that similar types of aggregates from different sources have thermal coefficients of expansion that correspond to their mineral compositions. The mineralogy of the aggregate, no doubt to a greatly affects the CTE of concrete. It is worth noting that Mindess, Young, and Darwin (2002) state that although the concrete CTE depends on cement content, the variation over the normal

range of cement contents may not be as great as the effect of changing the type of aggregate.

The different thermal expansion coefficients of concrete for different aggregates types used by Neville and Brooks (1987) are listed in Table 2.1. It may be observed that the type of aggregate used in a mixture ultimately affects the CTE of concrete to a greater extent than the other constituents of concrete.

Table 2.1: Coefficient of thermal expansion of concretes made with different aggregates (Neville and Brooks 1987)

Type of aggregate	Linear coefficient of thermal expansion			
	Air-cured concrete		Water-cured concrete	
	10^{-6} per °C	10^{-6} per °F	10^{-6} per °C	10^{-6} per °F
Gravel	13.1	7.3	12.2	6.8
Granite	9.5	5.3	8.6	4.8
Quartzite	12.8	7.1	12.2	6.8
Dolerite	9.5	5.3	8.5	4.7
Sandstone	11.7	6.5	10.1	5.6
Limestone	7.4	4.1	6.1	3.4
Portland stone	7.4	4.1	6.1	3.4
Blast-furnace slag	10.6	5.9	9.2	5.1
Foamed slag	12.1	6.7	9.2	5.1

Ziegeldorf, Kleiser and Hilsdorf (1978), after experimental works where limestone fines were substituted by quartzite fines, observed a relatively small increase of the CTE of concrete. This led them into concluding that the influence of fine aggregates on the concrete CTE is smaller than the effect of coarse aggregates.

2.1.2.2 Aggregate Volume

Aggregates occupy approximately 70 % to 80 % of the volume of concrete (Mehta and Monteiro 2006). Hence, it is logical to expect that the CTE of concrete will be largely dependent upon the CTE of the aggregates. Generally, an increase in the volume of the aggregate could either increase or decrease the CTE of concrete. This, of course, depends on the constituent minerals in the aggregate, as explained earlier. Mehta and Monteiro (2006) write that, concretes that contain high volumes of aggregates rich in quartzite will have a higher CTE than concretes that contain high volumes of aggregates rich in limestone. Emanuel and Hulsey (1977) state that because moisture has little effect upon the CTE of an aggregate, it is readily apparent that the proportion of aggregate is the primary factor contributing to the reduction of the effect of moisture content on the variation of the thermal coefficient of concrete as compared to cement paste. In other words, an increase in the amount of aggregate will decrease the moisture effect on concrete.

Figure 2.11 shows the effect of aggregate volume and mineralogical composition on the effect of CTE of concrete and mortar. From this plot, it may be seen that as the volume of siliceous sand increases, the CTE of the mortar increases, while when the volume of the limestone sand increases, the CTE of the mortar decreases, as shown in Figure 2.11(a). Similarly, it is observed from Figure 2.11(b) that as the coarse aggregate volume increases, for the case of limestone sand and crushed limestone rocks, the CTE of concrete keeps decreasing, a trend which is somehow similar to the case of siliceous sand and crushed limestone. Figure 2.11(b) also shows that for the case of siliceous sand and quartz gravel, although there is an increase in CTE of concrete, it is not as substantial as

in the case for limestone sand and quartz gravel. This shows the influence of the coarse aggregate type on concrete CTE and hence appears to be in agreement with Ziegeldorf, Kleiser and Hilsdorf (1978), who claim that the influence of fine aggregate on the CTE of concrete is smaller than the effect of coarse aggregate.

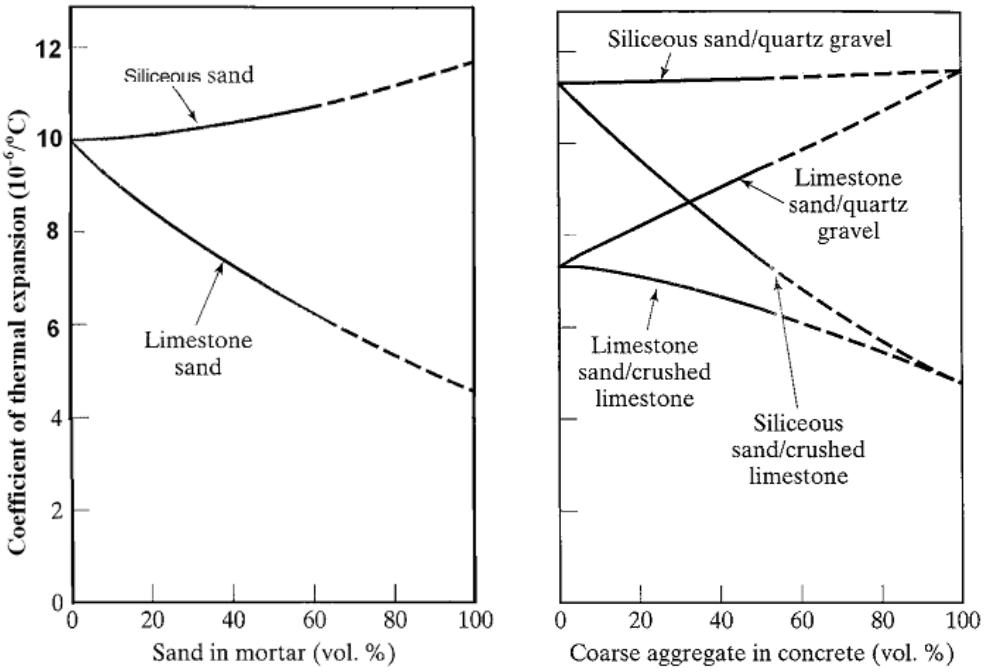

(a) (b)

Figure 2.11: (a) Effect of aggregate volume and mineralogy on the CTE of mortar. (b) Effect of aggregate volume and mineralogy on the CTE of concrete (Mindess, Young and Darwin 2002)

Neville and Brooks (1987) represented the influence of volumetric content of aggregate and of aggregate type on the concrete CTE using the model developed by Hobbs (1971). This is shown in Figure 2.12, from which it is apparent that, for a given type of aggregate, an increase in its volume concentration reduces the thermal coefficient

of expansion of concrete, while for a given volume concentration, a lower thermal coefficient of aggregate also reduces the concrete thermal expansion coefficient.

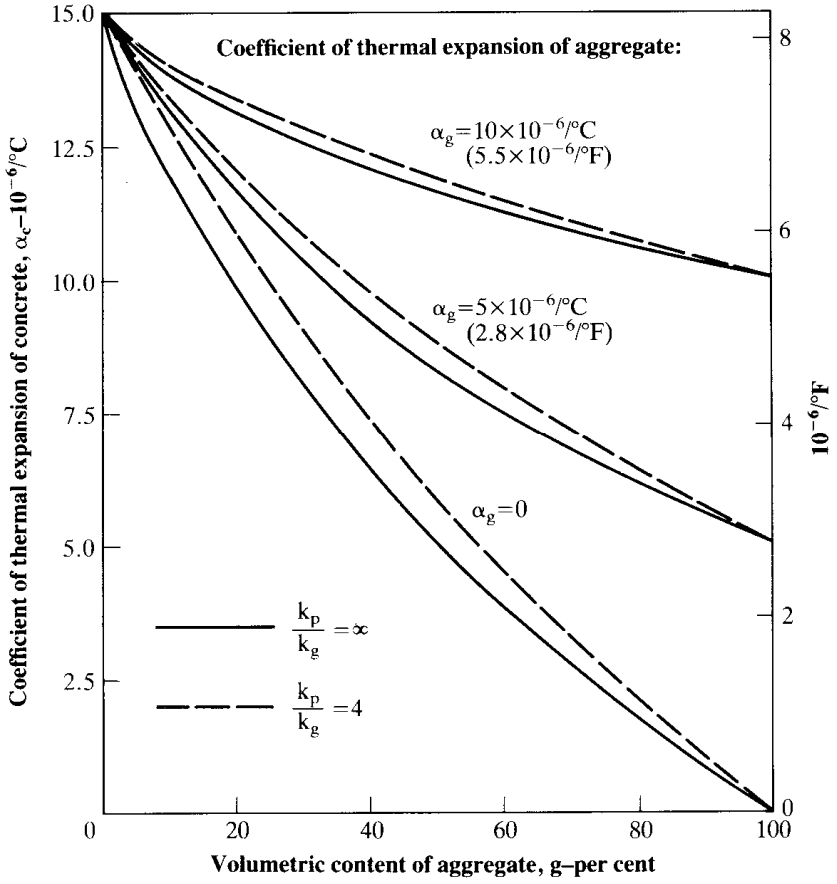

Figure 2.12: Influence of volumetric content of aggregate and of aggregate type on linear CTE of concrete (Neville and Brooks 1987)

2.1.3 AGE OF CONCRETE

Kada et al. (2002) concluded based on works they carried out that the CTE for studied concretes was significantly dependent on the age during the first few hours following concrete casting, and that any investigations aiming at evaluating the early-age strain development in high performance concrete structures should take into

consideration the effect of autogenous shrinkage on the CTE variations during concrete hardening. The CTE, as they believed, was important at a very young age, but after this time almost remained constant. This early-age variation of the CTE with time according to Kada et al. (2002) is shown in Figures 2.13 (a) and (b). It is observed that similar patterns are noted for different water-cement ratios. This early-age variation, they explained, is caused essentially by the presence of water not yet linked in the system, the water having a CTE of up to twenty times greater than the other constituents.

Berwanger and Sarkar (1976) found that the CTE for concretes made of normal portland cement, with a maximum aggregate size of ¾ in. (the coarse aggregate being 65 % limestone with about 25 % feldspar and the fine aggregate was 35 % quartz , 29 % carbonate and 23 % feldspar) at an applicable temperature range of -100 ^{o}F to 150 ^{o}F (-73 ^{o}C to 66 ^{o}C), increases by approximately 12 % and 20 % for above and below freezing, respectively, when tested between the ages of 7 days and 84 days. Bonnel and Harper (1950) reported, however, that age had a minor effect upon the thermal coefficient for concretes tested up to one year.

Experimental works conducted by Alungbe et al. (1992) show that the CTE of concrete decreases with increasing age for concretes tested at the ages of 28 days and 90 days, the mean CTE for concretes made of river gravel being 7.63 x $10^{-6}/^{o}$F (13.73 x $10^{-6}/^{o}$C) at 28 days and 6.77 x $10^{-6}/^{o}$F (12.20 x $10^{-6}/^{o}$C) at 90 days. This finding by Alungbe et al. (1977) appears to be in contrast with the work of Berwanger and Sarkar (1976) that concluded that the CTE increases with increasing age.

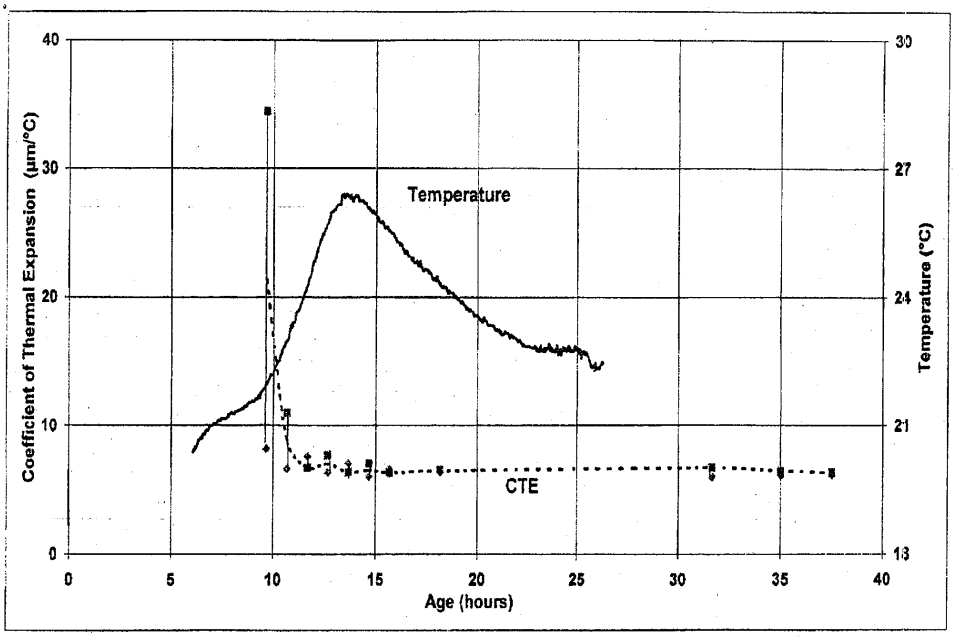

Figure 2.13: (a) Evolution of the CTE for a 0.45 water-cement ratio concrete during hydration (Kada et al. 2002)

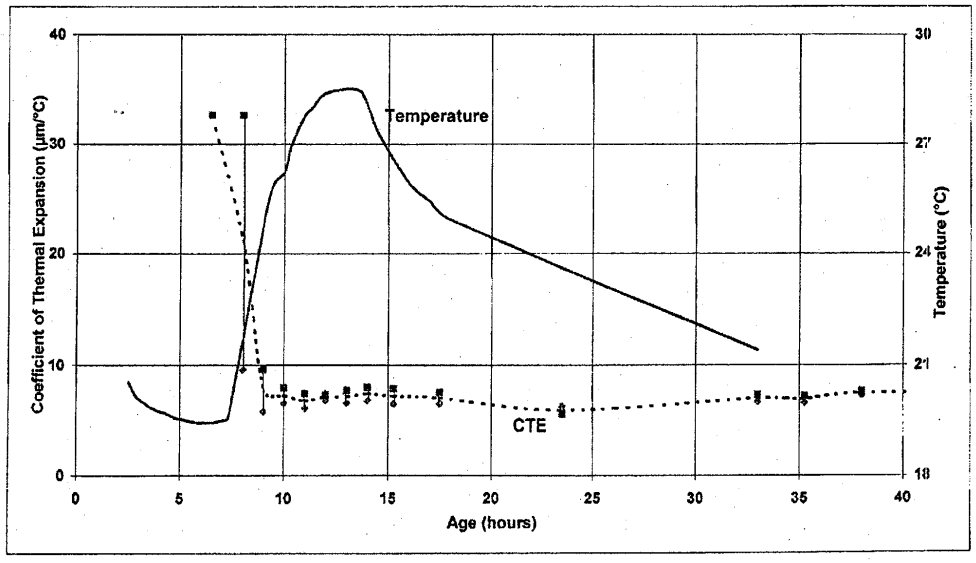

Figure 2.13: (b) Evolution of the CTE for a 0.35 water-cement ratio concrete during hydration (Kada et al. 2002)

In addition, Emanuel and Hulsey (1977) show that the CTE decreases with increasing age for a Type I cement *paste*. In Figure 2.14, Emanuel and Hulsey (1977) show this variation of CTE with age for cement paste.

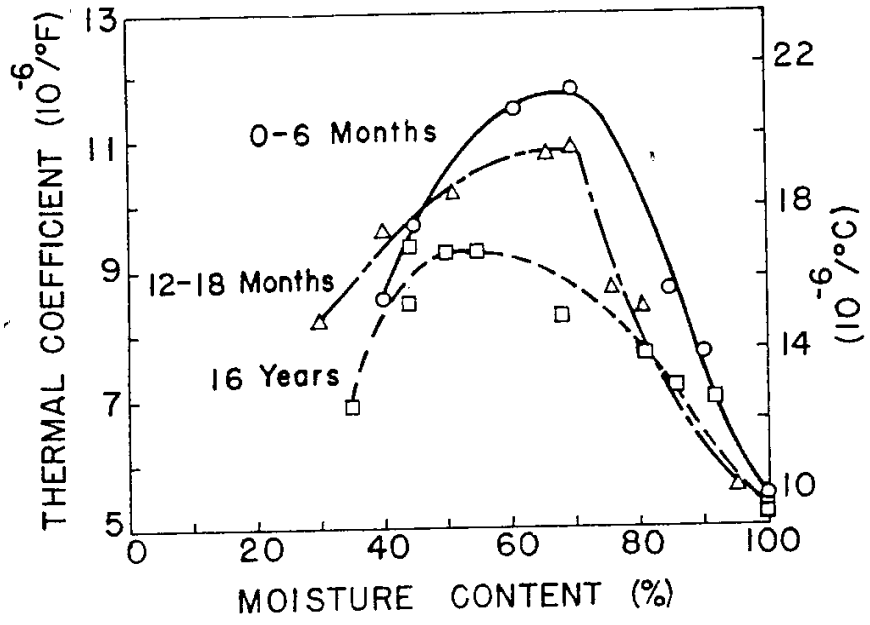

Figure 2.14: Variation of the CTE with moisture content and age for Type I cement *paste* (Emanuel and Hulsey 1977)

2.1.4 TEMPERATURE

Tests carried out on saturated concrete samples 55 days old and under different conditions of relative humidity showed that at a relative humidity of 90 %, the CTE increases with an increase in temperature as shown in Figure 2.15. Varying effects seem to have occurred at a relative humidity of 100 %.

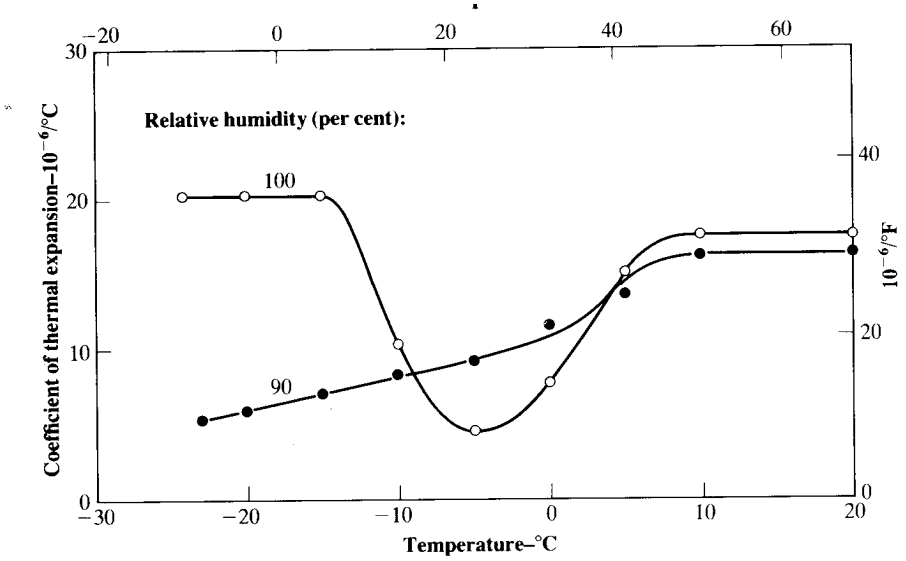

Figure 2.15: Relation between CTE and temperature of concrete specimens (Wittmann and Lukas 1974)

This finding by Neville and Brooks (1987) that the concrete CTE increases with an increase in temperature is in harmony with the works of Emanuel and Hulsey (1977). Hatt (1926) observed a coefficient of 4.0 x 10^{-6} /°F (7.2 x 10^{-6} /°C) at 60 °F (16 °C), and 6.5 x 10^{-6} /°F (11.7 x 10^{-6} /°C) at 150 °F (66 °C). However, this effect of temperature on CTE is noted in Mindness, Young, and Darwin (2002) to be much more pronounced in aggregates than in concrete. Thus rocks may lose their integrity due to chemical decomposition (limestone, basalt) or phase changes (quartzite); hence, it is a good practice to keep the temperature to a range that will make the rocks preserve their integrity. This issue is, however, not important in structures exposed to ambient temperatures.

2.1.4.1 Variation of Thermal Coefficient of Expansion with Expansion and Contraction

Chow (1953) found that the CTE of concrete was generally lower for contraction (temperature descending) than for expansion (temperature ascending). Experimental works as a preliminary step for clarifying the time dependence of the CTE in the initial hardening process of concretes, undertaken by Yamakawa et al. (1979) later on, also showed that the CTE of comparatively early-aged concrete in expansion tends to be greater than the CTE in contraction.

2.1.5 WATER-CEMENT RATIO

In a test on concrete and reinforced concrete samples to determine the CTE under short-term steady-state temperatures, -100 ^{o}F to 150 ^{o}F (-73 ^{o}C to 150 ^{o}C), Berwanger and Sarkar (1976) found that for a water-cement ratio of 0.672 to 0.445, the CTE increased with a decrease in the water-cement ratio. They explained further that the average increase is 30 % for above freezing and 20 % for the below freezing CTE for air-dried and saturated concrete for the water-cement ratio ranging from 0.672 to 0.445.

However, in a study to determine the CTE, for concretes with water-cement ratios of 0.53, 0.45 and 0.33 at varying paste volume, Alungbe et al. (1992) noted that the water-cement ratio did not show any effect on the concrete CTE. This observation was also noted by Mindness, Young, and Darwin (2002) from tests carried out on cement pastes with water-cement ratios of 0.4, 0.5 and 0.6.

2.1.6 PASTE CONTENT AND COMPOSITION

Bonnel and Harper (1950) report that the higher the paste content of the concrete, the higher its CTE; this they believe is due to the fact that the hydrated cement paste has a higher CTE than that of the aggregate constituent. Meyers (1940) also writes that the CTE appears to increase with the theoretical quantity of cement gel present if the cement gel is neither desiccated nor saturated with water. The CTE, Meyers (1940) further claims, decreases after long periods of time as the cement gel becomes a metacolloid and that any condition which accelerates this process decreases the CTE.

Works conducted by Mitchell (1953) indicated that the CTE of cement paste increases by 25 % when the cement fineness is increased from 1200 sq cm/g to 2700 sq cm/g, as shown in Figure 2.16.

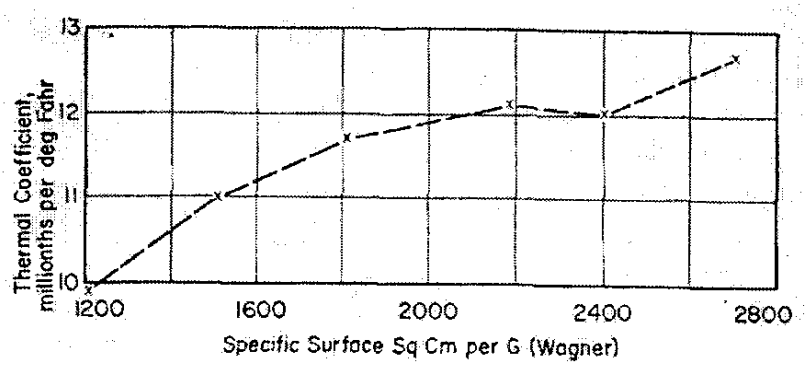

Figure 2.16: Variation of the CTE of neat cement paste with fineness (Mitchell 1953)

It is also reported by Emanuel and Hulsey (1977) that the CTE of cement paste increases by about 25 % with an increase the fineness of the cement. Since the concrete CTE depends on the aggregated constituents of the mixture and with the CTE of the cement paste being higher than that of the aggregate, an increase in the CTE of the

cement paste due to an increase in the cement fineness would consequently increase the concrete CTE. In fact, Hossain et al. (2006) have recently shown that increasing the volume of the cement paste increases the concrete CTE. However, tests conducted on concrete samples made of cement contents 508, 564, and 752 lb/yd^3 by Alungbe et al. (1992) showed no effect on the CTE.

In summary, based on the literature reviewed, the factors affecting the concrete CTE are shown in Table 2.2.

Table 2.2: Summary of the effect of variables on the concrete CTE

Variable	**Change**	**Effect on concrete CTE**	**Correlation**
Age	↑	Varies	Inconclusive
Water-Cement Ratio	↓	↑	Moderate
Moisture Content	Varies	Varies	Strong
Temperature	Varies		
Cement Fineness	↑	↑	Moderate
Paste Content	↑	↑	Strong
Coarse Aggregate Volume	↑	↑ or ↓	Strong
Coarse Aggregate Type	Quartz ↑ CaO ↑	↑ ↓	Strong
Fine Aggregate Volume	↑	↑ or ↓	Strong
Fine Aggregate Type	Siliceous ↑ CaO ↑	↑ ↓	Strong

Notation: Strong = Excellent Correlation; Moderate = Average Correlation.

↑ = Increase

↓ = Decrease

2.2 MEASUREMENT OF THE CONCRETE COEFFICIENT OF THERMAL EXPANSION

Various experimental methods have been proposed by researchers to measure the CTE of concrete. Some techniques measure directly unidirectional length changes while monitoring temperature variations. Others involve the measurement of some physical properties that are related to volumetric changes. These methods are discussed in the following sub-sections.

2.2.1 STANDARD METHOD OF TEST FOR COEFFICIENT OF THERMAL EXPANSION OF HYDRAULIC CEMENT CONCRETE - AASHTO TP 60 (2004)

This provisional test method was proposed by the American Association of State Highway and Transportation Officials (AASHTO), and it covers the determination of the coefficient of thermal expansion (CTE) of hydraulic cement concrete specimens. Since it is known that the degree of saturation of concrete influences its measured CTE, the moisture condition of the concrete specimens is controlled. Hence for this test, the specimens, 4 in. x 7 in. (100 mm x 175 mm) in size are tested in the saturated condition. This is achieved by submersion of the concrete specimen in saturated limewater at a temperature of around 73 ± 4 ^{o}F (23 ± 2 ^{o}C) for not less than 48 hours and until two successive weighings of the surface-dried sample at intervals of 24 hours show a change in weight of less than 0.5 percent. The specimen is removed from the saturation tank, and

its length and diameter are measured at room temperature to the nearest 0.004 in. (0.1 mm).

2.2.1.1 Testing Procedure

A measurement frame with the linear variable differential transformer (LVDT) attached is placed in the water bath and the bath is filled with water. A schematic of the apparatus is shown in Figure 2.17. Four temperature sensors are then placed in the bath at locations that will measure an average temperature for the water bath as a whole.

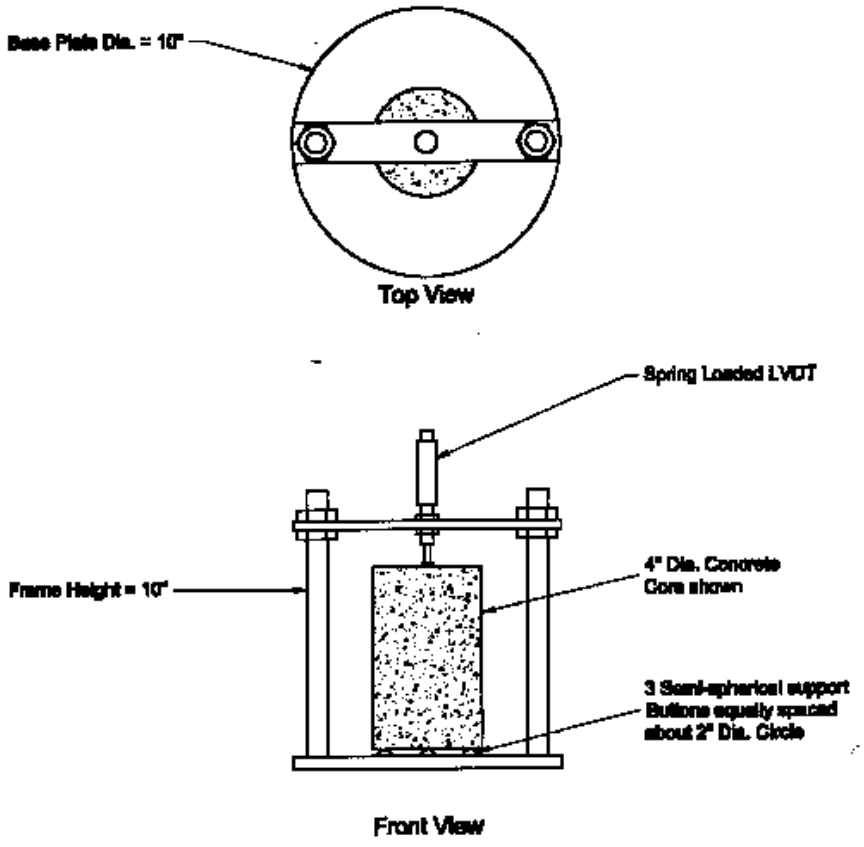

Figure 2.17: Schematic of a Measuring Frame (AASHTO TP 60 2004)

The specimen is next placed in the controlled temperature bath, making sure that the lower end of the specimen is firmly seated against the support buttons, and that the LVDT tip is seated against the upper end of the specimen (this is done taking into consideration the linear range of the LVDT over which it has been calibrated. The LVDT travel during the test should remain well within this range to ensure accurate results). The detail of the whole experimental set up used in this study is described in section 4.3.

The temperature of the water bath is set to 10 ^{o}C ± 1 ^{o}C (50 ^{o}F ± 2 ^{o}F) on the circulator, and when the bath reaches this temperature, it is allowed to remain at this temperature until thermal equilibrium of the specimen has been reached, as indicated by repeated readings of the LVDT within 0.00001 in. (0.00025 mm) taken over a one half hour time period.

The temperature readings are then recorded to the nearest 0.2 ^{o}F (0.1 ^{o}C), and the LVDT readings are also recorded to the nearest 0.00001 in. (0.00025 mm). These are the initial readings. Next the temperature of the water bath is set to 122 ^{o}F ± 2 ^{o}F (50 ^{o}C ± 1 ^{o}C). When the bath reaches this temperature, it is allowed to remain at this temperature until thermal equilibrium of the specimen has been reached. This is indicated by repeated readings of the LVDT within 0.00001 in. (0.00025 mm) taken every 10 minutes over a one half hour time period.

The temperature readings from the 4 sensors and the LVDT reading are then recorded. These form the second set of readings. The temperature of the water bath is next set to 50 ^{o}F ± 2 ^{o}F (10 ^{o}C ± 1 ^{o}C) on the circulator.

When the bath reaches this temperature, it is allowed to remain at this temperature, until thermal equilibrium of the specimen has been reached. This is indicated by repeated readings of the LVDT to the nearest 0.00001 in. (0.00025 mm) taken every 10 minutes over a one half hour time period. The temperature readings of the 4 sensors and the LVDT reading are recorded. These are the final readings.

The CTE of one expansion or contraction test segment of a concrete specimen is calculated as follows (reported in microstrain / ^{o}C):

$$CTE = \left(\Delta L_a \Big/ L_o \right) \div \Delta T \qquad \textit{Equation 2.4}$$

but, $$\Delta L_a = \Delta L_m + \Delta L_f \,, \qquad \textit{Equation 2.5}$$

Since the frame expands while the concrete specimen is expanding.

and, $$\Delta L_f = C_f \times L_o \times \Delta T \qquad \textit{Equation 2.6}$$

where,

ΔL_a = actual length change of specimen during temperature change, mm.

L_o = measured length of specimen at room temperature, mm.

ΔT = measured temperature change (average of four sensors), ^{o}C (increase = positive, decrease = negative).

ΔL_m = measured length change of specimen during temperature change, mm (increase = positive, decrease = negative).

ΔL_f = length change of measuring apparatus during temperature change, mm and

C_f = correction factor accounting for the change in length of the measuring apparatus with temperature, in /^{o}F (/^{o}C). (The derivation for the correction factor is presented in Chapter 4)

The test result is the average of the two CTE values obtained from the two test segments provided the two values are within 0.5 x 10^{-6} / ^{o}F (0.3 x 10^{-6} /^{o}C) of each other.

2.2.2 AASHTO TP 60 USING THE REGRESSION ANALYSIS METHOD

The Texas Department of Transportation (TxDOT) initiated an in-house study to identify the causes of the spalling in Continuously Reinforced Concrete Pavement (CRCP). Based on this study, Won (2005) observed that:

- The accuracy and repeatability of the AASHTO TP60 test method depends to a great extent on the stability and accuracy of the displacement readings at 50 ^{o}F (10 ^{o}C) and 122 ^{o}F (50 ^{o}C).

- The tolerance between two successive CTEs (the CTE during expansion phase or contraction phase) of less than 0.5 x 10^{-6} /^{o}F (0.3 x 10^{-6} /^{o}C) is not small enough for TxDOT to implement CTE requirements for actual paving projects.

Won (2005) further observed during these investigations of the AASHTO TP 60 test method that:

- The difference between two successive CTE tests varied significantly, and

- The displacements at 50 ^{o}F (10 ^{o}C) and 122 ^{o}F (50 ^{o}C) were not stable, which results in variability in the CTE results.

In view of these findings, Won (2005) postulated that a more accurate and repeatable CTE could be determined by using the close correlation observed between temperature and displacement changes. This correlation is shown in Figure 2.18.

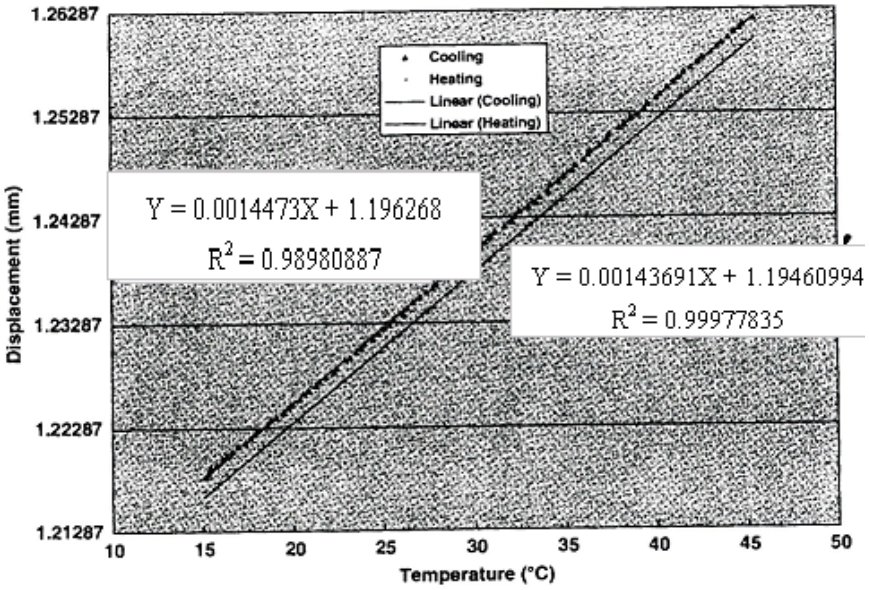

Figure 2.18: Correlation between concrete temperature and displacement (Won 2005)

The proposed revised testing procedure is presented below:

- Condition the test specimens by submerging them in saturated lime water at 73 ^{o}F ± 4 ^{o}F (23 ^{o}C ± 2 ^{o}C) for not less than 48 hours. Conditioning is complete when two successive weights of the surface dried sample taken at intervals of 24 hours show a change in weight of less than 0.5 %.

- Place a support frame for each test specimen, with LVDT attached in the water bath.

- Remove the test specimen from the saturation tank and measure its length at room temperature to the nearest 0.004 in. (0.1 mm). Record this length, L.

- Place the specimen in the measuring apparatus/frame located in the controlled temperature bath, making sure that the lower end of the specimen is firmly seated against the support buttons and that the LVDT tip is seated against the upper end of the specimen.

- Set the temperature of the water bath to 50 ^{o}F ± 2 ^{o}F (10 ^{o}C ± 1 ^{o}C).

- Record readings every minute of the LVDT (displacement), temperature, and time.

- Maintain the temperature of 50 ^{o}F ± 2 ^{o}F (10 ^{o}C ± 1 ^{o}C) for 1 hour.

- Set the temperature of the water bath to 122 ^{o}F ± 2 ^{o}F (50 ^{o}C ± 1 ^{o}C). Continue to take readings every minute of the LVDT (displacement), temperature, and time. Maintain 122 ^{o}F ± 2 ^{o}F (50 ^{o}C ± 1 ^{o}C) for 1 hour.

- Set the temperature of the water bath to 50 ^{o}F ± 2 ^{o}F (10 ^{o}C ± 1 ^{o}C). Continue to take readings every minute of the LVDT (displacement), temperature, and time. Maintain 50 ^{o}F ± 2 ^{o}F (10 ^{o}C ± 1 ^{o}C) for 1 hour.

- Plot the temperature versus displacement for each test specimen, and inspect the plot for any unusual behavior.

- Use only increasing or decreasing temperature points for the plot above. There will be two lines: one for the increasing temperature period and one for the decreasing temperature period. The lines should be basically on top of each other. Apply regression analysis between the temperature and displacement for temperature ranges of 59 ^{o}F (15 ^{o}C) to 113 ^{o}F (45 ^{o}C). Find the coefficient of determination (R^2) value for each line. The R^2 values should be greater than 0.999.

- The difference between the CTE values for the decreasing temperature period and the increasing temperature period must be less than or equal to 0.15 x 10^{-6} /^{o}F (0.3 x 10^{-6} /^{o}C). If this tolerance is exceeded, complete one or more additional test segments until two successive test segments yield CTE values within the allowable tolerance. Take the average of the two CTE values. This is the CTE value for the cylinder/concrete specimen.

These improvements in the AASHTO TP 60 testing method were evaluated by researchers (Kohler, Alvarado, and Jones 2007) at the University of California Pavement Research Center (UCPRC), Davis. These researchers found out using the TxDOT modified method that CTE results were on average slightly higher by about 0.09 x 10^{-6} /^{o}F (0.16 x 10^{-6} /^{o}C) than results obtained at Federal Highway Administration's (FHWA) Turner Fairbanks Highway Research Center Laboratory and at the concrete materials laboratory at TxDOT.

2.2.3 VIBRATING WIRE EXTENSOMETER METHOD

This test method was developed by Kada et al. (2002) to monitor the evolution of the CTE as a function of time from the beginning of hardening. This test method is particularly suitable for the early ages of concrete, especially during cement hydration.

The test is carried out on two replicate samples of concrete to be studied. Samples are cast in PVC molds of 4 in. x 4 in. x 16 in. (100 mm x 100 mm x 400 mm). Before the concrete is placed in the mould, a vibrating wire extensometer is installed at the center of the sample along its longitudinal axis as shown in Figure 2.19 and connected to a data acquisition system that monitors the strain and temperature variations within the specimen.

Demolding of the specimens is done just as the concrete begins to set (i.e. at the moment when the material is of the right consistency for demolding). The samples thereafter are wrapped in plastic bags to prevent any moisture exchange with the environment. One sample is then immersed in heat-controlled water bath set at a temperature of 122 ^{o}F (50 ^{o}C) and the other, is immersed in a bath of temperature 50 ^{o}F (10 ^{o}C), respectively.

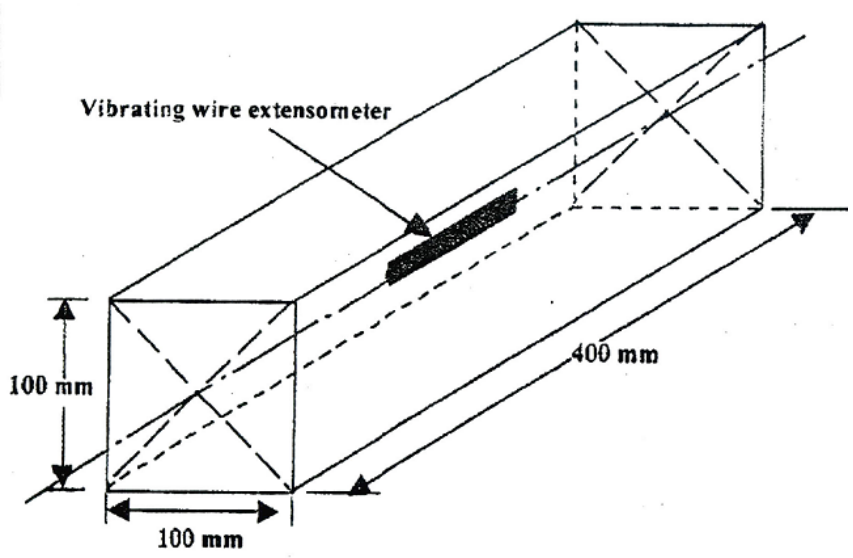

Figure 2.19: Schematic representation of the test sample (Kada et al. 2002)

Once a stable temperature is reached within the samples, each of the samples is subjected to a thermal shock of the order of 72 ^{o}F (40 ^{o}C). The samples are swapped in the water baths and less than an hour separates each thermal shock administered. A length of steel wire was stretched between two brackets that are in direct contact with the concrete in which the sensor is encased. Distortion of the concrete affects the extensometer, causing the distance between the two brackets to vary, resulting in a variation in the wire tension. The tension is measured by determining the resonant frequency of the wire. Afterwards, the gage factor, K, and the resonant frequency, F, of the wire, are used to obtain the gross strain according to the following equation:

$$\varepsilon_g = K \times F^2 \times 10^{-3} \qquad \textit{Equation 2.7}$$

The body of the vibrating wire extensometer is made of steel, whose CTE differs from that of the concrete, which results in a small error in the frequencies that are registered.

Consequently, corrections must be made to the gross strain values to eliminate the strain caused by the differences in the thermal expansion coefficients. The total deformation recorded by the sensor is equal to:

$$\varepsilon_{total} = \varepsilon_{Plastic} + \varepsilon_{drying} + \varepsilon_{carbonation} + \varepsilon_{thermal} + \varepsilon_{autogeneous} \qquad \textit{Equation 2.8}$$

where,

$\varepsilon_{plastic}$ = the shrinkage due to the evaporation of water from the fresh concrete when it is still at the plastic state.

ε_{drying} = the shrinkage caused by the evaporation of water from capillary pores in the hardened concrete.

$\varepsilon_{carbonation}$ = the shrinkage caused by the reaction of the hydrated cement paste with the carbon dioxide in the air when humidity is present.

$\varepsilon_{thermal}$ = the thermal deformation linked to the expansion and contraction of the mass accompanying cement hydration. This deformation accounts for both the concrete and the vibrating wire sensor.

$\varepsilon_{autogeneous}$ = the deformation caused by the reduction of available water for hydration because of the hydration process itself. In the course of this study, the duration of the thermal expansion coefficient measurement being less than one hour, at first approximation, this deformation can be neglected in this interval of time.

Therefore, under the experimental conditions for this study, the deformation corresponding to the thermal shock, during which a temperature variation of ΔT occurs is represented by:

$$\varepsilon_{total} = \varepsilon_{thermal} = \alpha_c \Delta T + \alpha_e \Delta T \qquad \textit{Equation 2.9}$$

where,

α_c and α_e = the CTE of the concrete and the vibrating wire extensometer respectively. Thus:

$$\alpha_c = \frac{\varepsilon_{total} - \alpha_e \Delta T}{\Delta T} \qquad \textit{Equation 2.10}$$

2.2.4 ENVIRONMENTAL EXTENSOMETER METHOD

This test method was developed by Ndon (1990) for hardened concrete cores in the laboratory. The apparatus is as shown in Figure 2.20. The concrete core is placed in the environmental chamber and heated to a temperature of about 140 ^{o}F (60 ^{o}C) or cooled to 7 ^{o}F (-14 ^{o}C). Heating and cooling were accomplished by circulating methanol from a controlled-temperature bath through a coil around each core as shown. Temperatures in the concrete cores, and thermal elongation, ΔL, were recorded every 10 minutes by a data acquisition system.

The CTE is calculated from the formula:

$$\alpha_c = \frac{\Delta L}{\Delta T \times L_i} \qquad \textit{Equation 2.11}$$

Where,

α_c = the CTE of concrete

ΔT = temperature change (^oF)

ΔL = change in length of concrete specimen (in.)

L_i = initial length of concrete specimen (in.)

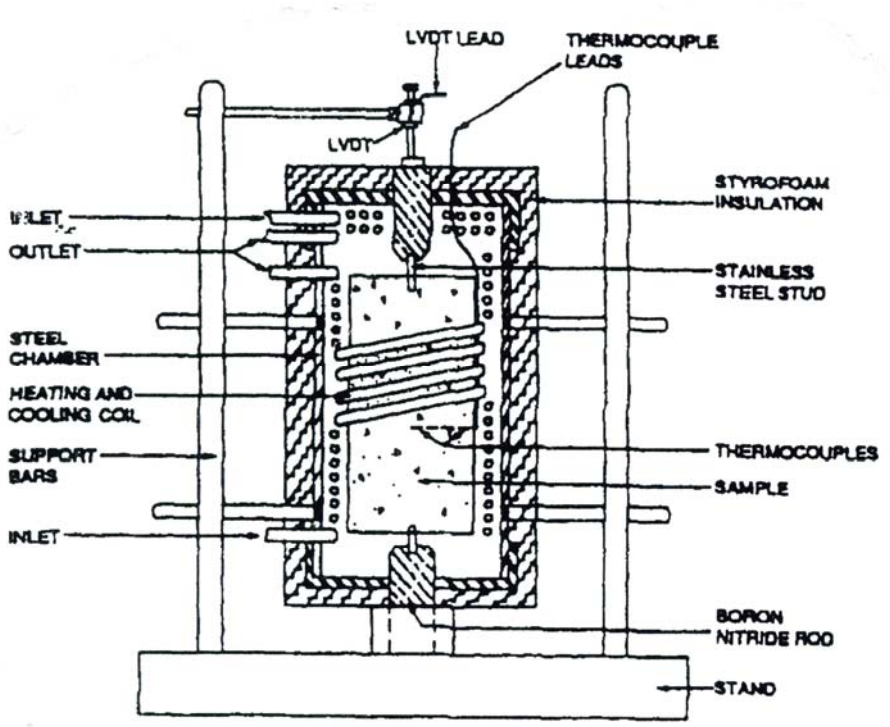

Figure 2.20: Environmental Extensometer (Ndon 1990)

2.2.5 LOUBSER AND BRYDEN APPARATUS

This method was developed by Loubser and Bryden (1972). The apparatus used is able to measure the CTE of rocks, mortar, and concretes. The apparatus is as shown in

Figure 2.21. The base plate is an aluminum casting, measuring 14 in. x 14 in. x 2 in. (350 mm x 350 mm x 50 mm), except for a longitudinal center section 1.5 in. (38 mm) wide and a wall thickness all round of 0.5 in. (12.5mm). On the left are shown the oven and its container and the fused silica tube supporting the specimen. This tube passes through a hollow aluminum cylinder. Tap water passes through this cylinder at a rate of 150 ml per minute, cooling the fused tube and preventing heat flow from the oven to the base of the apparatus. Two neoprene O-rings serve to secure the fused silica tube to the aluminum cylinder and prevent water leakage from the specimen chamber. The aluminum cylinder for the cooling water has a shoulder at its upper end. This shoulder and an encircling threaded and knurled ring serve to clamp the two concentric brass tubes to the cylinder. A third O-ring seals the base of the tubes to the aluminum cylinder. This arrangement permits measurements to be made on the specimen immersed in water. The inner of the two concentric tubes is the specimen chamber, and the annulus between the two tubes contains the oven.

The heat flow from the oven to the specimen is thus across the inner tube, and this improves the even distribution of heat over the specimen. A hollow aluminum cap, with steps and recesses machined in its lower face to fit the brass tubes and oven, encloses the top of this section of the apparatus. The center of the cap has a hole serving as a guide for a solid silica rod 2.6 in. (66 mm) long by 0.2 in. (5 mm) in diameter. This rod rests on the top of the specimen being measured, and transmits the movement of the specimen to the Invar beam above it.

Through three more holes in the cap at appropriate radii, rods of fused alumina are passed. These carry and insulate the temperature thermocouple leads, the control thermocouple leads, and the leads to the oven winding.

Beneath the left hand side of the Invar beam, which is 12 in. (300mm) long by 0.16 in. (4 mm) thick, and is machined to a symmetrical shape as shown in Figure 2.21, there is a fixed Invar disc which presses onto the silica rod, which touches the specimen.

A wedge fixed to the center of the beam fits into a V in the silica tube in the center of the apparatus. This V is formed by heating the tube and pressing it while still plastic onto a hard steel section. A silica rod carrying the slug of the linear variable differential transformer (LVDT) hangs from the right side of the beam. The LVDT is a solid state device with the transformer, the oscillator, the demodulator and its amplifier all contained in a metal cylinder 1.8 in. (45mm) long by 0.8 in. (20 mm) in diameter. The output from the LVDT is proportional to the expansion of the specimen. This output is attenuated 24dB by a voltage divider, and after passing through a zero suppressor, it is fed to the recorder.

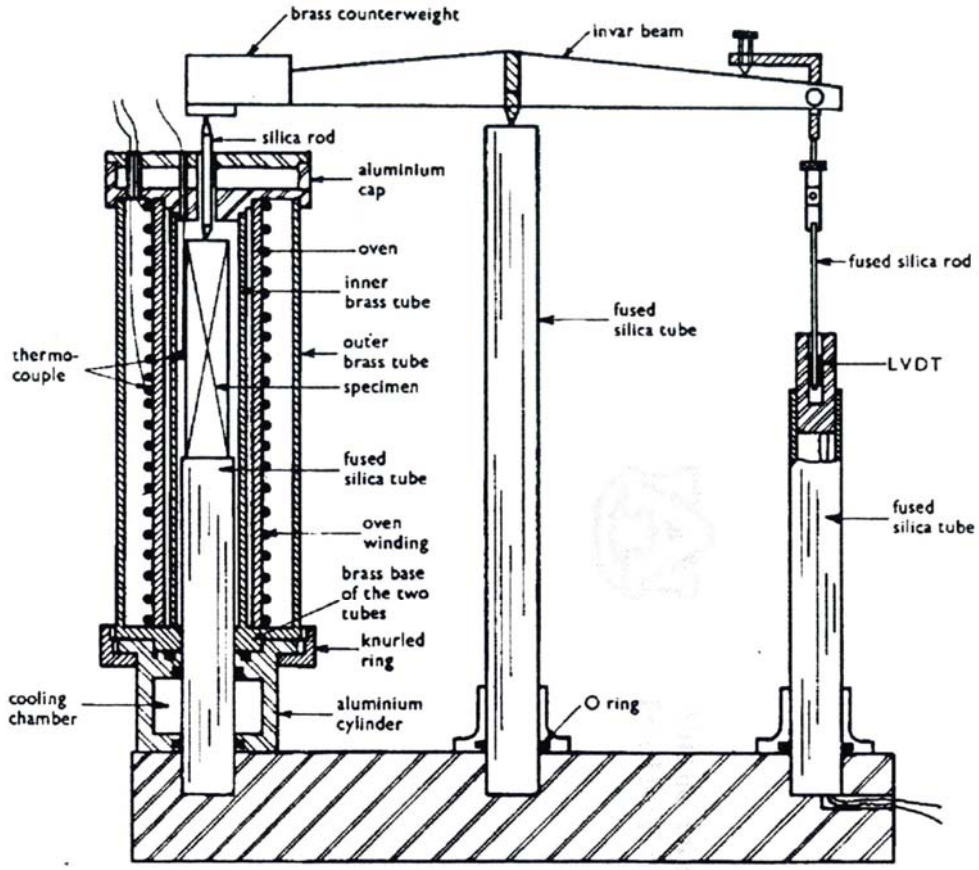

Figure 2.21: Cross section of the apparatus (Loubser and Bryden 1972)

2.2.6 ZIEGELDORF, KLEISER AND HILSDORF METHOD

The apparatus for the determination of the thermal expansion coefficient of the concrete consists of a steel vessel equipped with three LVDTs as shown schematically in Figure 2.22. The vessels are capable of being sealed for testing saturated samples. In running the experiment, the vessel containing the sample is heated to 356 ^{o}F (180 ^{o}C) in increments of 54 ^{o}F (30 ^{o}C) per hour. Expansion of the vessel is taken into account by proper calibration. A plot is then made of the strain against the temperature rise. The slope is determined as the expansion coefficient of concrete. This procedure is applied in Figures 2.23 (a) and (b) for determining the thermal expansion coefficient of concrete.

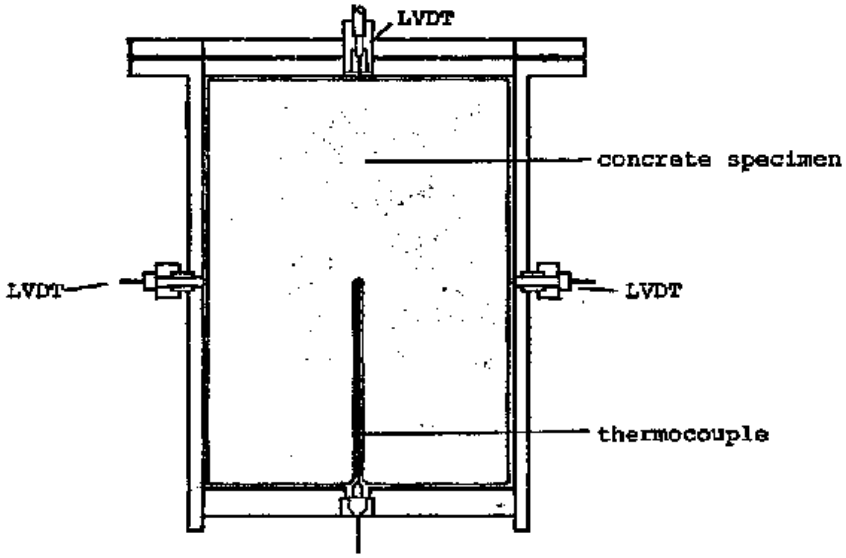

Figure 2.22: Cross section of apparatus for measuring thermal expansion of concrete (Ziegeldorf, Kleiser and Hilsdorf 1978)

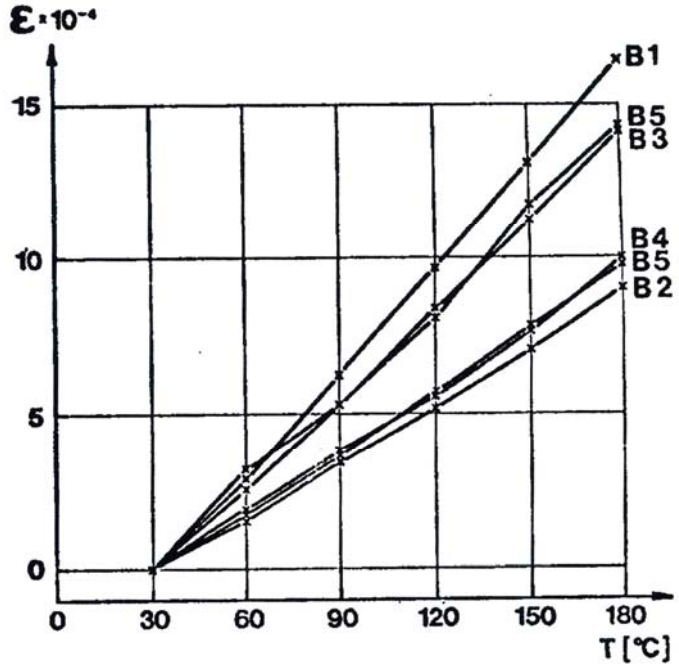

Figure 2.23: (a) Effect of temperature on the thermal expansion of dry concrete specimens (Ziegeldorf, Kleiser and Hilsdorf 1978)

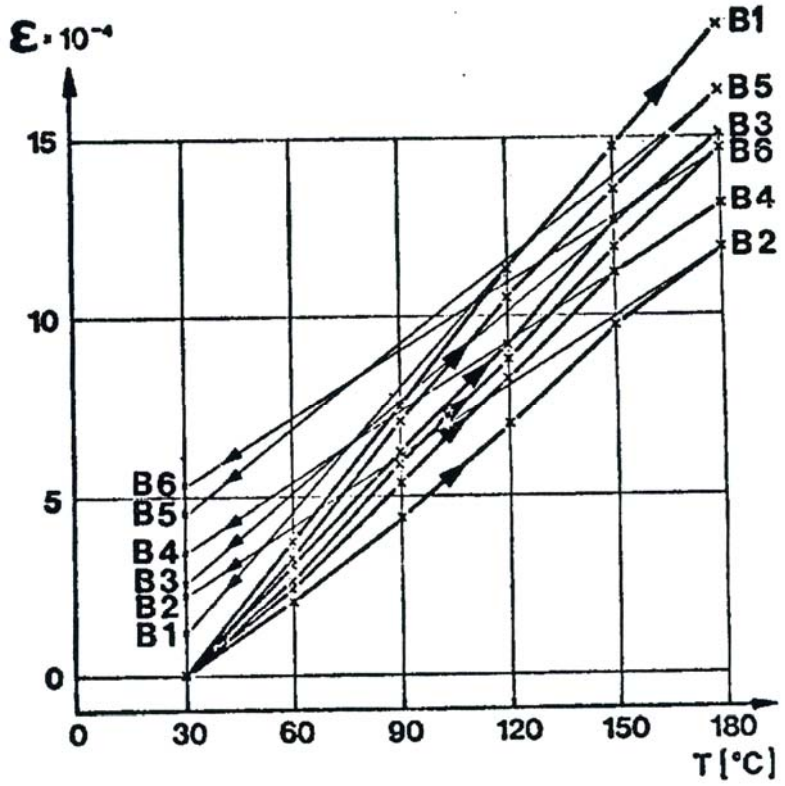

Figure 2.23: (b) Effect of temperature on the thermal expansion of sealed concrete specimens (Ziegeldorf, Kleiser and Hilsdorf 1978)

2.3 MODELS FOR CALCULATING THE CONCRETE COEFFICIENT OF THERMAL EXPANSION

In this section, models for determining the CTE are presented and also discussed.

2.3.1 EMANUEL AND HULSEY'S MODEL

From literature (Meyers 1950; Mitchell 1953; Bonnel and Harper 1950 and Detling 1964) and experimental works conducted by Emanuel and Hulsey (1977), it is noted that:

- The concrete CTE is dependent upon the volumetric weighted average of its ingredients.

$$\text{I.e. } \beta_P + \beta_{FA} + \beta_{CA} = 1.0 \qquad \textit{Equation 2.12}$$

Where,

β_P = Proportion by volume of hardened cement paste (ratio)

β_{CA} = Proportion by volume of coarse aggregate (ratio)

β_{FA} = Proportion by volume of fine aggregate (ratio)

- The CTE is lowest for saturated concrete, is slightly higher for oven dry concrete, and is a highest, at some partially dry condition. The maximum value for the partially dry state is approximately 15 % higher than for the saturated state and is dependent upon the proportion of aggregate present in the concrete.

It is noted in the works of Meyers (1950) that the dependency of the concrete CTE on moisture and age is mainly due to the presence of the paste content in the concrete. Hence, in arriving at the CTE for the paste, correction factors f_A and f_M will have to be applied to the original (saturated) paste CTE to account for age and moisture dependency.

Hence,

$$\alpha_P = f_M f_A \alpha_S \qquad \textit{Equation 2.13}$$

From equations 2.12 and 2.13 above, we have:

$$\alpha_C = f_T\left[f_M f_A \beta_P \alpha_S + \beta_{FA}\alpha_{FA} + \beta_{CA}\alpha_{CA}\right] \qquad \textit{Equation 2.14}$$

Where,

α_C= Concrete CTE (in./in. /^{o}F)

α_S = CTE of saturated paste (in./in. /^{o}F)

α_{FA} = CTE of fine aggregate (in./in. /^{o}F)

α_{CA} = CTE of coarse aggregate (in./in. /^{o}F)

f_A = Correction factor for age

f_M = Correction factor for moisture

f_T = Correction factor for temperature

2.3.2 CHEM 2 MODEL

In Texas Department of Transportation Project 422/1244, a methodology is presented for improving the predictive ability of oxide based chemical models that predict aggregate material properties using the chemical composition of the coarse aggregate. Because portland cement concrete is composed of 70 % to 85 % coarse and fine aggregates, by weight (Dossey, McCullough, and Dumas 1994), the aggregate material properties have a profound effect on the material properties of the finished concrete and ultimately on pavement and bridge deck performance. An existing computer program, CHEM 1 has been used to estimate these concrete properties (compressive and tensile strength, elastic modulus, and drying shrinkage) through stochastic models based

on user input oxide residues. This approach, although adequate for some applications, suffers from the fact that concrete properties are influenced more by the mineralogy of the aggregate than by the oxides formed from their decomposition (Dossey et al. 1994). Using stoichiometric analysis, the new computer program CHEM 2 back-calculates the original mineral composition from the oxides and thereby improves the accuracy of the models.

With the mineral contents determined, Dossey et al. (1994) used regression to model the CTE as a function of mineral content in the sample as follows:

$$\alpha_C = e^{1.098}.(quartz)^{0.486}.(calcite)^{-0.106}.(dolomite)^{0.415}.(PF)^{-2.37}.(albite)^{1.635} \qquad \textit{Equation 2.15}$$

Where,

Quartz = percent quartz by weight (ratio)

Calcite = percent calcite by weight (ratio)

Dolomite = percent dolomite by weight (ratio)

PF = percent potassium feldspar by weight (ratio)

Albite = percent albite by weight (ratio)

FS = albite + PF, all feldspars by weight (ratio)

α_C = CTE (microstrain /^{o}F)

This model was developed for eight Texas aggregates used in the analysis; however, it provides reasonable predictions in most cases for additional aggregates (Dossey et al. 1994). The eight aggregates are shown in Table 2.3.

Table 2.3: Eight Texas aggregates used in developing the model (Dossey et al. 1994)

Source	Aggregate Type
McKelligan #1	Dolomite
Western – Tascosa	Siliceous River Gravel
Bridgeport + TinTop	Limestone + Siliceous River Gravel
Feld (TCS)	Limestone
Fordyce	Siliceous River Gravel
Vega	Siliceous River Gravel
Ferris #1	Limestone
Scotland	Granite

2.3.3 NEVILLE AND BROOKS MODEL

In their book *Concrete Technology*, Neville and Brooks (1987) report that the CTE value for concrete depends on both its composition and on its moisture condition at the time of temperature change. The influence of mixture proportions, they noted, arises from the fact that the two main constituents of concrete, cement paste and aggregate,

have dissimilar CTE. The concrete CTE is affected by these two values and also by the volumetric proportions and elastic properties of the two constituents.

The concrete CTE, $\alpha_{c,}$ is related to the thermal coefficient of aggregate, $\alpha_{g,}$ and of cement paste, $\alpha_{P,}$ as follows:

$$\alpha_C = \alpha_P - \frac{2g(\alpha_P - \alpha_g)}{1 + \frac{k_P}{k_g} + g\left[1 - \frac{k_P}{k_g}\right]} \qquad \textit{Equation 2.16}$$

Where,

g = volumetric content of aggregate, and

$\frac{k_p}{k_g}$ = stiffness ratio of cement paste to aggregate, approximately equal to the ratio of their moduli of elasticity.

The models predicted by Emanuel and Hulsey (1977) and Neville and Brooks (1987) are represented in Figure 2.24. Table 2.4 shows the aggregate CTE values used and their sources. From this figure, it is apparent that, for a given type of aggregate, an increase in its volume concentration reduces the concrete CTE, while for a given volume concentration, a lower aggregate CTE also reduces the concrete CTE. It is realized from the plots that, for a mixture of river gravel and limestone, in a ratio of 60 % to 40 %, the Emanuel and Hulsey model (E & H model) predicts a higher value than the Neville and Brooks model (N & B model).

Table 2.4: Aggregate CTE values used for developing Figure 2.24

Aggregate Type	CTE Value	Units	Source
Siliceous River Gravel (SRG)	6.80×10^{-6}	/°F	Emanuel and Hulsey(1977)
Limestone (LS)	3.30×10^{-6}	/°F	Mindess,Young and Darwin (2002)
Cement Paste	1.00×10^{-5}	/°F	Mindess,Young and Darwin (2002)

Where,

N & B Model = Neville and Brooks's Model

E & H Model = Emanuel and Hulsey's Mode

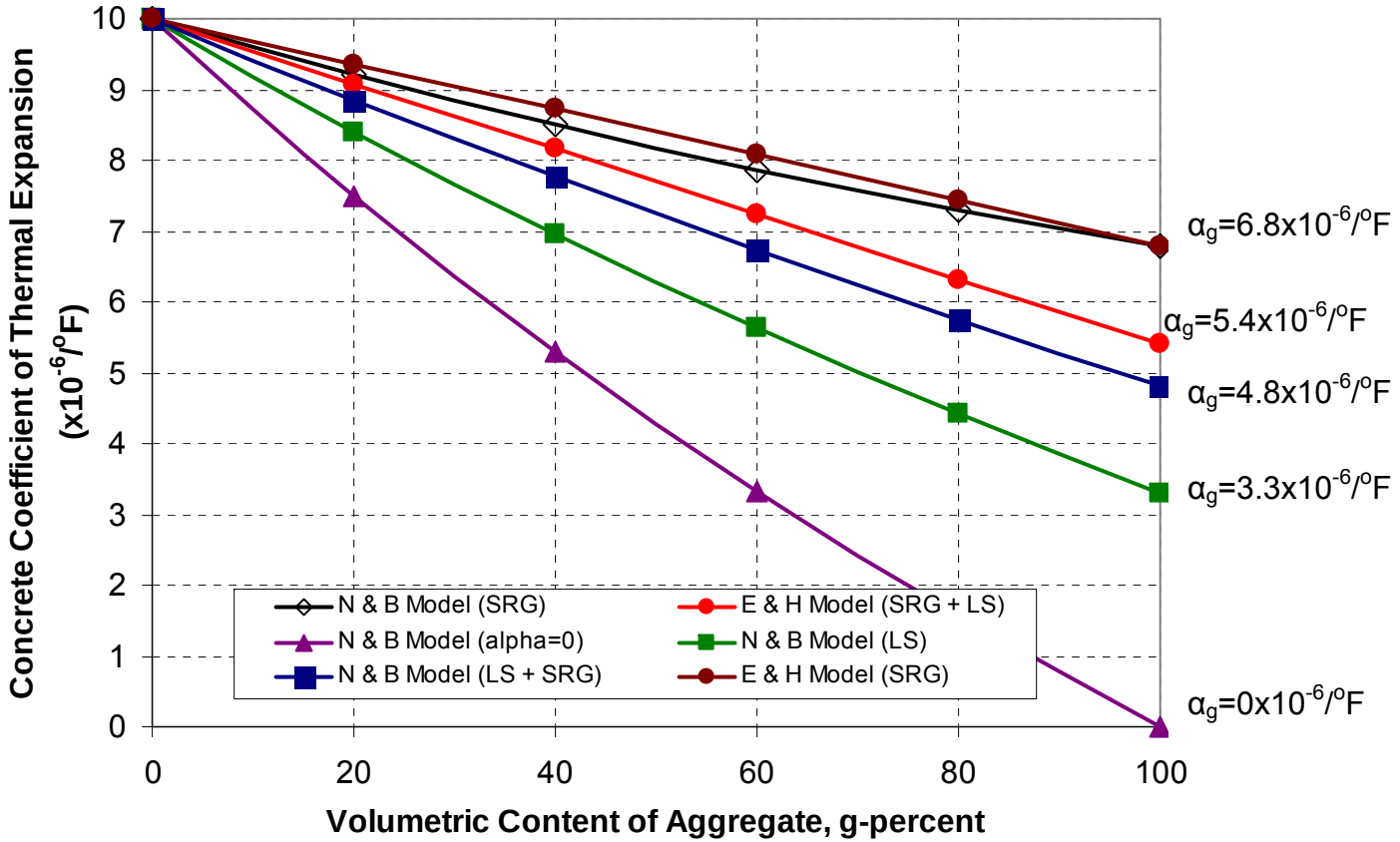

Figure 2.24: Influence of volumetric content of aggregate and of aggregate type on linear CTE of concrete using Neville and Brooks Model as well as the Emanuel and Hulsey Model

CHAPTER 3

SUMMARY OF THE GEOLOGY OF ALABAMA RELEVANT TO CONCRETE AGGREGATES

The geology of Alabama is briefly summarized in this section. The importance of knowledge of the geology to this study is also covered. The major aggregate types commonly used in the Alabama concrete industry are presented and discussed here.

3.1 IMPORTANCE OF THE KNOWLEDGE OF GEOLOGY

Concrete is known to comprise about 70 % to 80 % by volume of aggregates (Emanuel and Hulsey 1977). The type (mineralogical content and source) and the amount of an aggregate used in a concrete mixture have the greatest influence on the coefficient of thermal expansion (CTE) of the concrete (Mindess, Young, and Darwin 2003; Emanuel and Hulsey 1977, and Dossey et al. 2002). It is thus important to evaluate the source and mineralogical composition of these aggregates. This will help predict with a greater accuracy the CTE for the concrete sample being used. An adequate prediction of the CTE will help in the design of concrete bridge decks and pavements that are exposed to ambient temperature.

With a proper evaluation of the sources and mineral content of the aggregates, it becomes easier to understand, for instance, why limestone from different quarries in Alabama could give different values of the CTE when used in a concrete mixture.

3.2 GENERAL GEOLOGY OF ALABAMA

The word “geology” is made up of two ancient Greek words, namely, “geo” and “logos”. Geo means “the earth,” and logos mean “the study of” (Daniel et al. 1966). Therefore, geology can be interpreted to mean “the study of the earth.” Daniel et al. (1966) in their book, *Rocks and Minerals of Alabama,* therefore, write that the study of rocks and minerals is only one phase of the science of geology.

There are three principal geologic areas in Alabama, each with its own characteristic rocks and geologic structure (Daniel et al. 1966). These areas are shown on the map of Alabama in Figure 3.1. The oldest rocks in Alabama occur in the Piedmont area, or the east-central part of the state. The next oldest rocks occur in the Paleozoic area in north Alabama, and the young and unconsolidated rocks occur in the Coastal Plain area, or in south and west Alabama (Daniel et al. 1966). Following is a brief description of these geologic areas of Alabama.

3.2.1 PIEDMONT AREA

Investigations conducted by Daniel et al. (1966), reveal that the Piedmont area is underlain by igneous and metamorphic rocks. These rocks lie in the northeastward-trending belts and are highly deformed and complexly faulted. To the south and over lapping these rocks are the younger rocks of the Coastal Plain area. The sedimentary rocks of the Paleozoic area lie to the northwest of the Piedmont area. Most of the igneous and metamorphic rocks of the Piedmont area according to Daniel et al. (1966) are granite, schist, diorite, gneiss, pegmatite, slate, phyllite, quartzite, and marble.

Adams et al. (1926) also report in their book, *Geology of Alabama,* that the Piedmont area corresponds in extent to the area of crystalline rocks. They further write that this area exhibits two rather distinct topographic divisions. The lower division, which is called the Opelika Plateau, occupies the area underlain by the Archean rocks. The higher topographic division of the Piedmont area is the Ashland Plateau, which is diversified by ridges. The Ashland Plateau is the mountainous portion of the Piedmont and includes Cheaha Mountain, the highest point in the State of Alabama.

3.2.2 Paleozoic Area

Daniel et al. (1966) report that the Paleozoic area is underlain predominantly by hard, sedimentary rocks. In the northeastern part of Alabama, these layers of rock have been pushed into upfolds, or anticlines, and downfolds, or synclines. While these rocks were being pushed gradually into upfolds, they fractured along the crests and allowed water to seep into the cracks and start erosion. After a long period of time, streams eroded the anticlines into valleys. The rocks in the synclines did not fracture and erode like the anticlines; therefore, the synclines have now become mountains. These rocks are made up of layers of limestone, dolomite, shale, sandstone, conglomerate, and coal.

3.2.3 Coastal Plain Area

According to Daniel et al. (1966), the Coastal Plain area is underlain by rocks similar to those in the Paleozoic area, except that they are much younger and most of them are soft and unconsolidated. They further write that these younger rocks overlie the rocks of the Paleozoic and Piedmont areas. The oldest strata of the Coastal Plain rocks lie on top of and are in contact with the youngest strata of Paleozoic rocks. They claim these Coastal Plain rock formations were deposited layer upon layer, and traveled southward

from the Paleozoic area to the beaches of Baldwin County, and crossed outcrops of the oldest to the youngest Coastal Plain sedimentary rocks. These rocks consist of limestone, shale or clay, sandstone or sand, gravel or conglomerate, and lignite. Additionally, there are some rocks which are also a mixture of these rock types.

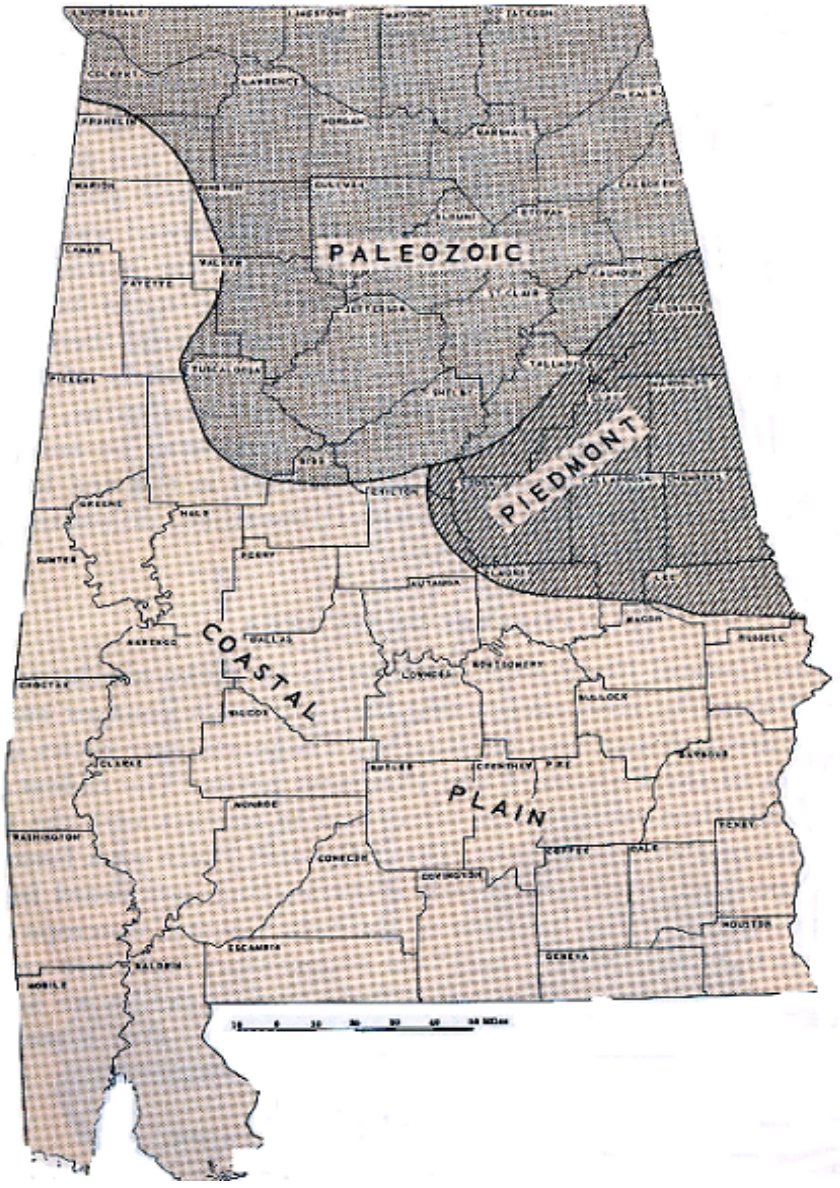

Figure 3.1: Geologic areas of Alabama (Daniel et al. 1966)

3.3 MAJOR ROCK TYPES / FORMATIONS FOUND IN ALABAMA

3.3.1 INTRODUCTION

There are three kinds of rocks that make up the crust of the earth: igneous rocks, metamorphic rocks, and sedimentary rocks. A rock is mainly a mixture of particles or grains of two or more minerals. A mineral is any naturally occurring inorganic substance having a characteristic chemical composition, usually possessing a definite crystalline structure (Daniel et al. 1966).

3.3.1.1 Igneous Rocks

Igneous rocks originate far below the surface of the earth in the form of molten material, or magma. Activated by crystal movements, the magma flows and fills openings in the crust of the earth. As it cools, mineral crystals are formed; the size of the crystals depends on the rate of cooling (Daniel et al. 1966).

Igneous rocks in Alabama occur in the eastern part of the state. The granites in Randolph, Tallapoosa, Clay, and Coosa Counties are believed by some geologists to be of igneous origin. Diabase dikes in Chambers, Lee, and Tallapoosa Counties are also thought to be of igneous origin (Daniel et al. 1966).

3.3.1.2 Metamorphic Rocks

Metamorphic rocks are produced by the action of heat, pressure, crustal movements, and the chemical action of liquids and gases acting on igneous, sedimentary, or other metamorphic rocks (Daniel et al. 1966). Most metamorphic rocks do not show

the structure of the original igneous or sedimentary rocks. The schist, gneiss, phyllite, slate, and marble of eastern Alabama are typical metamorphic rocks (Daniel et al. 1966).

3.3.1.3 Sedimentary Rocks

The grains and particles that make up sedimentary rocks may have come from igneous, metamorphic, or other sedimentary rocks themselves. The original rocks exposed on the surface of the earth are gradually worn or eroded by the forces of nature, such as temperature change, rain, wind, and running water. Small particles of rock, and often large boulders, are transported by streams and wind to the ocean or other large bodies of water, where they are deposited layer upon layer. These layers of sediment may accumulate into rocks many thousands of feet thick (Daniel et al. 1966).

The major rock formations found in Alabama, according to Adams et al. (1926), can be further grouped into four main categories: Crystalline rock, Paleozoic rock, Mesozoic rock and Cenozoic formations.

3.3.2 CRYSTALLINE ROCKS

These rocks occur in the area generally corresponding in extent to the Piedmont Upland and to some extent, parts of the coastal plains. According to Adams et al. (1926) the Piedmont Upland at the south east is underlain by igneous rocks and crystalline schist, mainly of the Archean and Algonkian ages which are thrust-faulted and have a very complex structure. The Piedmont Upland, as earlier reported, exhibits two rather distinct topographic divisions: one being the lower division which is called the Opelika Plateau which occupies the area underlain by the Archean rocks. These Archean rocks consist principally of schists and gniesses, which have in general the chemical

composition of igneous rocks. Typical rocks of the Algonkian age reported by Adams et al. (1926) include: Ashland mica schist, Hollis quartzite, and Chewacla marble, etc. In the coastal plain, the crystalline rocks constitute a part of the floor on which the formations of the coastal plains were deposited, but have been reduced to a generally even surface.

3.3.3 PALEOZOIC ROCKS

The term "Paleozoic" means ancient life. Adams et al. (1926) write that the Paleozoic rocks of Alabama include the great succession of phyllite, slate, shale, sandstone, conglomerate, dolomite, and limestone formations that were accumulated during the Paleozoic era.

The Paleozoic rocks occupy an area in the northern part of Alabama. In its general relations, the Paleozoic area of Alabama, which houses the Paleozoic rocks, falls into the large geographic division of the eastern United States known as the Appalachian highlands which extends from the Coastal Plain on the east to the Interior Lowlands of the Mississippi valley region on the west (Adams et al. 1926). The Appalachian highlands comprise the Appalachian Mountains, Appalachian Valley, and the Appalachian Plateaus (Adams et al. 1926).

Adams et al. (1926) reports that the Appalachian Mountains occupy an area well outside of Alabama, from northern Georgia to southern Virginia, and it reaches a maximum breadth of 75 miles in southeastern Tennessee and southwestern North Carolina.

The rocks of the Appalachian valley are of sedimentary origin, such as shale, sandstone, and limestone, which preserve their original stratification and have not undergone any more metamorphism than the change of limestone to marble on a

relatively small scale. There have also been such slight mineralogical changes as might accompany the development of the slaty cleavage (Adams et al. 1926).

West of the Appalachian Valley lies the Appalachian Plateau; like the valley, the plateau region extends from Alabama to New York (Adams et al. 1926).

The rocks of the Appalachian Plateau and of the Highland Rim in Tennessee Valley consist of limestone, sandstone, and shale as in the Appalachian Valley. But unlike the rocks of the valley they are in most of the plateau areas and slightly deformed from their original horizontal attitude. The exceptions are along the anticlinal Big Wills and Sequatchie valleys and along the margins of Lookout and Sand Mountains in which some of the strata are sharply upturned to steeply inclined or even to vertical attitudes (Adams et al. 1926).

3.3.4 MESOZOIC ROCKS

Adams et al. (1926) write that the upper cretaceous formations of Alabama, which developed to form the Mesozoic rocks, crop out from the northern part of the coastal plain province in a belt 50 miles to 75 miles wide, which trends westward in the eastern part of the state and swings around to northwestward in the western part of the state. The Upper Cretaceous formations are composed of sedimentary deposits, including beds of sand, gravel, clay, and chalk, most of which were deposited in relatively shallow marine waters. However, some of the coarser, more irregularly bedded parts were deposited by streams on low plains that bordered the coast.

The Mesozoic rocks developed as a result of the deposition of sediments from streams. These deposits presented here developed into four formations: the Tuscaloosa Formation, Eutaw Formation, Selma Chalk, and Ripley Formation (Adams et al. 1926).

3.3.5 CENOZOIC FORMATIONS

Adams et al. (1926) write that the Cenozoic era in Alabama is divided into various epochal formations such as, the Eocene, Oligocene, Miocene, Pliocene, Pleistocene, and recent epochs. All the Cenozoic formations except certain comparatively young river terrace deposits are confined to the coastal plain. Most of the deposits formed during the Cenozoic era were laid down on the bottom of the sea as sand, clay, mud, or calcareous ooze and many of them include different kinds of sea shells, sea urchins, or other marine fossils. However, a few show evidence of having been formed in swamps, marshes, lagoons, or on floodplains.

3.4 DESCRIPTION OF ROCKS COMMONLY USED IN THE ALABAMA CONCRETE INDUSTRY

This section describes the characteristics and properties of the commonly used rocks in the Alabama concrete industry. The most commonly used rocks in the Alabama concrete industry include granite, dolomite, limestone, and gravel.

3.4.1 GRANITE

Daniel et al. (1966) describe granite as a light-colored, medium- to fine-grained rock composed of feldspar, quartz, muscovite, and either hornblende augite or biotite. The minerals are usually well mixed together, having a “salt and pepper” appearance. Exposures of granite show smooth erosional surfaces and thus resemble exposures of diorite and gneiss. Upon chipping a small fragment from the outcrop, identification can be made easily because of color and composition. The color of granitic rocks varies from white to reddish gray to gray, depending on the percentage of the various minerals

present. This (mineral content) is one reason why granites from different sources may impact differently on the value of the concrete CTE.

Granitic rocks, according to Daniel et al. (1966), have been interpreted by many petrologists as being the last products of igneous activity; however, some studies indicate that many granitic rocks previously interpreted as igneous in origin are really metamorphic rocks representing a higher degree of metamorphism than gneiss. The Piedmont area of Alabama has many examples of metamorphic granite. Granitic rocks are very hard and durable and are hence used in many building applications. Daniel et al. (1966) report that granites may be collected from the following counties and localities in Alabama:

Table 3.1: Granite locations in Alabama (Daniel et al. 1966)

COUNTY	AREA
Coosa	Thomas Crossroad area
Tallapoosa	Alexander City area
Clay	Ashville area

3.4.2 DOLOMITE

Dolomite, according to Daniel et al. (1966), is a rock having a variable mixture of calcium and magnesium carbonate. It can be quickly distinguished from limestone by application of cold hydrochloric acid; dolomite is only slightly effervescent in acid,

whereas limestone is highly effervescent. True dolomite will only effervesce in hot hydrochloric acid. Dolomite varies from cream white to black and usually has a coarse crystalline texture.

Dolomite has a widespread occurrence in the sedimentary strata of the Paleozoic area of Alabama. It is believed to have originated through the transformation of limestone by magnesium-bearing solutions. Dolomite can be used as a road pavement material. Dolomite may be collected from the following locations in Alabama (Daniel et al. 1966):

Table 3.2: Dolomite locations in Alabama (Daniel et al. 1966)

COUNTY	AREA
Lee	Auburn area, Chewacla State Park
Jefferson	Irondale area, Dolcito quarry, North Birmingham area, Ketona area
Shelby	Montevallo area
Talladega	Sylacauga area

3.4.3 LIMESTONE

Limestone is a sedimentary rock mostly composed of calcium carbonate and contains varying amounts of impurities (Daniel et al. 1966). Often limestone is associated with dolomite, the calcium magnesium carbonate. The two carbonate rock minerals can be quickly distinguished by the application of cold dilute hydrochloric acid; limestone will effervesce briskly, whereas dolomite will, but very slightly. Limestone varies in

color from snow white to black and in texture from very fine grained to very coarse grained also depending on the mineralogical composition (Daniel et al. 1966). This also explains why limestone from different sources may produce concretes with different CTE values.

Daniel et al. (1966) further report that limestone is of organic origin, being composed of calcareous remains of foraminifers, corals, mollusks, and other ocean life which occur as fossils in the limestone. Other limestone is deposited directly from solution and is generally found in veinlets and in other rocks as stalactites and stalagmites. Limestone is generally graded and classified according to the texture and impurities. Limestone is used in many applications such as: cement, brick, and building stones, and in steel making.

Limestone and dolomite are found in great quantities and are quarried in the northern parts of Alabama in the Paleozoic area. Specimens of limestone can be found in the counties and areas listed in Table 3.3.

Table 3.3: Limestone locations in Alabama (Daniel et al. 1966)

COUNTY	**AREA**
Franklin	Russellville area
Crenshaw	Luverne area
Limestone	Elkmont area

3.4.4 GRAVEL

Schumann (1993) in his book *Rocks, Minerals, and Gemstones* defines gravel as an accumulation of more or less rounded and polished rock fragments comprising of pebbles and drift. Pirsson (1908) describes gravel as pieces of individual rocks that are generally made up of grains of different kinds of minerals of which quartz is by far the most common, and sometimes feldspar. Szabo (1967) describes gravel as materials passing a U.S standard size sieve of $3\frac{1}{2}$ in. and retained on a U.S. standard number 4 mesh sieve.

Gravel, like conglomerates, is a sedimentary rock which may be composed of all kinds of rock fragments depending upon their source. Most of these gravels are found in the Paleozoic area of Alabama. However, a few occurrences of substantial quantities have been reported in the coastal plain area of Alabama, claim Daniel et al. (1966).

Szabo (1967), in agreement with Daniel et al. (1966), reports that gravels occur as alluvial deposits, i.e. conglomerates in the northern parts of the state, and as beach deposits and unconsolidated beds in the southern part of the state, and these are as a result of the weathering and disintegration of consolidated rocks.

Gravel is used in the construction industry as concrete aggregate, fill material, and railroad ballast. Quartz gravel is often used for concrete aggregate, while gravel for use as fill material and railroad ballast may consist of any material that is tough, durable and chemically stable (Daniel et al. 1966). Gravels can be found in the areas of Alabama listed in Table 3.4.

Table 3.4: Gravel locations in Alabama (Daniel et al. 1966)

COUNTY	AREA
Dekalb	Fort Payne area, Desota State Park
Shelby County	Helena area

3.5 CONCLUSION

Since aggregates compose 70 % to 80 % of the concrete volume (Emanuel and Hulsey 1977), their CTEs significantly influences the concrete CTE. The CTE can vary extensively among aggregates due to the mineralogical differences between them. Even the same aggregate type from the same state can present different CTEs as a result of the differences in the mineralogical content. The source of an aggregate therefore becomes important when designing concrete pavements and bridge decks.

CHAPTER 4

EXPERIMENTAL PLAN AND WORK

The testing procedures adopted, and a description of the AASHTO TP 60 (2004) test setup used to test the CTE of concrete samples is presented in this chapter. The raw materials used in this study are also described in this chapter.

4.1 EXPERIMENTAL TESTING PROGRAM

The testing program was developed considering some of the main factors affecting the coefficient of thermal expansion (CTE) of concrete and also time constraints. The testing program was developed to evaluate the effects of coarse aggregate type and volume, water-cement ratio, and sand-aggregate ratio on the concrete CTE. A total of fifty-four concrete samples were tested at the concrete age of 28 days for their CTE and compressive strength. Table 4.1 shows the experimental testing program adopted. Siliceous river gravel, dolomitic limestone, and granite are the coarse aggregates and siliceous sand is the only fine aggregate used in this study.

The sand-aggregate ratios used in this study were 0.40, 0.45, and 0.50, with the water-cement ratios being 0.32, 0.38, and 0.44. These ranges of sand-aggregate ratio and water-cement ratio capture those typically used in the Alabama concrete industry. For each coarse aggregate type, a total of nine concrete mixtures were thus made and tested.

Type I portland cement was used and all samples were tested in the saturated state as required by AASHTO TP 60 (2004).

Table 4.1: Experimental Testing Program

Coarse Aggregate Type	Fine Aggregate Type	Sand - Aggregate Ratio (By Volume)	Water - Cement Ratio	Concrete Sample Identification
Siliceous River Gravel	**Siliceous Sand**	0.40	0.32	RG-40-32
			0.38	RG-40-38
			0.44	RG-40-44
		0.45	0.32	RG-45-32
			0.38	RG-45-38
			0.44	RG-45-44
		0.50	0.32	RG-50-32
			0.38	RG-50-38
			0.44	RG-50-44
Dolomitic Limestone		0.40	0.32	DL-40-32
			0.38	DL-40-38
			0.44	DL-40-44
		0.45	0.32	DL-45-32
			0.38	DL-45-38
			0.44	DL-45-44
		0.50	0.32	DL-50-32
			0.38	DL-50-38
			0.44	DL-50-44
Granite		0.40	0.32	GR-40-32
			0.38	GR-40-38
			0.44	GR-40-44
		0.45	0.32	GR-45-32
			0.38	GR-45-38
			0.44	GR-45-44
		0.50	0.32	GR-50-32
			0.38	GR-50-38
			0.44	GR-50-44

4.2 SAMPLE IDENTIFICATION

The methodology adopted to label and identify the laboratory-prepared concrete samples is shown in Figure 4.1. The sample identification method was developed with

consideration of the type of coarse aggregates used, the sand-aggregate ratio, and the water-cement ratio. The concrete sample identification for all the mixtures tested as part of this study is shown in Table 4.1.

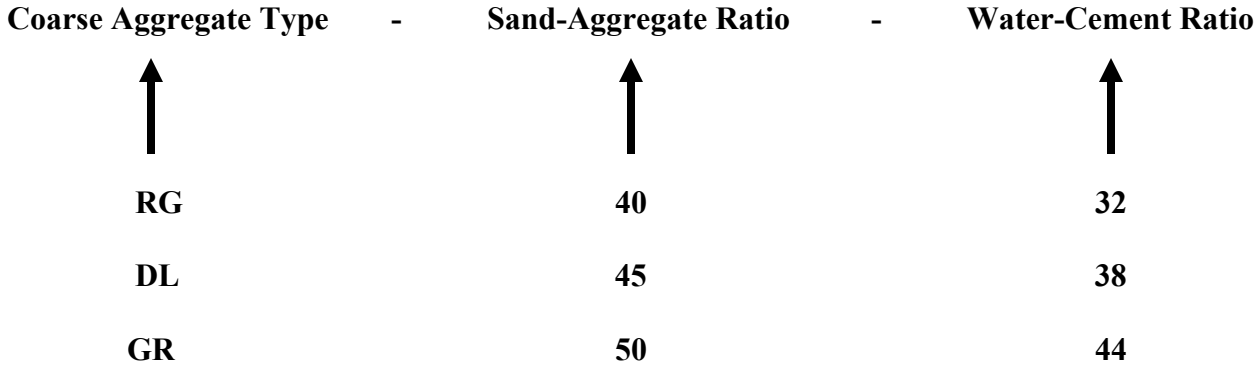

Identification Code:

Coarse Aggregate	Water-Cement Ratio	Sand-Aggregate Ratio
RG = Siliceous River Gravel	32 = 0.32	40 = 0.40
DL = Dolomitic Limestone	38 = 0.38	45 = 0.45
GR = Granite	44 = 0.44	50 = 0.50

***Example*: RG-40-32 =** Concrete sample made with siliceous river gravel, at a sand-aggregate ratio of 0.40, and a water-cement ratio of 0.32.

Figure 4.1: Concrete Sample Identification Code

4.3 COEFFICIENT OF THERMAL EXPANSION EQUIPMENT

This section describes in detail the equipment and procedure used for the concrete CTE test, which was performed in accordance with AASHTO TP 60 (2004).

This test method determines the CTE of concrete sample maintained in a saturated condition, by measuring the length change of the sample due to a specified temperature change. The measured length change is corrected for any change in length of the measuring apparatus (previously determined), and the CTE is then calculated by dividing the corrected length change by the temperature change and then the sample length.

4.3.1 CIRCULATOR

The Polyscience circulator model 9612 shown in Figure 4.2 was used. It provides precise temperature control of fluids for open- or closed-loop circulation to attached external equipment. This model features a 28-liter reservoir with a maximum fill level of about 1 in. (25 mm) below the top of the reservoir. For optimum cooling efficiency, the fluid level in the reservoir is kept above the coils at all times. All parts exposed to moisture are corrosion-resistant 300-series stainless steel. The operational temperature range is from -13 ºF (-25 ºC) to 302 ºF (150 ºC) with a temperature stability of ± 0.018 ºF (± 0.01 ºC). The read out accuracy is ± 0.45 ºF (± 0.25 ºC). The circulator has a duplex pump that permits circulation to and from an attached external open bath.

4.3.2 LINEAR VARIABLE DIFFERENTIAL TRANSFORMER READOUT

The Schaevitz MP2000 linear variable differential transformer (LVDT) readout was used in this study and is shown in Figure 4.3. The Schaevitz MP2000, from Measurement Specialties, is an integrated microprocessor–based LVDT readout

controller. It is designed to provide excitation and to display the calibrated voltage of alternating current (AC) operated LVDTs. In addition to displaying real-time readings of LVDTs, and gage heads, the MP2000 also displays minimum and maximum values etc. Physical variables such as displacement, force and weight can be displayed directly in engineering units on the 5-digit display. This readout has a bitmap liquefied crystal display (LCD) with legible characters, and has two output channels, A and B.

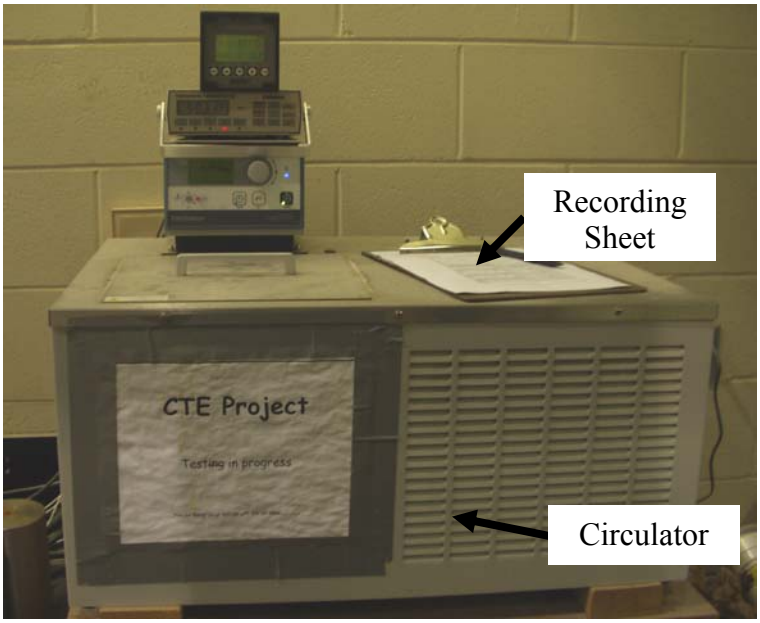

Figure 4.2: Circulator

Figure 4.3: Thermistor Display and MP2000 Readout

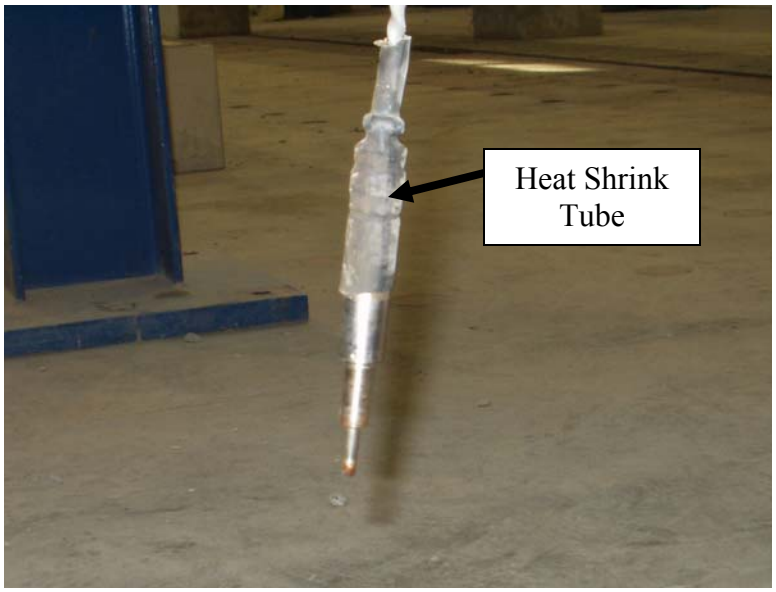

Figure 4.4: Typical Linear Variable Differential Transformer

4.3.3 LINEAR VARIABLE DIFFERENTIAL TRANSFORMER

The linear variable differential transformer (LVDT) used in this study is shown in Figure 4.4. It uses alternating current (AC) and has a ±0.125 in. (3.18 mm) range. It was manufactured by Measurement Specialties Incorporated and has the model number GCA-121-125. The GCA series gage head is made from stainless steel, which enables it to perform in environments containing moisture, dirt, and other contaminants. Electronic components are hermetically sealed for added protection against hostile conditions. Additionally, these LVDTs were further protected from moisture by the use of heat-shrink tubes as shown in Figure 4.4. These LVDTs have ranges up to ± 2.0 in. (50 mm). In Table 4.2, the other specifications of these LVDTs are shown. As can be seen, it works well in a wide range of temperatures, i.e. -65 °F to 300 °F (-55 °C to 150 °C), and has a linearity of ± 0.25 % of full range output, which makes it suitable for this study. The LVDT requires calibration on its first use. The next section describes the calibration procedure.

Table 4.2: Specifications of an AC-LVDT operated model (Measurement Specialties, Inc. 2008)

Frequency Range	400 Hz to 10 kHz
Linearity	±0.25% of full range output
Repeatability	0.000025 in. (0.0006 mm)
Operating temperature range	-65 °F to 300 °F (-55 °C to 150 °C)
Housing Material	AISI 400 series stainless steel
Electrical Termination	6-pin connector

4.3.3.1 Calibration Procedure for the LVDT

A micrometer screw gage was used to apply a controlled displacement of 0.1 in. to the LVDT as shown in Figure 4.5. The amount of displacement exceeds the largest displacement anticipated during a CTE test.

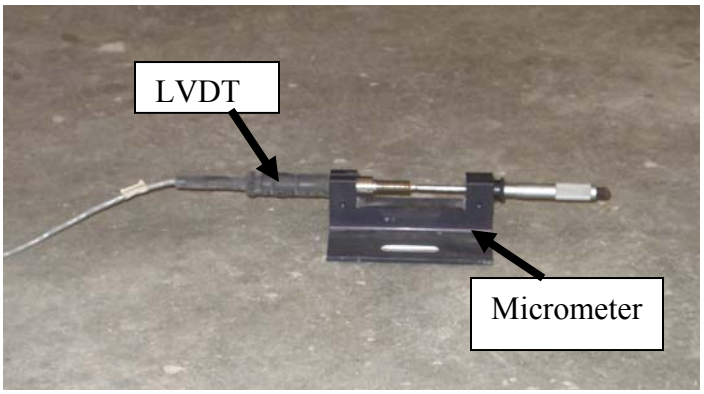

Figure 4.5: LVDT connected to a micrometer screw gage

The following steps were followed in the calibration of the LVDT:

Step 1. Determine the LVDT Sensitivity:

The sensitivity of the LVDT was obtained from the calibration sheet accompanying the LVDT unit. This was defined as 2.39390 mV/V/0.001in.

Where,

mV/V/0.001in. = Millivolt of output, per volt of excitation, per 0.001 in. of displacement from the null position.

Step 2. Determine the Full-Scale LVDT output:

Two calculations were performed.

Calculation 1: Multiply the sensitivity by 1V by the full-scale displacement (in thousandths of an inch). i.e. Sensitivity x 1V x full-scale displacement.

Calculation 2: Multiply the sensitivity by 3 V by the full-scale displacement (in thousandths of an inch). i.e. Sensitivity x 3 V x full-scale displacement.

Thus, using a Schaevitz GCA-121-125 with sensitivity of 2.39390 mV/V/.001in. (at 2.5 kHz) and full-scale displacement of 0.100 in.:

Calculation 1: 2.39390 x 1 x (0.1 in./0.001 in.) = 2.39390 x 100 = 239.390 mV

Calculation 2: 2.39390 x 3 x (0.1 in./0.001 in.) = 7.18170 x 100 = 718.170 mV

Step 3. Determine the Full-scale Meter Sensitivity:

The full-scale LVDT output is the closest voltage associated with the full-scale sensitivity of the meter without exceeding it. The full-scale sensitivity of the meter is 600 mV in high gain or 1200 mV in low gain. Since *Calculation 2* in this example resulted in a full-scale output (718.170 mV) that was close enough to the low gain (1200 mV) sensitivity of the meter, *Calculation 2* was used for the set up. The full-scale meter sensitivity was determined to be 1200 mV.

Step 4. Determine and set the drive frequency, drive voltage, and gain.

The drive voltage and gain, like in *Calculation 2,* selection was based on:

- If the value (*Calculation 1* output) is close to 600mV, select gain *High*.
- If the value (*Calculation 2* output) is close to 1200mV, select gain *Low*.

In this particular case, gain *Low* was selected since 718.170 mV is closer to 1200mV than 239.390 mV is to 600mV.

Step 5: Plug the LVDT into the meter, and turn the power on, and then leave it to warm up for approximately 10 minutes as recommended by the manufacturer.

Step 6: Set the *Calibration Switch* to enable.

Step 7: Set the *Decimal Point* to five decimal places.

Step 8: Set the *Preset value* to zero.

The *Preset value* is a constant added to or subtracted from the scaled and zeroed value prior to being displayed.

Step 9: Determine and set the *Cal Value*.

The *Cal Value* or calibration displacement is the distance the transducer will be moved during calibration. The *Cal Value* was set to 0.1 in.

Step 10: Set the *Full-scale* (FS) *value*.

The FS value is used to keep track of the transducer's position relative to the electrical zero (null) of the LVDT when the auto zero button is used to off-set the meter zero. The full-scale value was set to 0.125 in. (3.125 mm).

Step 11: Calibrate Channel A.

The following procedure was used to calibrate this channel:

- The LVDT was positioned at the center of its stroke (zero output position).
- In the *Run* mode, the *Cal* button was pressed to get the readout into the calibration menu.
- With the LVDT positioned at the center of its stroke, the *Enter* button was pressed; this was taken as the first point of calibration. All necessary precautions were taken to ensure that the LVDT did not exceed the *Full-scale* setting, in the next step.
- The sensor was displaced the exact distance, as defined by the *Cal Value*, in a positive direction (i.e. toward the leads), using the micrometer screw gauge.
- Next the *Enter* button was pressed and this was taken as the second point of the calibration.

- The calibration process of channel A was thus completed.

Step 12: Calibrate Channel B. Use the same process as described for Channel A.

4.3.3.2 Validation of the Linear Variable Differential Transformer Readings

After calibration of the linear variable differential transformer (LVDT), its readings were often validated to ensure it read accurately and linearly. Controlled displacements were introduced to the LVDT using the micrometer shown in Figure 4.5. The gage outputs recorded were compared with the controlled displacements introduced. This section describes the steps taken to validate typical LVDT readings:

Step 1: Connect the cable end of the LVDT to the MP2000, and then connect the LVDT itself to the Schaevitz micrometer.

Step 2: Introduce controlled displacements in multiples of 0.025 in. (0.625 mm) to the LVDT using the micrometer (i.e. from 0 to 0.1 and back to 0).

Step 3: Record the output values from the MP2000 readout.

Step 4: Repeat Steps 2 and 3 two more times for each LVDT.

Step 5: Construct a validation plot by plotting the values obtained from the micrometer against the values displaced for the LVDT.

In Table 4.3 and Figure 4.6, the results for a typical LVDT validation are shown.

Table 4.3 Data for a typical LVDT Validation

	Actual Displa-cement (in.)	Gauge Output (in.)	Calculated Displacement (in.)	Percent Error	Tolerable Limits of Error	
					Upper Limit (+5 %)	Lower Limit (-5 %)
Increasing	0.0000	0.0103	0.0000	0.0000	0.0000	0.0000
	0.0250	0.0340	0.0237	-5.3200	0.0263	0.0238
	0.0500	0.0591	0.0488	-2.4600	0.0525	0.0475
	0.0750	0.0840	0.0737	-1.7733	0.0788	0.0713
	0.1000	0.1087	0.0984	-1.5800	0.1050	0.0950
Decreasing	0.0750	0.0856	0.0753	0.4267	0.0788	0.0713
	0.0500	0.0606	0.0503	0.6600	0.0525	0.0475
	0.0250	0.0356	0.0253	1.1600	0.0263	0.0238
	0.0000	0.0104	0.0001	0.0000	0.0000	0.0000

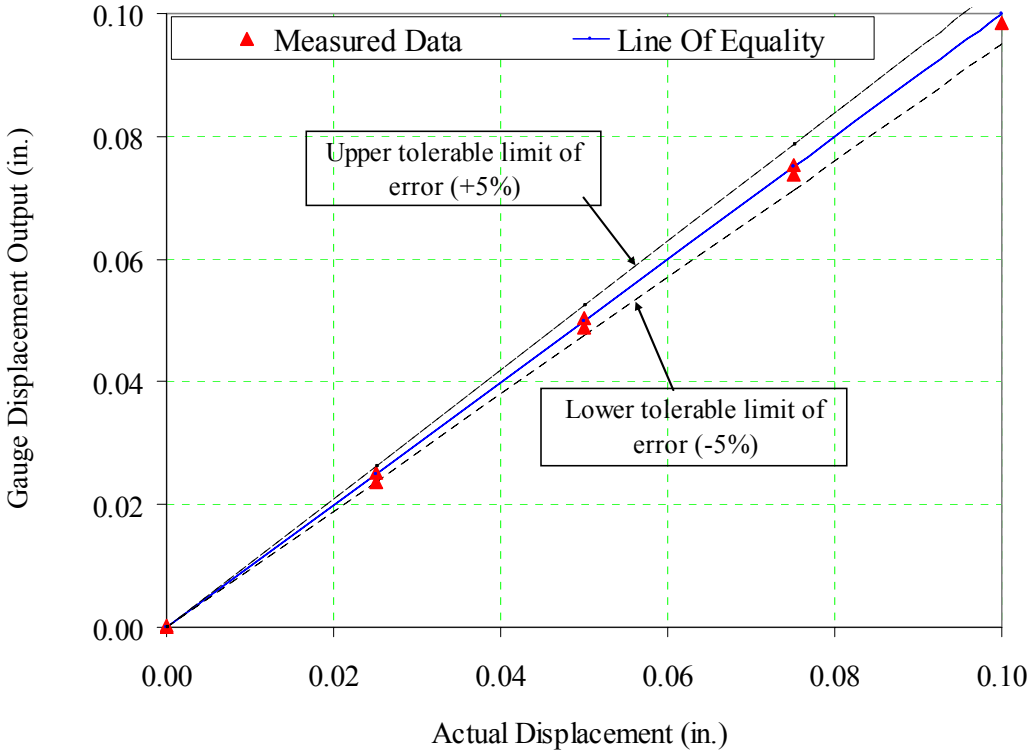

Figure 4.6: Typical LVDT Validation Plot

It was observed that, in all cases, the data collected during the calibration test fell within the tolerable limits of ± 5 %, except for one point that was consistently an outlier. The first recorded point was consistently slightly above 5%. The average error for this was calculated to be 6.4 %, differing by 1.4 % from the tolerable error of 5 %. This was however tolerated as it probably was occurring due to seating issues between the LVDT and the micrometer.

4.3.4 External Water Tank

A rectangular stainless steel tank was used as shown in Figure 4.7. It has dimensions of 23 in. (length) x 21 in. (width) x 20 in. (height) (575 mm x 525 mm x 500 mm) with a thickness of 1 in. (25 mm). Within each wall of the tank is insulation to help prevent loss of temperature.

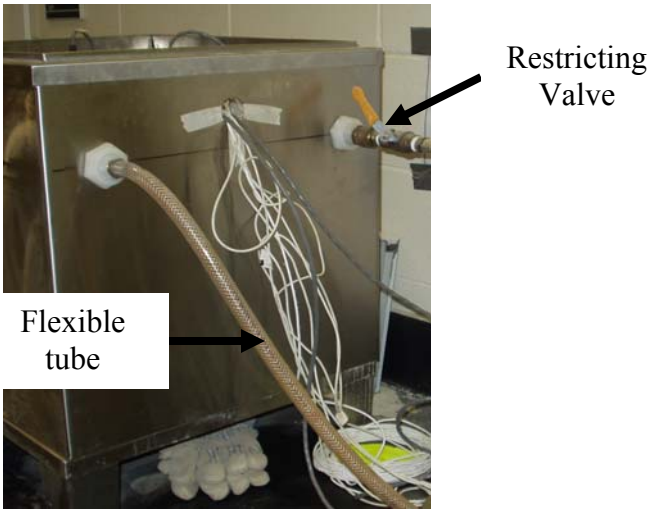

Figure 4.7: External water tank

4.3.5 THERMISTOR READER

A thermistor is a temperature-sensing element composed of sintered semiconductor material which exhibits a change in resistance proportional to a small change in temperature (Omega Engineering, Inc. 2008). The thermistor reader used is shown in Figure 4.3. It was manufactured by Omega Engineering, Inc. and has the model number 5830. It is a portable instrument which measures and displays the temperature of up to five different readings from -22 ^{o}F to 212 ^{o}F (-30 ^{o}C to 100 ^{o}C). The thermistor reader reads thermistor probes and displays the readings on a five digit LCD on the front panel. Each thermistor probe plugs into its own jack in the back of the instrument and is represented by a front panel light and a labeled membrane key. When one or more of the panel probe keys is pressed, its corresponding light comes on to show that it has been selected and is currently active.

4.3.5.1 Thermistor Probes

The thermistor probes with model number ON-403-PP were used as shown in Figure 4.8. It was manufactured by Omega Engineering, Inc. It is made of stainless steel and has a diameter of 1/8 in. and a length of 4 ½ in.

Figure 4.8: Thermistor Probe

4.3.5.2 Calibration of the Thermistor Reader

The Omega thermistor reader required calibration before use. Five resistors, 106.2K Ohm ± 0.05%, each wired across a separate standard 1/4" phone plug and hence marked "*Hi Cal*" and Five resistors, 407.1 Ohm ± 0.05 %, each wired across a separate standard 1/4" phone plug and hence marked "*Lo Cal*" were required for the calibration. The following steps were used in the calibration.

Step 1: Turn off the thermistor reader.

Step 2: Press probe number one key and keep it pressed in.

Step 3: Turn on the power while pressing and holding in probe number one key for 3 to 4 seconds before releasing; the display will show "*Hi Cal*" or "*USrCal*". If "*USrCal*" is displayed, continue to step 5, however, if "*Hi Cal*" is displayed, proceed to step 6.

In this particular case, "*Hi Cal*" was displayed and hence step 6 was followed.

Step 5: Press the probe number five key and the display will show "*Hi Cal*".

Step 6: Plug all five "*Hi Cal*" phone plugs into the probe jacks at the rear of the instrument.

Step 7: Press any probe number and hold it for 3 to 4 seconds and then release the key. "*Lo Cal*" will be displayed on the screen. In this instance, probe number two key was pressed and held for about 3 to 4 seconds and then released. The display showed "*Lo Cal*".

Step 8: Remove all five "*Hi Cal*" phone plugs and set aside. Insert all five "*Lo Cal*" phone plugs into the probe jacks at the rear of the instrument.

Step 9: Press any probe number key and hold it in for 3 or 4 seconds. The thermistor reader will then go into the run mode.

With this calibration, probe number three key was pressed and held for about 3 to 4 seconds and then released. The unit went into the run mode.

Step 10: Remove all five "*Lo Cal*" phone plugs.

The calibration procedure is complete.

4.3.6 FRAMES

The frame used in this study is shown in Figure 4.9. It is made of Invar and has a total height of 13.75 in. The supporting vertical bars have a diameter of 0.75 in. The base plate has dimensions of 10.25 in. (length) x 10.25 in. (width) x 0.75 in. (thickness). The cross bar with dimensions of 9.75 in. (length) x 2.0 in. (width) x 0.75 in. (thickness) is usually positioned by nuts at a height of about 8.0 in. above the top of the base plate.

Figure 4.9: Invar Frame

4.3.7 Assembly of the Components for the AASHTO TP 60 (2004) Test Setup

The AASHTO TP 60 (2004) test setup is shown in Figure 4.10. The circulator was connected to the external water tank by means of suction and pressure flexible tubing. A restriction valve (Figure 4.7) was installed on the pressure (outlet) tubing and adjusted to match the return suction (inlet) flow rate.

Figure 4.10: AASHTO TP 60 (2004) Test setup

The circulator's water reservoir was filled to a level of 1 in. (25 mm) below the top, while the water level in the external water tank was filled such that the level matched that of the water level in the circulator's reservoir. The cables of the thermistor probes were plugged into the rear of the thermistor reader with the temperature probes positioned using plexiglass plates in the external water bath (see Figure 4.11) specifically prepared to hold these probes. The LVDTs were then connected by cables to the MP2000 reader. The LVDT was held in position on the Invar cross bar by a nut. The cross bar was then fixed onto the Invar frames by nuts. Two frames were used, and they were made to sit side by side in the external water tank.

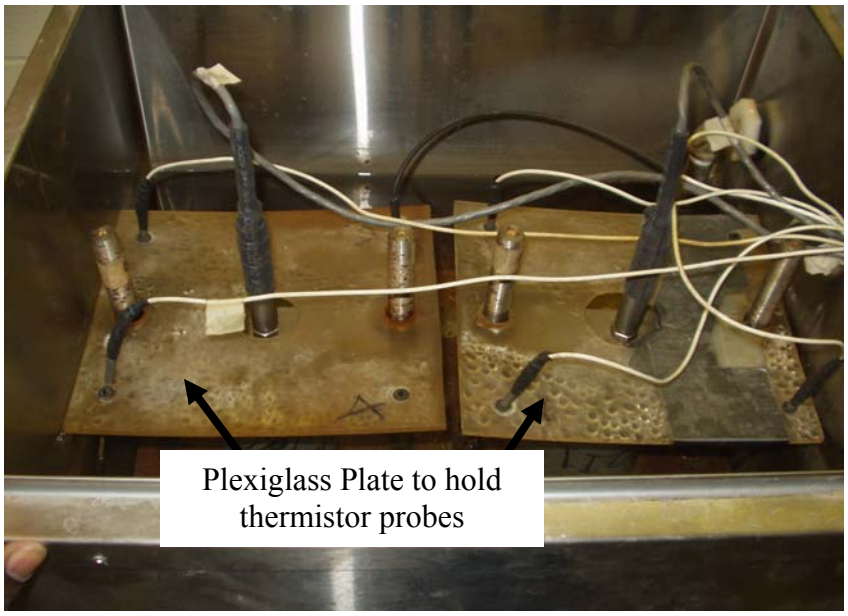

Figure 4.11: External water bath housing the two Invar frames containing concrete samples

4.4 LABORATORY PROCEDURES

This section describes the procedures for the laboratory work undertaken. All concrete mixing performed in this project was conducted in an enclosed, air-conditioned concrete laboratory. The raw materials used to produce the concrete were also stored in the laboratory. Portland cement was received and stored in standard 94-lb sacks. The coarse and fine aggregates were stored in sealed 55-gallon drums. The aggregates were replenished from large stockpiles stored outdoors at Sherman Industries Ready Mixed Concrete Plant in Auburn, Alabama.

4.4.1 BATCHING

Prior to batching, moisture corrections were performed on both the fine and coarse aggregates. These moisture corrections were carried out with a small digital scale and two hot plates. Once the moisture corrections were performed, all the materials were batched using weight batching into 5-gallon buckets. In an attempt to prevent moisture gain or loss, the buckets were sealed with lids. The chemical admixtures were batched in terms of volume using 60-ml syringes. The total batch size made was three cubic feet, usually with about 50 % being waste. A complete table of mixture proportions used in this study is shown in Appendix A.

4.4.2 MIXING PROCEDURE

A total of three cubic feet of concrete was always mixed. Figure 4.12 shows the mixing room where all the concrete was mixed. The procedure used to mix concrete was in accordance with AASHTO T 126 (2001), which is summarized below:

- Prior to mixing, the mixer was buttered to thoroughly coat the mixer with mortar. This mortar was drained out of the mixer before adding the batched materials.
- The coarse and fine aggregates were placed in the rotating drum mixer, together with 80 % of water mixed with the air-entraining admixture.
- Next, the cementitious material was added followed by the remaining water mixed with the appropriate water-reducing admixture.
- Mixing was done for the next three minutes, stopped for three minutes, and followed by a final two minutes of mixing.

Figure 4.12: Concrete mixing room

4.4.3 Assessment of Fresh Concrete Properties

On completion of mixing, the following tests were performed to assess fresh concrete properties according to the standards indicated:

- Slump according to ASTM C 143 (2003),
- Unit weight according to ASTM C 138 (2001),
- Total air content according to ASTM C 231 (2004), and
- Fresh concrete temperature according to ASTM C 1064 (2004).

4.4.4 SAMPLE PREPARATION

The concrete samples were prepared to conduct hardened concrete tests as detailed in the following sections.

4.4.4.1 Making Cylinders

The AASHTO TP60 (2004) procedure requires that tests should be carried out on 4 in. diameter x 7 in. high (100 mm x 175 mm) concrete samples. Therefore, before mixing, the 4 in. x 8 in. (100 mm x 200 mm) plastic cylinder molds were trimmed to 7 in. (175 mm) in height using an electric-powered saw blade.

All test specimens were made in accordance with ASTM C 192 (2002). A total of nine cylinders were made for each concrete batch. This comprised of six 4 in. x 7 in. (100 mm x 175 mm) cylinders and three 6 in. x 12 in. cylinders. Each 6 in. x 12 in. (150 mm x 300 mm) cylinder was made in three equal lifts of concrete, and each layer was rodded 25 times with a 5/8-in. tamping rod. For the 4 in. x 7 in. (100 mm x 175 mm) cylinders, each was made in two equal lifts of concrete, and each layer rodded 25 times with a 3/8-in. tamping rod. The sides of the molds were slightly tapped with a rubber mallet each time a layer was rodded. A wooden trowel was then used to strike off the surface of the concrete sample. Next, the cylinders were covered with plastic caps to prevent any loss of moisture. Figure 4.13 shows concrete samples being made, while Figure 4.14 shows typical concrete samples in the hardened state with their identification numbers.

Figure 4.13: Concrete samples being made in the Laboratory

Figure 4.14: Typical tested samples ready to be discarded

4.4.4.2 Curing of Concrete Samples

Using the ASTM C 192 (2002) test method, the concrete samples were stripped after a concrete age of 24 hours and transferred to the moist curing room, where they

were kept until a concrete age of 28 days and then prepared for the hardened concrete testing. The moist curing, apart from helping in hydration, also helps to keep the concrete samples saturated for the CTE test as required by AASHTO TP 60 (2004).

4.4.5 HARDENED CONCRETE PROPERTIES TESTING

The following hardened concrete property tests were performed on each concrete sample prepared.

4.4.5.1 Compressive Strength Testing

The compressive strength testing was conducted on the three 6 in. x 12 in. (150 mm x 300 mm) cylinders using a compressive testing machine manufactured by Forney. This machine is shown in Figure 4.15. All three samples were tested in accordance with ASTM C 39 (2003) and the load rate used was kept around 60,000 lb/min. The load at failure was recorded and a spreadsheet (shown in Appendix C) was used to calculate the compressive strength of the concrete samples.

Figure 4.15: Forney compressive testing machines

4.4.5.2 Coefficient of Thermal Expansion

A total of fifty-four samples were tested for their coefficient of thermal expansion (CTE). This test was conducted in accordance with the specifications of AASHTO TP 60 (2004). The CTE test was carried out on two 4 in. x 7 in. (100 mm x 175 mm) concrete samples at a time, hence two Invar frames A and B were used at a time. The frames were made to sit side-by-side in the external water bath. With the samples removed from the curing room, their dimensions (length and diameter) were measured using the vernier caliper and recorded. The length and diameter measurements were taken at four different points along the circumference to ensure accuracy. The samples were next setup in the frames, making sure that the lower end of the sample was firmly seated against the support buttons, and that the LVDT tip was seated against the upper end of the sample.

The temperature of the water bath was set to 50 ^{o}F (10 ^{o}C) on the circulator, and when the external water bath reached this temperature, it was allowed to remain at this temperature until thermal equilibrium of the concrete samples was reached as was indicated by consistent readings of the LVDT to the nearest 0.00001 in. (0.00025 mm) taken over a one half hour time period at 10 minute intervals.

The temperature readings were then recorded to the nearest 0.2 ^{o}F (0.1 ^{o}C), and the LVDT readings were also recorded to the nearest 0.00001 in. (0.00025 mm). These were the initial readings. Next the temperature of the water bath was set to 122 ^{o}F (50 ^{o}C). When the bath reached this temperature, it was allowed to remain at this temperature until thermal equilibrium of the concrete samples was reached, as explained earlier.

The temperature readings from each of the four sensors and LVDT readings were then recorded. These formed the second set of readings. The temperature of the water bath was next set to 50 ^{o}F (10 ^{o}C) on the circulator. When the bath reached this temperature, it was allowed to remain at this temperature until thermal equilibrium of the sample was reached. The temperature readings of the four sensors and LVDT readings were again recorded as stated previously. These were the final readings for a complete cycle. The whole process was repeated two more times. A data recording sheet (shown in Appendix C), was prepared for the recording of the CTE test data.

4.5 DATA PROCESSING

The CTE test data recorded were processed using a spreadsheet (shown in Appendix C) designed for calculating the CTE of the concrete samples. However, prior to calculating the CTEs of the concrete samples, a correction factor for the Invar frames had to be determined and applied. It was observed that, and as noted in AASHTO TP 60 (2004), during the heating and cooling segments, the Invar frames expand and contract simultaneously with the concrete sample. Therefore the readings as noted on the MP2000 do not represent the actual amount of expansion or contraction of the concrete samples during the heating and cooling segments, so there was the need to correct for this. Accordingly, the AASHTO TP 60 (2004) test was run on stainless steel samples (see Figure 4.16) to establish the correction factors for each frame (A and B) to be applied during the calculation of the CTE of the concrete samples. In the next section, the derivation and calculation of the correction factor is presented.

Figure 4.16: Stainless steel samples used in determining the correction factor

4.5.1 Derivation and Calculation of the Correction Factor for the Invar Frames

This section details the correction factor derivation and its calculation for the two Invar frames used in testing for the CTE of the concrete samples.

4.5.1.1 Derivation of Correction Factor

Consider the schematic CTE test frame shown in Figure 4.17:

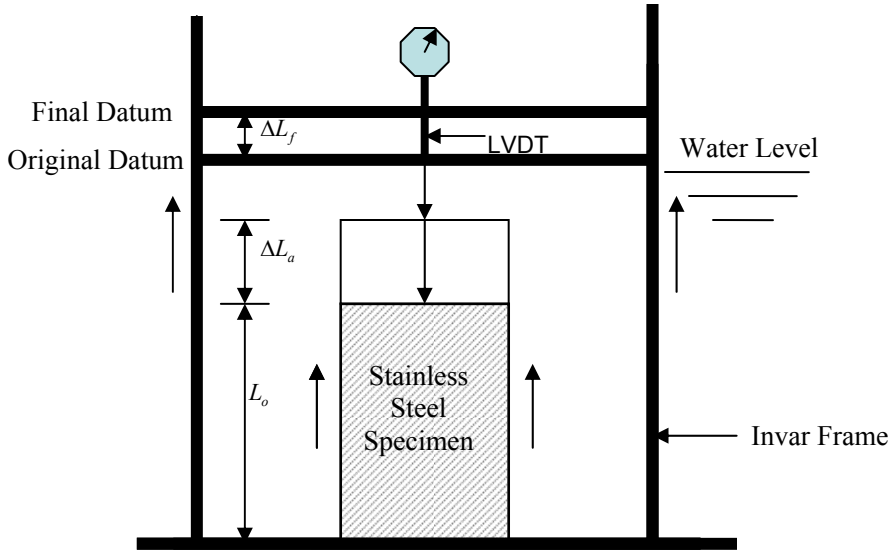

Figure 4.17: Schematic of the CTE test frame (Drawing not to Scale)

The following symbols are used in the derivation of the correction factor:

ΔL_f = Expansion of Invar frame/displacement of datum due to temperature change,

ΔT = Temperature change through which the sample is subjected,

ΔL_a = Actual expansion of the concrete sample due to the temperature change,

ΔL_m = Measured length change of the concrete sample on the LVDT due to the temperature change,

α_c = CTE of the concrete sample, and

L_o = Original length of concrete sample.

Due to the simultaneous expansion of the Invar frame and the concrete sample, the actual measured expansion on the LVDT is:

$$\Delta L_m = \Delta L_a - \Delta L_f \qquad \textit{Equation 4.1}$$

Hence,

$$\Delta L_a = \Delta L_m + \Delta L_f \qquad \textit{Equation 4.2}$$

And,

$$\alpha_c = \frac{\Delta L_a}{L_o \times \Delta T} \qquad \textit{Equation 4.3}$$

Substituting *Equation 4.2* into *Equation 4.3* yields:

$$\alpha_c = \frac{(\Delta L_m + \Delta L_f)}{L_o \times \Delta T} \qquad \textit{Equation 4.4}$$

Therefore,

$$\alpha_c = \frac{\Delta L_m}{L_o \times \Delta T} + \frac{\Delta L_f}{L_o \times \Delta T} \qquad \textit{Equation 4.5}$$

Where,

$\frac{\Delta L_m}{L_o \times \Delta T}$, = the CTE corresponding to the *measured* length change of the concrete sample, and

$C_f = \frac{\Delta L_f}{L_o \times \Delta T}$ = the correction factor, accounting for the expansion of the Invar frame.

To determine ΔL_f, AASHTO TP 60 (2004) requires the use of a sample of known CTE, and should be composed of a material that is linearly elastic and has a thermal coefficient of expansion close to that of concrete. Assume the length change of the apparatus varies linearly with temperature. The actual expansion of the calibration specimen when it undergoes a temperature change ΔT, is given by:

$$\Delta L_{a(cs)} = L_{cs} \times \alpha_{cs} \times \Delta T \qquad \textit{Equation 4.6}$$

But,

$$\Delta L_{m(cs)} = \Delta L_{a(cs)} - \Delta L_f \qquad \textit{Equation 4.7}$$

Hence,

$$\Delta L_f = (\Delta L_{a(cs)} - \Delta L_{m(cs)}) = L_{cs} \times \alpha_{cs} \times \Delta T - \Delta L_{m(cs)} \qquad \textit{Equation 4.8}$$

Or,

$$C_f = \frac{\left(L_{cs} \times \alpha_{cs} \times \Delta T - \Delta L_{m(cs)}\right)}{L_o \times \Delta T} \qquad \textit{Equation 4.9}$$

Where,

L_{cs} = Original length of calibration sample,

$\Delta L_{m(cs)}$ = Measured length change of the calibration sample on the LVDT due to the temperature change,

$\Delta L_{a(cs)}$ = Actual expansion of the calibration sample due to the temperature change, and

α_{cs} = CTE of the calibration specimen.

4.5.1.2 Calculation of the Correction Factor

A total of eight tests were carried out in accordance with AASHTO TP60 (2004) using the stainless steel samples of Figure 4.16 to determine the linear displacement of the LVDT due to the expansion and contraction of the stainless steel sample. The stainless steel samples were labeled as A and B respectively, with each being set up in the frame with the same corresponding label. So stainless steel sample marked with an A was set up in frame A, etc. Four different LVDTs labeled B, C, D and E were used interchangeably in both frames A and B, and the linear displacements of the LVDTs for each test were recorded as shown in Table 4.4. The average range of temperature change during the process was 71.30 ^{o}F.

Table 4.4: Measured displacement of LVDT for test run on stainless steel samples

Test Number	Frame	LVDT	Net Displacement
Test 1	A	C	0.00474
Test 2	A	C	0.00473
	B	B	0.00452
Test 3	A	C	0.00472
	B	B	0.00466
Test 4	A	C	0.00474
	B	B	0.00466
Test 5	A	C	0.00476
	B	B	0.00472
Test 6	A	C	0.00485
	B	B	0.00474
Test 7	A	C	0.00481
	B	B	0.00474
Test 8	A	D	0.00495
	B	E	0.00467

A sensitivity analysis was carried out to determine the effect of a unit change in the linear displacement of the LVDT on the concrete CTE. This was done using a single

test result run on concrete for the range of LVDT displacements shown in Table 4.4. The results is as shown in Figure 4.18; it was observed that the concrete CTE was dependent on the unit change in the linear displacement of the LVDT as indicated by the slope of about 0.002 /in.^{o}F. Hence the average of the most repeatable values of displacement for each frame as measured on the LVDT was used in the calculation of the correction factor for both frames A and B.

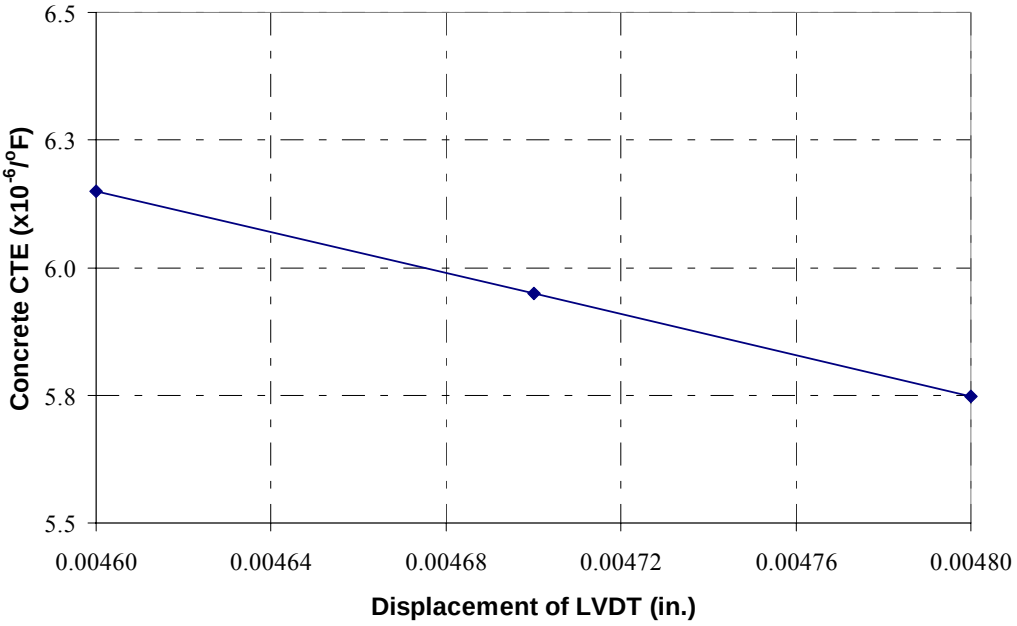

Figure 4.18: Sensitivity analysis of CTE dependence on net displacement of LVDT

The calculation of the Correction Factors, as described in AASHTO TP 60 (2004) were performed as follows:

The CTE of the stainless steel sample as given by AASHTO TP 60 (2004) and used in the calculations is 17.3 x 10^{-6} in./in./^{o}C (9.61 x 10^{-6} in./in./^{o}F). The average temperature change calculated and used is 71.30 ^{o}F.

For frame A:

Average measured linear displacement: $\Delta L_m = 0.00474$ in.

Expected actual linear displacement of calibration specimen:

$\Delta L_a = L_{CS} \times \alpha_{CS} \times \Delta T = (7.00 \text{ in.})(\frac{5}{9} \text{ x } 17.3 \text{ x } 10^{-6}/^{o}\text{F})(71.30\ ^{o}\text{F}) = 4.80 \text{ x } 10^{-3} \text{ in.}$

Expansion of frame A ΔL_{fa} due to temperature change ΔT is:

$\Delta L_{fa} = \Delta L_a - \Delta L_m = 4.80 \times 10^{-3} - 4.74 \times 10^{-3} = 6 \times 10^{-5} \text{ in.}$

Hence the Correction Factor:

$C_{fa} = \left[\left(\frac{\Delta L_{fa}}{L_O} \right) \div \Delta T \right] = [(\frac{6x10^{-5}}{7.00} \text{ in. /in.}) / 71.30\ ^{o}\text{F}] = 1.1 \text{ x } 10^{-7}\ /^{o}\text{F}$

For frame B:

Average measured linear displacement: $\Delta L_m = 0.00470$ in.

Expected actual linear displacement:

$\Delta L_a = L_{CS} \times \alpha_C \times \Delta T = (7.00 \text{ in.})(\frac{5}{9} \text{ x } 17.3 \text{ x } 10^{-6}/^{o}\text{F})(71.30\ ^{o}\text{F}) = 4.80 \text{ x } 10^{-3} \text{ in.}$

Expansion of frame B ΔL_{fb} due to temperature change ΔT is:

$\Delta L_{fb} = \Delta L_a - \Delta L_m = 4.80 \text{ x } 10^{-3} - 4.70 \text{ x } 10^{-3} = 10 \text{ x } 10^{-5} \text{ in.}$

Hence the Correction Factor

$C_{fb} = \left[\left(\frac{\Delta L_{fb}}{L_O} \right) \div \Delta T \right] = [(\frac{10x10^{-5}}{7.00} \text{ in. /in.}) / 71.30\ ^{o}\text{F}] = 1.9 \text{ x } 10^{-7}\ /^{o}\text{F}$

4.5.2 CALCULATION OF THE COEFFICIENT OF THERMAL EXPANSION OF CONCRETE

With the correction factors determined for each frame, a spreadsheet developed in accordance with AASHTO TP60 (2004) was used to calculate the CTE of concrete samples. The calculated values of concrete CTE are presented in Chapter 5.

4.6 RAW MATERIALS USED

This section presents the properties of all the raw materials used in this study.

4.6.1 AGGREGATES

Three types of coarse aggregates, namely siliceous river gravel, dolomitic limestone, and granite, were used in this study. They were of gradation No. 67 according to ASTM C 33 (2003). These aggregates were selected for this study since they are the types of aggregates commonly used by the Alabama concrete industry. The type of fine aggregate used was siliceous sand. The different types of aggregates together with their properties are outlined in Table 4.5. The gradation plots of these aggregates are also shown in Figures 4.19a – 4.19d.

Table 4.5: Aggregate Properties

Aggregate Type	Source	Gradation	Bulk Specific Gravity	Absorption Capacity (%)
Siliceous River Gravel	Martin Marietta, Shorter, Alabama	No. 67	2.568	0.820
Dolomitic Limestone	Vulcan Materials, Calera, Alabama	No. 67	2.753	0.378
Granite	Florida Rock Industries, Forest Park, Georgia	No. 67	2.687	0.640
Siliceous Sand	Martin Marietta, Shorter, Alabama	ASTM C 33 Sand	2.626	0.301

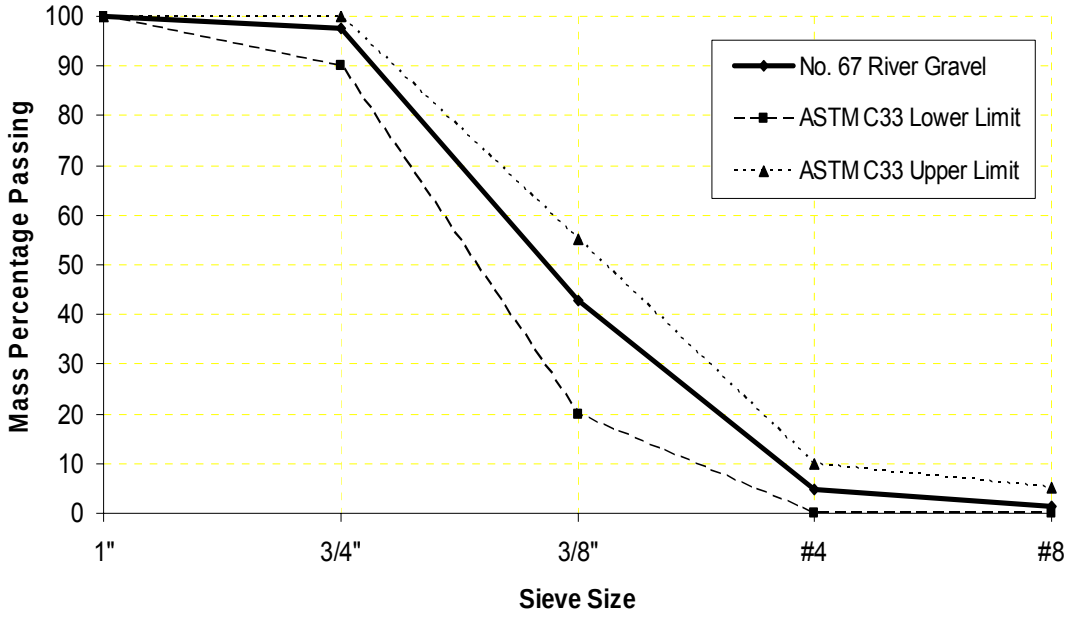

Figure 4.19a: Gradation test results for Martin Marietta No. 67 Siliceous River Gravel

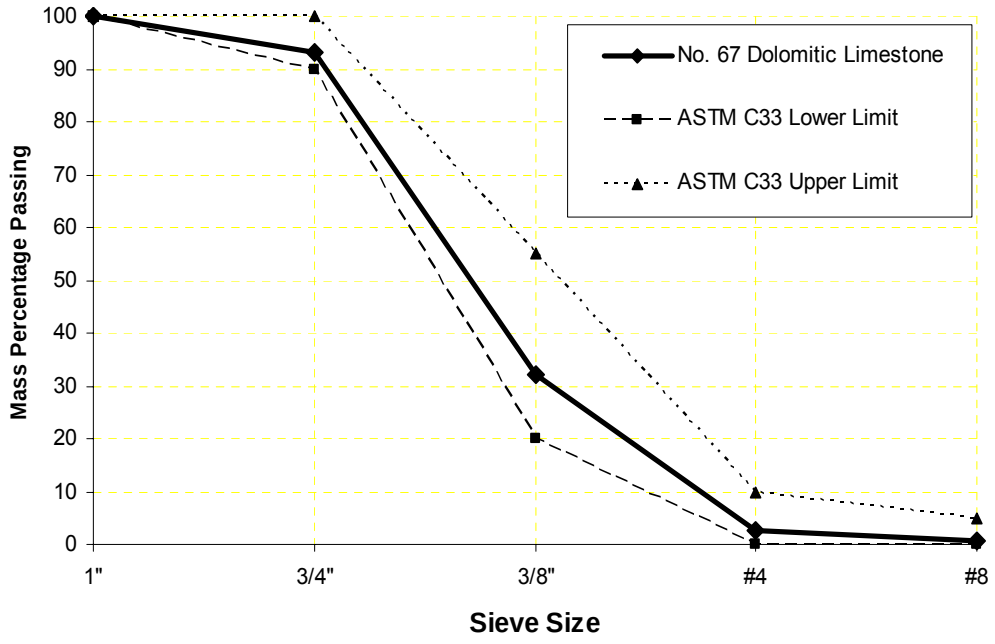

Figure 4.19b: Gradation test results for Vulcan Materials No. 67 Dolomitic Limestone

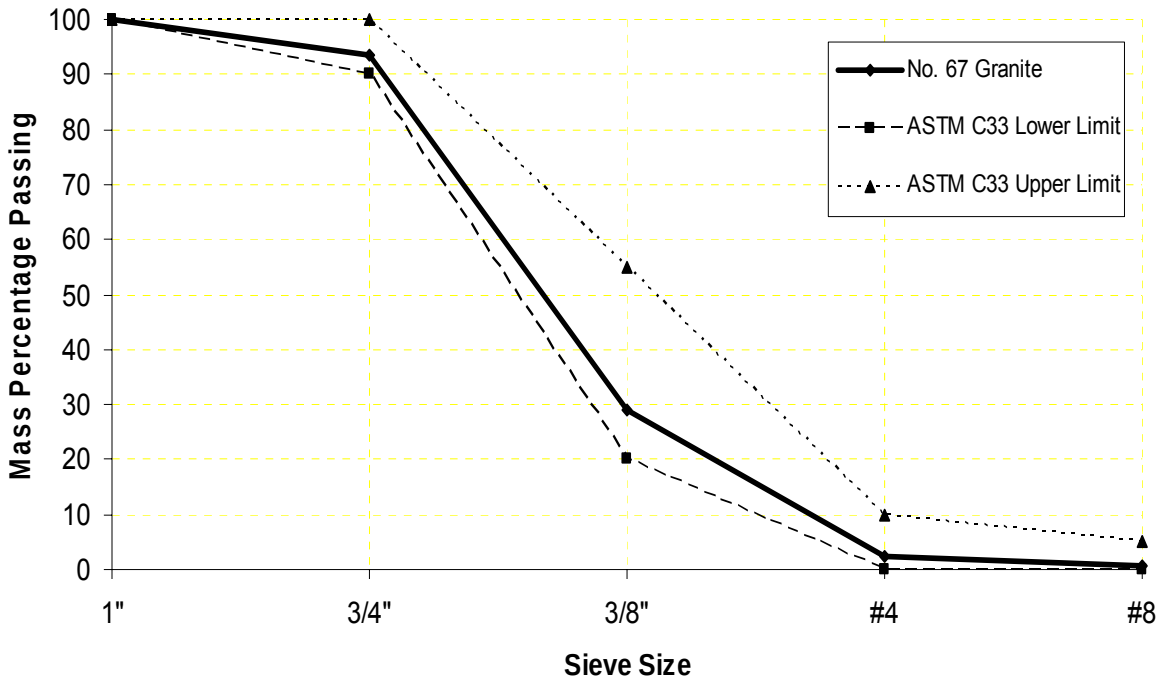

Figure 4.19c: Gradation test results for Florida Rock Industry No. 67 Granite

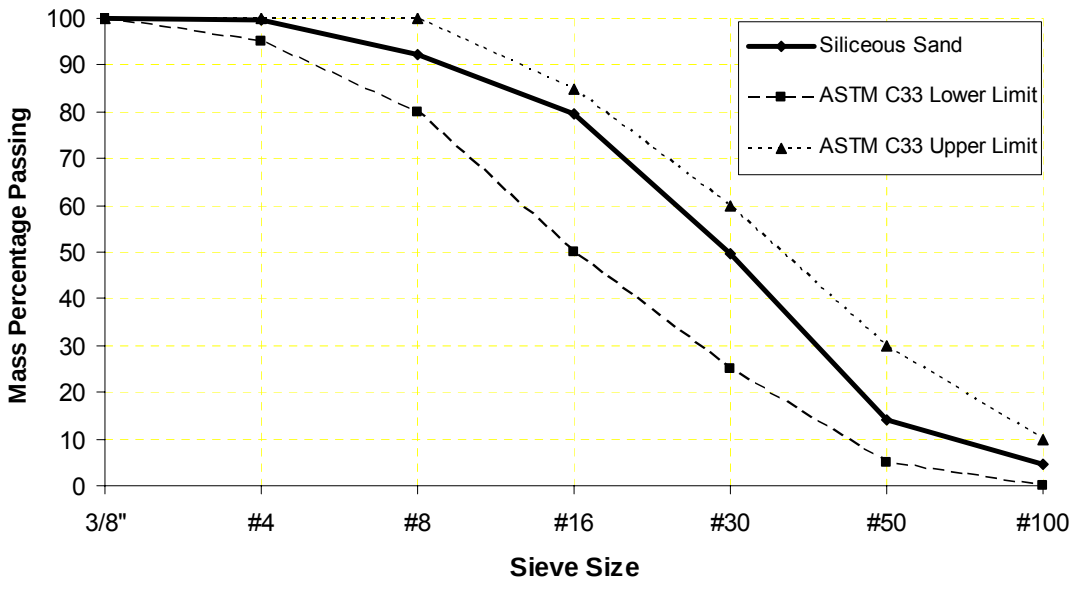

Figure 4.19d: Gradation test results for Martin Marietta, Shorter Siliceous Sand

4.6.1.1 Aggregate Chemical Analysis Testing

Samples of the aggregate were prepared for their chemical composition testing. The preparation involved crushing the aggregate samples to minus 3/8-in. in size. They were then sent to Wyoming Analytical Laboratories in Golden, Colorado for the chemical test. The chemical test involved the determination of the oxide residues in the compound. The main oxide residues tested for were silicon dioxide (SiO_2), calcium oxide (CaO), magnessium oxide (MgO), cardon dioxide (CO_2), manganese oxide (MnO), iron oxide (Fe_2O_3), aluminium oxide (Al_2O_3), sodium oxide (Na_2O), potassium oxide (K_2O), and titanium oxide (TiO_2). Table 4.6 shows the proportions of these oxide residues in the various aggregates.

Table 4.6: Chemical Analysis Results (Wyoming Analytical Laboratories 2008)

Oxide Residue	**Percent by Weight**			
	River Gravel	**Dolomitic Limestone**	**Granite**	**Siliceous Sand**
SiO_2	99.20	3.12	65.87	97.42
AL_2O_3	0.21	0.23	13.99	1.12
Fe_2O_3	0.24	0.11	3.26	0.48
CaO	0.03	40.16	5.68	0.08
MgO	0.05	11.82	1.69	0.07
Na_2O	0.05	0.01	3.90	0.03
K_2O	0.02	0.07	2.16	0.37
TiO_2	0.03	0.00	0.42	0.14
MnO	0.01	0.01	0.10	0.01
CO_2	0.07	44.31	2.62	0.17
Others	0.09	0.18	0.31	0.11

4.6.2 CHEMICAL ADMIXTURES

Chemical admixtures were used as needed in the concrete mixtures to control the slump and the total air content of the fresh concrete. All chemical admixtures were supplied by BASF Admixtures, Inc. Pozzolith 200N was used as a low-range water-reducing admixture, the dosage of which depended on the water-cement ratio used. Polyheed 1025 was used as a medium-range water-reducing admixture, the dosage of which also depended on the water-cement ratio used. MB AE 90 was used as the air-entraining admixture.

4.6.3 CEMENTITIOUS MATERIALS

In order to evaluate the effect of cementitious materials on the CTE of concrete, various cementitious materials, i.e. Type I and III portland cements, slag, and class C fly ash, were proposed to be considered for use in preparing the concrete samples, but this could not be done due to time constraints. Therefore only Type I portland cement was used. The Type I portland cement used was manufactured by Lafarge in Calera, Alabama.

CHAPTER 5

PRESENTATION AND DISCUSSION OF RESULTS

The results obtained from the laboratory testing program are presented in this chapter. Thus the test results of the fresh concrete properties as well as the hardened concrete properties are presented. The effect of the coarse aggregate type and volume, water-cement ratio, and sand-aggregate ratio on concrete CTE are statistically analyzed and discussed. At the end of the chapter, results from this experimental work are compared with those of the Federal Highway Administration (FHWA).

5.1 FRESH CONCRETE PROPERTY TEST RESULTS

Several tests were performed on the fresh concrete as described in Chapter 4. These included temperature, slump, total air content, and unit weight, all of which were performed in accordance with the appropriate ASTM standard. Table 5.1 shows the results of the fresh concrete properties. The normal range of slump observed was from 2 in. (50 mm) to 7.5 in. (190 mm). The target slump range was from 2 in. (50 mm) to 7 in. (180 mm). The average unit weight for samples made with river gravel was 148.4 pcf (2.38 g/cm^3), and that for samples made with granite was 150.3 pcf (2.41 g/cm^3), while that for samples made with dolomitic limestone was 152.0 pcf (2.44 g/cm^3). The range of total air content obtained was 1.5 % to 5.8 %.

Table 5.1: Results of fresh concrete properties

Concrete Mixture Identification	Slump (in.)	Temperature (^{o}F)	Air Content (%)	Unit Weight (pcf)
RG-40-32	5.5	68	2.1	151.2
RG-40-38	2.5	67	2.4	149.8
RG-40-44	5.0	68	4.8	146.1
RG-45-32	2.5	68	2.8	149.9
RG-45-38	3.0	70	2.8	149.3
RG-45-44	5.5	68	5.3	144.5
RG-50-32	3.3	75	3.0	149.9
RG-50-38	4.5	72	3.6	147.4
RG-50-44	2.0	70	3.7	147.2
GR-40-32	6.0	77	1.5	152.8
GR-40-38	2.0	72	2.0	152.3
GR-40-44	2.5	66	3.6	148.7
GR-45-32	5.0	76	2.0	152.4
GR-45-38	3.5	71	2.4	151.1
GR-45-44	2.0	73	4.8	147.7
GR-50-32	2.0	76	2.6	151.8
GR-50-38	3.5	72	2.8	150.2
GR-50-44	2.5	72	5.8	145.4
DL-40-32	7.0	71	1.5	155.1
DL-40-38	4.0	72	1.9	153.5
DL-40-44	3.0	76	3.5	150.3
DL-45-32	7.5	74	2.5	152.8
DL-45-38	4.0	69	2.5	152.5
DL-45-44	2.3	74	2.9	150.8
DL-50-32	3.5	72	2.5	154.0
DL-50-38	2.0	71	3.4	150.1
DL-50-44	2.0	72	3.9	149.2

5.2 HARDENED CONCRETE TEST RESULTS

The two main hardened concrete properties tested were the compressive strength and coefficient of thermal expansion (CTE) of concrete at a concrete age of 28 days. In Table 5.2, a summary of the tests is shown. The complete table of test results is shown in Appendix A.

Table 5.2 (a): CTE and compressive strength test results at a concrete age of 28 days

Concrete Sample Identification	CTE ($x10^{-6}$ in./in./°F)	Compressive Strength (psi)
RG-40-32	7.01	8270
RG-40-38	7.07	7520
RG-40-44	7.23	7580
RG-45-32	6.82	8580
RG-45-38	6.93	7490
RG-45-44	6.86	6420
RG-50-32	6.94	8960
RG-50-38	6.82	7250
RG-50-44	6.87	6330
DL-40-32	5.66	9800
DL-40-38	5.59	8730
DL-40-44	5.52	8340
DL-45-32	5.31	9150
DL-45-38	5.61	8790
DL-45-44	5.45	7200
DL-50-32	5.41	9910
DL-50-38	5.54	7770
DL-50-44	5.62	7250

Table 5.2 (b): CTE and compressive strength Test Results at a concrete age of 28 days

Concrete Sample Identification	CTE ($x10^{-6}$ in./in./°F)	Compressive Strength (psi)
GR-40-32	5.64	10300
GR-40-38	5.48	8390
GR-40-44	5.37	7430
GR-45-32	5.69	10600
GR-45-38	5.52	8670
GR-45-44	5.57	7990
GR-50-32	5.91	10260
GR-50-38	5.75	8400
GR-50-44	5.47	7820

From Tables 5.2 (a) and (b), it is evident that the CTEs of concretes made with river gravel are relatively higher than those of granite and dolomitic limestone. The average CTE for concretes made with river gravel is 6.95 x 10^{-6} in./in/^{o}F (12.5 x 10^{-6} in./in/^{o}C), and that for concretes made with granite is 5.60 x 10^{-6} in./in/^{o}F (10.1 x 10^{-6} in./in/^{o}C), while that for concretes made with dolomitic limestone is 5.52 x 10^{-6} in./in/^{o}F (9.9 x 10^{-6} in./in/^{o}C). These results are further presented graphically in Figures 5.1 (a) and (b). The concrete CTEs during the contraction segment (fall CTE) are plotted against the concrete CTEs during the expansion stage (rise CTE) for all aggregate types. Figure 5.1 shows that nearly all the data points have rise and fall CTEs within 0.5 x 10^{-6} /^{o}F (0.3 x 10^{-6} /^{o}C) range of each other as required by AASHTO TP 60 (2004), except for a single specimen. These plots further reveal that for most of the data points, the rise CTE was slightly greater than the fall CTE with the exception of a few cases where the reverse held true.

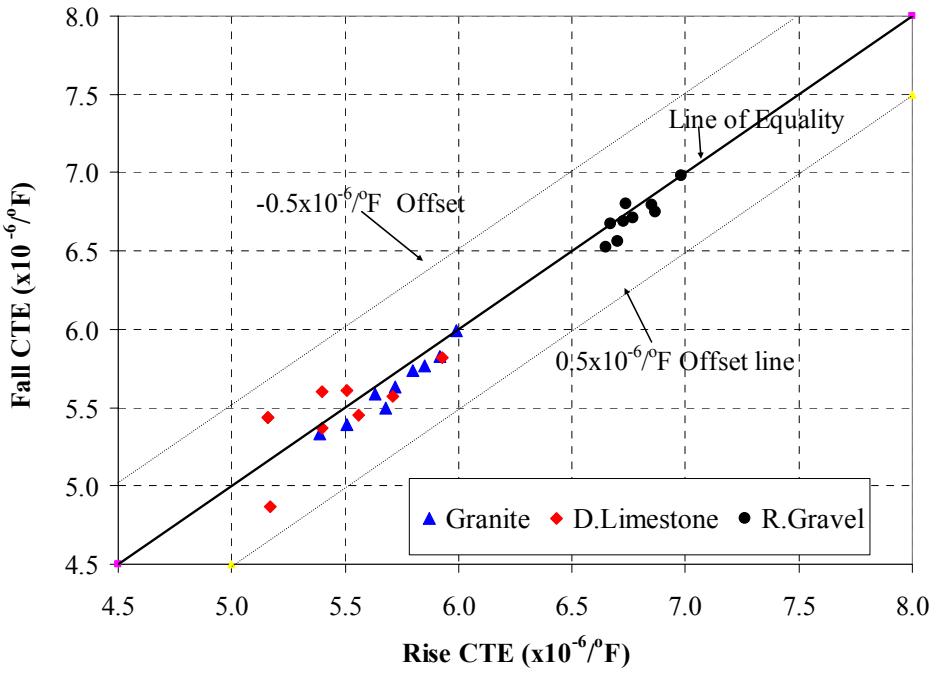

Figure 5.1 (a) Presentation of test results for Frame A

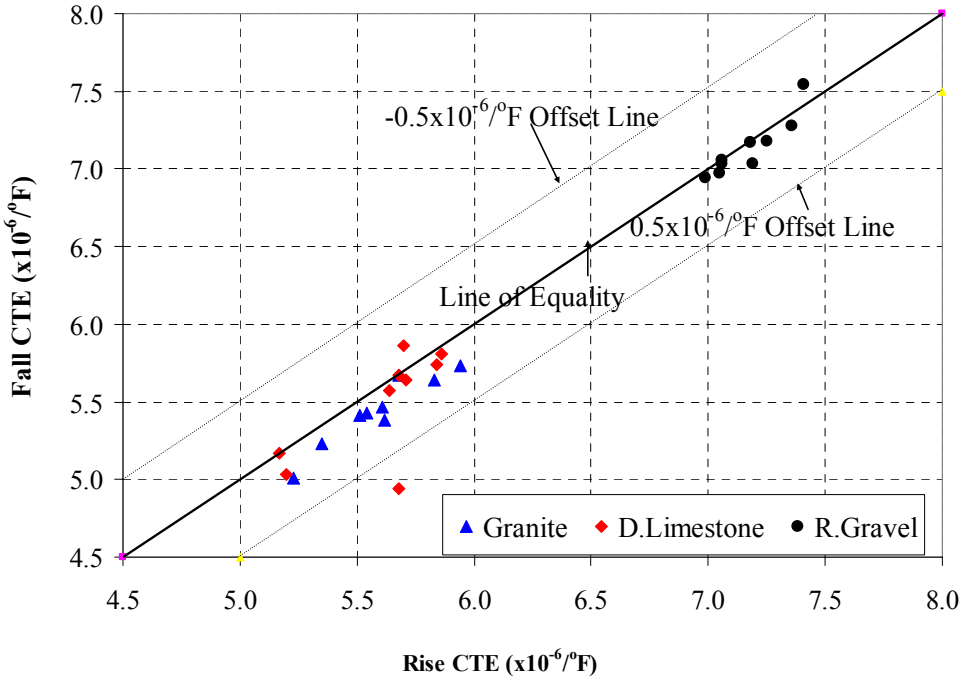

Figure 5.1(b): Presentation of test results for Frame B

5.3 STATISTICAL ANALYSIS AND INFERENCES FROM THE CTE TEST RESULTS

A statistical analysis was carried out on the CTE test results using the statistical software SAS 9.1 developed by the SAS Institute, Inc. The CTE test results were analyzed using the analysis of variance (ANOVA), generalized linear models (GLM), and the t-test methods. Hence PROC ANOVA, PROC GLM and PROC TTEST routines of SAS were used in the analyses. Proc GLM is a SAS procedure using the least squares method to fit general linear models (Suhr, 2002). GLM handles classification of variables that have discrete levels, as well as continuous variables, which measure quantities. The t-test and ANOVA examine whether group means differ from one another. The t-test compares two groups, while the ANOVA can be used with more than two groups. The t-test and ANOVA are based on three assumptions: independence, normality, and equality of variances assumptions, all of which were satisfied. PROCS GLM and ANOVA can be used interchangeably when the number of observations for each level of a factor is the same. PROC GLM is an "all-purpose" procedure that can be used to analyze all types of general linear models. It correctly handles unbalanced data in ANOVA (data is unbalanced when the levels of the independent variables have unequal sizes). Because PROC GLM will do many things, it is generally not as efficient as PROC ANOVA when the data is balanced (i.e. PROC GLM will use more computer resources to generate the same output as PROC ANOVA when the data is balanced. PROC GLM has to be used if the data is unbalanced (Diestelkamp, 2001).

The results from the statistical analyses are shown in Appendix B.

A P-value indicates the probability of error of the statement that a factor has a significant effect on the measured parameter. A lower P-value for a factor means that such factor has a higher level of significance. A probability of error (α) level of 0.05 was used. A factor is considered to be significant if the P-value of the factor is equal or less than 0.05. It should be noted, however, that a statistical significance may not necessary mean a practical significance.

The coefficient of determination, r^2, gives the proportion of the variance (fluctuation) of one variable that is predictable from the other variable. It is a measure that allows one to determine how certain one can be in making predictions from a certain linear relation. The coefficient of determination is such that $0 \leq r^2 \leq 1$. A coefficient of determination of 1 means that 100 % of the total variation in the dependent variable can be explained by the linear relationship between the independent variable and the dependent variable while for a coefficient of determination of 0, it implies that the total variation in the dependent variable cannot be explained by the linear relationship.

The analyses were undertaken to determine:

A. The difference in values between :

- The rise and fall CTEs,
- Frames A and B CTEs, and
- The CTEs of concretes made with the different rock types.

B. The effect of :

- Water-cement ratio on the concrete CTE, and
- Sand-aggregate ratio on the concrete CTE.

5.3.1 Statistical Analysis of the Coefficient of Thermal Expansion Values for the Rise and Fall Test Segments

A t-test carried out at a 95 % confidence level for the rise and fall CTE values for frame A, returned a P-value of 0.91. By statistical inference, a P-value = 0.91 > alpha (α) = 0.05 suggests evidence of no difference in the mean values between the rise and fall CTEs for frame A.

Similarly, a P-value of 0.72 was obtained for a t-test performed at 95 % confidence level on the rise and fall CTE values for frame B. Since the P-value = 0.72 > alpha (α) = 0.05, statistically, this gives an indication of no difference in the mean values between the rise and fall CTEs for frame B.

Moreover, the AASHTO TP 60 (2004) test procedure requires the test result to be the average of two CTE values, provided they are within 0.5 x 10^{-6} /^{o}F (0.3 x 10^{-6} /^{o}C) of each other. This requirement is satisfied by the pairs of rise and fall CTEs for all the specimens for both frames A and B as shown in Table A1 in Appendix A and also in Figures 5.1 (a) and (b). The averages of the rise and fall CTE were therefore used as the representative CTE for each concrete sample for each frame.

5.3.2 Statistical analysis of the Coefficient of Thermal Expansion Values for Frames A and B

A t-test carried out at a 95 % confidence level on the CTE values for frames A and B returned a P-value of 0.16. Statistically, a P-value = 0.16 > alpha (α) = 0.05, suggest evidence of no difference in values between the CTEs of frames A and B.

A closer examination of the CTE values for both frames A and B also reveals that, almost all of the CTEs are within 0.5 x 10^{-6} /^{o}F (0.3 x 10^{-6} /^{o}C) of each other as required

by AASHTO TP 60 (2004). Hence the CTE value for a concrete sample can be reported as the average of the CTEs for both frames A and B.

5.3.3 Statistical Analysis of the Coefficient of Thermal Expansion Values for Concretes Made of the Different Rock Types

Results of the analysis of variance (ANOVA) test carried out on the CTE values for concretes made of the different rock types suggest that there is substantial evidence of a difference in the mean CTE values. This is evidenced by a P-value of < 0.0001, since the P-value = $< 0.0001 \ll$ alpha (α) = 0.05 at a 95 % confidence level.

Additionally, when using the procedure GLM with the t-test option (see Table 5.3), it was observed that there is substantial difference in the mean CTEs for the concretes made of river gravel, granite and dolomitic limestone. In Table 5.3, this is shown by the t-test grouping, where the mean concrete CTEs with the same letter i.e. Y, are not significantly different while means with different letters i.e. X and Y are significantly different. The analysis revealed that the mean CTEs for concretes made of granite and dolomitic limestone are not significantly different from each other but are significantly different from that of concretes made of river gravel.

Table 5.3: Proc GLM t-test grouping of the mean CTEs for concretes made with the different coarse aggregates

t-Test Grouping	Mean (x 10^{-6} /^{o}F)	Coarse Aggregate Type
X	6.95	River Gravel
Y	5.60	Granite
Y	5.52	Dolomitic Limestone

5.3.4 Statistical Analysis to Show the Effect of the Water-Cement Ratio on the Concrete Coefficient of Thermal Expansion

An ANOVA test was carried out to determine the effect of the water-cement ratio (0.32, 0.38, and 0.44) on the concrete CTE and a P-value of 0.991 was found. Statistically, a P-value = 0.991 > alpha (α) = 0.05 gives an indication of no difference in the means of the CTEs. Hence it can be inferred that the water-cement ratio has no significant effect on the concrete CTE.

Further statistical analysis, using procedure GLM in SAS also confirmed the above findings. In Table 5.4, the results of the GLM procedure are shown. It is observed that the mean CTEs for concretes made with the different water-cement ratios i.e. 0.32, 0.38, and 0.44, are not significantly different from each other. Hence this is indicated by the same letter in the t-test grouping. That is to say, mean CTEs that are statistically the same are represented by the same letter i.e. Y while those that differ from each other statistically are represented by different letters i.e. X and Y.

Table 5.4: Proc GLM t-test grouping of the mean CTEs of concretes made with the different water-cement ratios

t-Test Grouping	Mean (x 10^{-6} /^{o}F)	Water-Cement Ratio
Y	6.03	0.38
Y	6.01	0.44
Y	5.99	0.32

5.3.5 Statistical Analysis to Show the Effect of the Sand-Aggregate Ratio on the Concrete Coefficient of Thermal Expansion

The ANOVA test carried out to determine the effect of sand-aggregate ratio on the concrete CTE returned a P-value of 0.960. Statistically, a P-value=0.960 > alpha (α) = 0.05 gives an indication of no difference in the means of the CTEs. Hence, it maybe inferred that the sand-aggregate ratio has no significant effect on the concrete CTE.

Further statistical analysis, using procedure GLM in SAS, also confirmed the above findings. In Table 5.5, the results of the GLM procedure are shown. It is observed that the mean CTEs for concretes made at the different sand-aggregate ratios, i.e. 0.40, 0.45, and 0.50, are not significantly different from each other. Hence, it is indicated by the same letter, Y, in the t-test grouping.

Table 5.5: Proc GLM t-test grouping of the mean CTEs for concretes made of the different sand-aggregate ratios

t-Test Grouping	Mean (x 10^{-6} /^{o}F)	Sand-Aggregate Ratio
Y	6.06	0.40
Y	6.00	0.50
Y	5.97	0.45

5.3.6 Summary

Table 5.6 summarizes the P-values and correlation coefficients (r^2) obtained from the statistical analysis carried out on the concrete CTE values. Table 5.6 shows that coarse aggregate type has the most significant effect on the concrete CTE. This is evidenced by a correlation coefficient of 0.96085, and a P-value of < 0.0001. The sand-aggregate ratio, with a correlation coefficient value of 0.00302 and a P-value of 0.960 has

a greater effect on the concrete CTE than the water-cement ratio. The water-cement ratio with a correlation coefficient value of 0.00076 and a P-value of 0.991 has the least effect on the concrete CTE.

Table 5.6: Summary of p-values and correlation coefficients

Parameter	P-Value	Correlation Coefficient
Coarse aggregate type	< 0.0001	0.96085
Sand-aggregate ratio	0.960	0.00302
Water-cement ratio	0.991	0.00076

5.4 DISCUSSION OF COEFFICIENT OF THERMAL EXPANSION TEST RESULTS

Statistical analysis presented in Section 5.3 revealed that there is no difference in the mean values of the concrete CTE between those of the rise and fall and also those of frames A and B.

The AASHTO TP 60 (2004) requires test results from different test segments to be within 0.5 x 10^{-6} /^{o}F (0.3 x 10^{-6} /^{o}C) of each other. This requirement is fulfilled by the CTE test results as shown in Table A1 in Appendix A. The average of the CTE values from frames A and B were therefore used in representing the CTE for a concrete sample.

The plots of the average concrete CTE versus the water-cement ratio are shown in Figures 5.2 (a), (b), and (c). This was plotted for the different sand-aggregate ratios of 0.40, 0.45, and 0.50. In this section, a discussion on how the water-cement ratio, sand-aggregate ratio, and the coarse aggregate type affect concrete CTE is presented.

Explanations are also provided as to why and how each of these parameters affects the concrete CTE.

5.4.1 Variation of the Concrete Coefficient of Thermal Expansion with the Coarse Aggregate Type

From Figures 5.2 (a), (b), and (c), it is observed that the CTEs of concretes made with river gravel (average = 6.95 x 10^{-6} /^{o}F), are highest compared with those made of granite (average = 5.60 x 10^{-6} /^{o}F) and dolomitic limestone (average = 5.52 x 10^{-6} /^{o}F).

This is believed to be due to the chemical composition (Table 4.6) of the coarse aggregates. The river gravel has the highest percentage of silicon dioxide, i.e. 99.20 %, while the granite has 65.87 %, and the dolomitic limestone has 3.12 %. In Section 2.1.2.1 and Table 2.2, it was noted that aggregate mineral composition strongly affects the CTE of concrete and that an increase in the volume of the silicon dioxide increases the concrete CTE (Figure 2.9). Hence, concretes made of river gravels will have the highest CTE, and dolomitic limestone, which has the lowest percentage of silicon dioxide, will have the lowest CTE. Also, it was noted that the CTEs of concretes made of granite and dolomitic limestone are similar. However, concretes with granite have a slightly higher CTE than those made of dolomitic limestone.

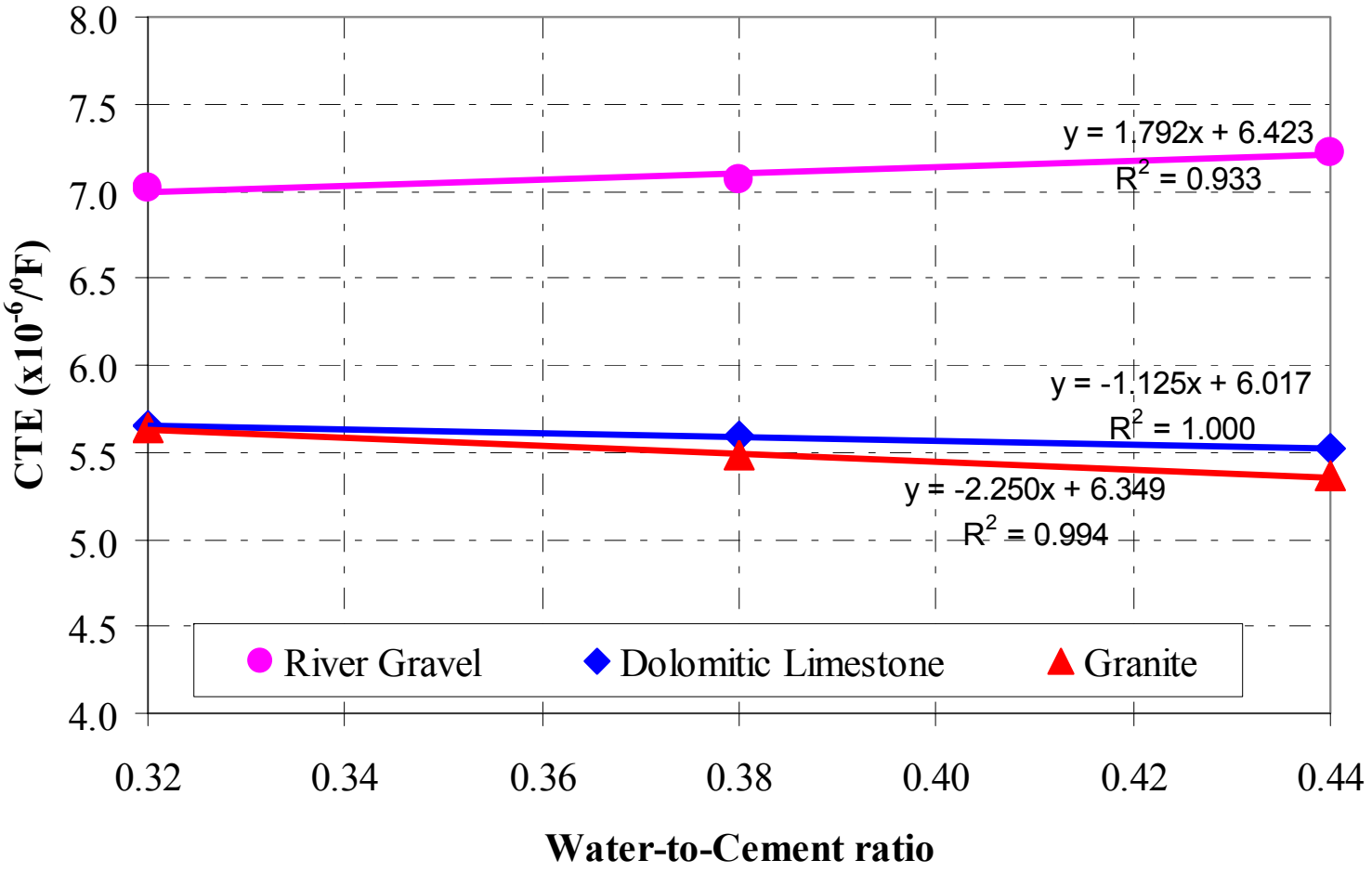

Figure 5.2 (a): Effect of water-cement ratio on the concrete CTE for sand-aggregate ratio of 0.40

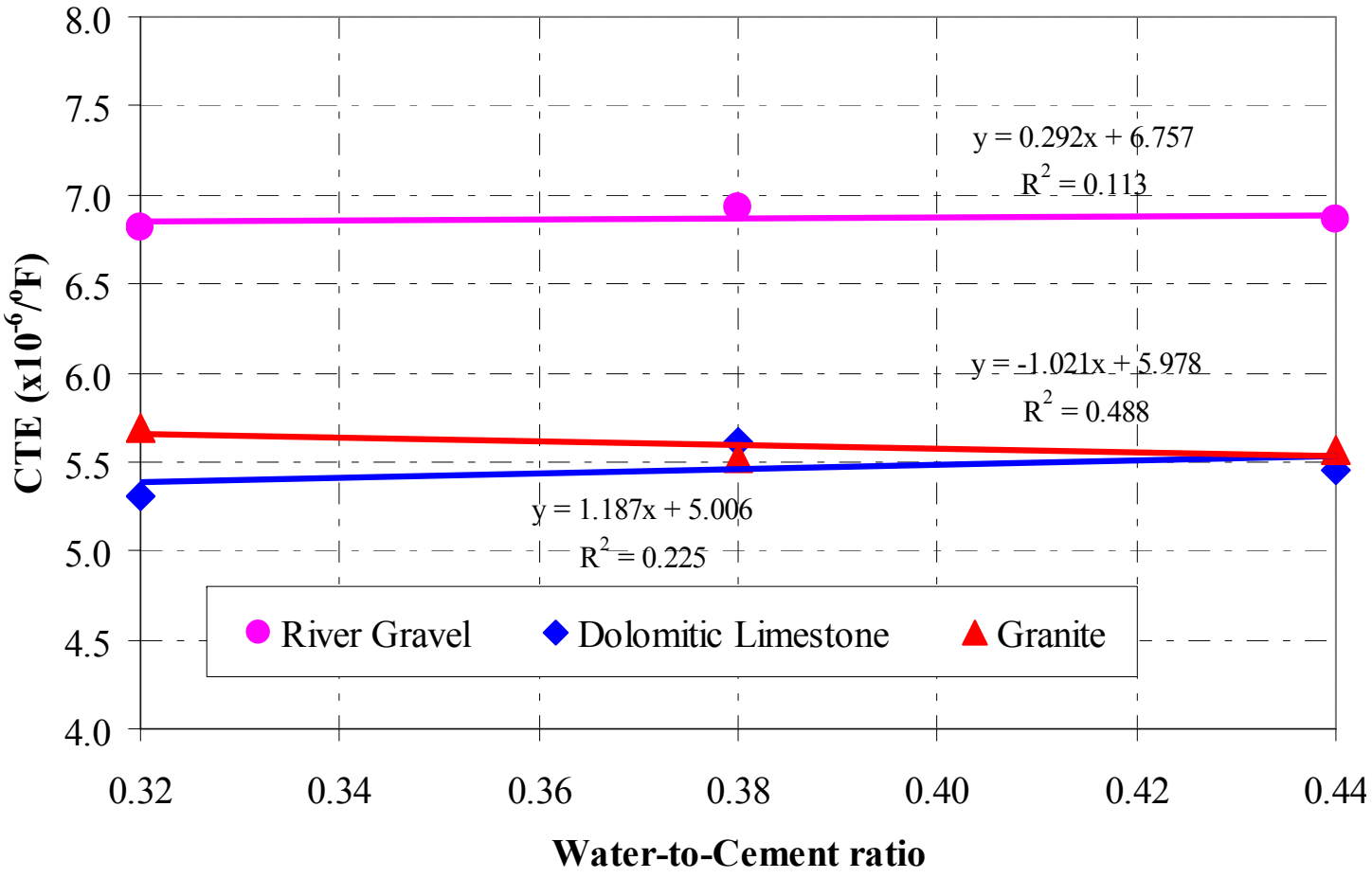

Figure 5.2 (b): Effect of water-cement ratio on the concrete CTE for a sand- aggregate ratio of 0.45

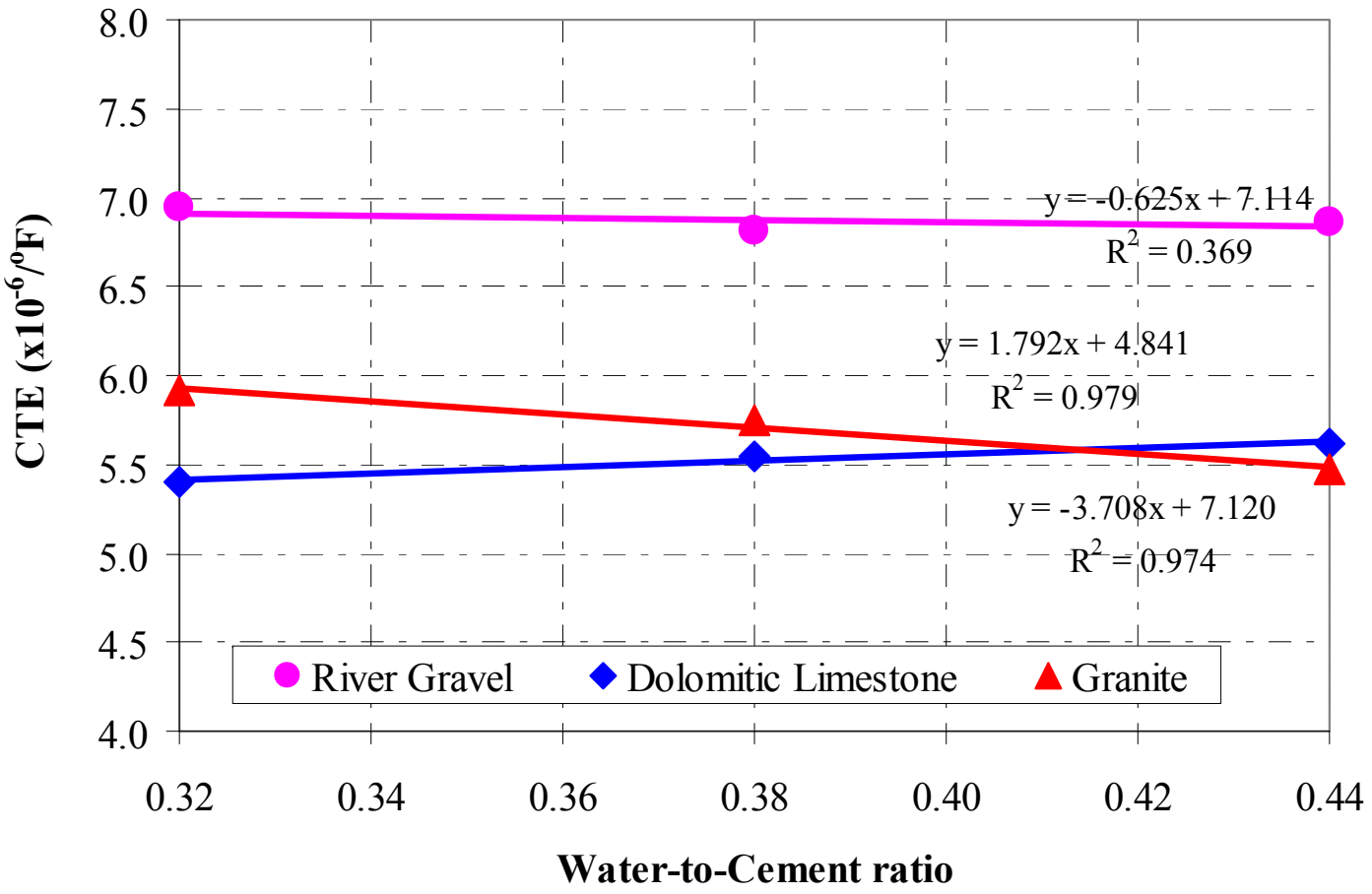

Figure 5.2(c): Effect of water-cement ratio on the concrete CTE for sand-aggregate ratio of 0.50

5.4.2 CONCRETES MADE OF RIVER GRAVEL

In this section, the variation of the concrete CTE with the sand-aggregate ratio and the water-cement ratio is discussed for concretes made of river gravel.

5.4.2.1 Variation of the Concrete Coefficient of Thermal Expansion with Sand-Aggregate Ratio

The CTEs of concretes made with river gravel, as observed from Figures 5.2 (a), (b), and (c) and summarized in Table 5.7, are highest for the sand-aggregate ratio of 0.40. They are lowest for a sand-aggregate ratio of 0.50 at a constant paste volume. At a sand-aggregate ratio of 0.40, the concrete mixture has higher river gravel content (i.e. 40 % of total concrete mixture) than at a sand-aggregate ratio of 0.50 (i.e. 34 % of total concrete mixture). Conversely, the siliceous sand content increases by the same amount as the decrease in river gravel content from a sand-aggregate ratio of 0.40 to a sand-aggregate ratio of 0.50.

Table 5.7: Effect of water-cement ratio and sand-aggregate ratio on CTE of concretes made of river gravel

Water-cement ratio		0.32		0.44	
Sand-aggregate ratio		0.40	0.50	0.40	0.50
Concrete CTE	**(x 10^{-6}) /^{o}F**	7.01	6.94	7.23	6.87
	(x 10^{-6}) /^{o}C	12.62	12.49	13.01	12.37

In Table 4.6, it was noted that the silicon dioxide content of river gravel, i.e. 99.20%, was higher than that for siliceous sand, i.e. 97.42 %. From Figure 2.9 and the discussion in Section 2.1.2.1, it was found out that the higher the silicon dioxide content, the higher the CTE of the aggregate and hence the concrete mixture. Similarly, in Section 2.1.2.2, it was noted that increasing the volume of the siliceous river gravel will increase the concrete CTE. From the above discussions, it is realized that the increase in volume of the siliceous river gravel from a sand-aggregate ratio of 0.50 to a sand-aggregate ratio of 0.40 will cause a slight increase in the concrete CTE as noted in the statistical analysis.

5.4.2.2 Variation of the Concrete Coefficient of Thermal Expansion with Water-Cement Ratio

It was observed from Figures 5.2 (a), (b), and (c) that as the water-cement ratio increases from 0.32 to 0.44, the concrete CTE increases. This was observed for all cases except for the case of sand-aggregate ratio of 0.50 where the concrete CTE tends to decrease with an increase in the water-cement ratio.

As the water-cement ratio increases from 0.32 to 0.44, the total volume of cement paste decreases from approximately 35 % to approximately 31 % of the total volume of the concrete mixture. Ideally, this decrease in the paste content should have caused a corresponding decrease in the concrete CTE. However, this was observed not to be the case. The total volume of the aggregates also increases from approximately 65 % to approximately 69 % of the total volume of the concrete mixture when the water-cement ratio increases from 0.32 to 0.44. This increment in the volume of the total aggregate content is believed to be the cause of the increase in the concrete CTE. The aggregates

having a total volume of approximately 69 % of the total volume of the concrete mixture are believed to have a greater influence on the concrete CTE than does the cement paste, although the CTE of the paste is known to be higher than that of the aggregates.

Moreover, the siliceous river gravel and siliceous sand have higher percentages of silicon dioxide i.e. 99.20 % and 97.42 % (Table 4.6). As shown and discussed in Figure 2.9, and in Sections 2.1.2.1 and 2.1.2.2, an increase in the volume of the total aggregates and hence the silicon dioxide content, will cause a corresponding increase in the CTE.

Hence, increasing the water-cement ratio causes a slight increase in the concrete CTE despite the decrease in the total volume of the paste.

At a constant sand-aggregate ratio of 0.45, the total volume of the siliceous sand in the concrete mixture is 3 % higher, and that of the river gravel is 3 % lower compared to the case of sand-aggregate ratio being 0.40. The total volume of aggregates in the concrete mixture is approximately 65 % at a water-cement ratio of 0.32 and approximately 69 % at a water-cement ratio of 0.44.

As discussed earlier, the volume and type of the aggregate is known to have a greater influence on the concrete CTE. Therefore, with the increase in the total volume of the aggregates, i.e. siliceous river gravel and siliceous sand, the CTE will increase. However, this increase was observed not to be of the same proportion as for the case when the sand-aggregate ratio was 0.40. It was observed to be less as evidenced in the slopes of the graph, with the slope of the graph for the case when the sand-aggregate ratio is 0.45 being less. This is believed to be due to the increase in the siliceous sand content, and the decrease in the siliceous river gravel content. The reason for this is that the

volume of the siliceous river gravel in the concrete mixture is greater than that of the siliceous sand; hence the effect of a 3 % decrease in the volume of the siliceous river gravel will be greater than that of a 3 % increase in the volume of the siliceous sand. Moreover, in experimental works to determine the effect of fine aggregate type on the concrete CTE, Ziegeldorf, Kleiser and Hilsdorf (1978) concluded that the effect of coarse aggregate on the concrete CTE is greater than that of the fine aggregate.

At a constant sand-aggregate ratio of 0.50, the total volume of the siliceous sand has increased to approximately 49 % of the total aggregate content in the concrete mixture. Compared with the case of the sand-aggregate ratio being 0.45, it is noted that the volume of siliceous sand in the concrete mixture has increased by approximately 3 % and that of river gravel decreased by approximately 3 % at a constant water-cement ratio. The total volume of the aggregate, therefore, remains unchanged. However, it increases from 65 % at a water-cement ratio of 0.32 to 69 % at a water-cement ratio of 0.44 as observed in the previous cases. It was expected that with the increase in the water-cement ratio, and hence an increase in the total aggregate content, there would have been a corresponding increase in the concrete CTE as observed in earlier cases. However, this was not the case; rather there was a decrease in the concrete CTE. A possible reason for this could be that perhaps, the decrease in the volume of the coarse aggregate has a greater effect on the concrete CTE than does the increase in the volume of the siliceous sand, even when the volume of the siliceous sand is 49 % of the total aggregate content. As stated earlier, Ziegeldorf, Kleiser and Hilsdorf (1978) reported that the effect of fine aggregate on the concrete CTE is smaller, compared to the effect of coarse aggregate.

Hence it is believed that the decrease in the river gravel content might have caused a decrease in the concrete CTE.

The case of sand-aggregate ratio of 0.50 appears to follow the trend observed by Berwanger and Sarkar (1976). Based on research works conducted to determine the CTE of concrete and reinforced concrete samples, they concluded that the CTE increases with a decrease in the water-cement ratio.

In conclusion, it is noted that the water-cement ratio slightly affects the CTE of concretes made with siliceous river gravel for the ranges of water-cement ratios, 0.32 to 0.44, and at varying paste contents as confirmed in the statistical analysis. However, this result contrasts with the research findings by Alungbe et al. (1992). Their research work to determine the effect of aggregates and water-cement ratio on concrete CTE concluded that the water-cement ratio did not show any effect on the CTE.

5.4.3 CONCRETES MADE WITH GRANITE

In this section, the variation of the concrete CTE with the sand-aggregate ratio and the water-cement ratio are discussed for concretes made with granite.

5.4.3.1 Variation of the Concrete Coefficient of Thermal Expansion with Sand-Aggregate Ratio

As observed from Figures 5.2 (a), (b), and (c), and summarized in Table 5.8, when the sand-aggregate ratio increases from 0.40 to 0.50 at a constant water-cement ratio, the concrete CTE also slightly increases. The concrete CTE was observed to be highest for the case when the sand-aggregate ratio is 0.50 and lowest when the sand-aggregate ratio is 0.40, unlike in the case of the river gravel.

Table 5.8: Effect of water-cement ratio and sand-aggregate ratio on CTE of concretes made of granite

Water-cement ratio		0.32		0.44	
Sand-aggregate ratio		0.40	0.50	0.40	0.50
Concrete CTE	**(**x 10^{-6}) /^{o}**F**	5.64	5.91	5.37	5.47
	(x 10^{-6}) /^{o}**C**	10.15	10.64	9.67	9.85

As the sand-aggregate ratio increases from 0.40 to 0.50, the volume of the siliceous sand in the concrete mixture increases by approximately 6 % of its original volume, and that of the granitic rock also decreases by approximately 6 % of its original volume. In Table 4.6, it was noted that granite has a calcium oxide content of 5.68 % and a silicon dioxide content of 65.87 %, while the siliceous sand has a calcium oxide content of 0.08 % and a silicon dioxide content of 97.42 %. When the sand-aggregate ratio increases from 0.40 to 0.50, and hence the volume of the siliceous sand in the mixture increases, the concrete CTE increases although the volume of the granite decreases. This is not to say that the decrease in the volume of the granite has little or no effect on the concrete CTE. Rather, when the volume of the granite decreases, the calcium oxide content contributed by the coarse aggregate decreases as well, and as discussed in Section 2.1.2.1, and shown in Figure 2.10, a decrease in the calcium oxide content will increase the concrete CTE. Moreover, the volume of the siliceous sand increases, and this causes an increase in the silicon dioxide content; hence, as shown in Figure 2.9, this will also cause a slight increase in the concrete CTE.

5.4.3.2 Variation of the Concrete Coefficient of Thermal Expansion with Water-Cement Ratio

It was also observed from Figures 5.2 (a), (b), and (c) that when the water-cement ratio increases from 0.32 to 0.44, and for all cases of the sand-aggregate ratio (i.e. 0.40, 0.45, and 0.50), the concrete CTE slightly decreases.

As the water-cement ratio increases from 0.32 to 0.44, at a constant sand-aggregate ratio, the total paste volume in the concrete mixture decreases by approximately 3 %. Correspondingly, the total aggregate volume increases by approximately 3 %. At a water-cement ratio of 0.32, the paste content of the concrete mixture is estimated to be approximately 35 %, while at a water-cement ratio of 0.44 it is estimated to be about 32 % of the total volume of the concrete mixture. Therefore, at a water-cement ratio of 0.44 the volume of the granite must be higher than at a water-cement ratio of 0.32, since the sand-aggregate ratio is constant. In Table 4.6, it was noted that granite has a calcium oxide content of 5.68 % and a silicon dioxide content of 65.87% while the siliceous sand has a calcium oxide content of 0.08 % and a silicon dioxide content of 97.42 %. Hence at a water-cement ratio of 0.44, with a higher volume of granite, there will be a higher percentage of calcium oxide in the concrete mixture than at a water-cement ratio of 0.32. Therefore, in line with the discussions of Sections 2.1.2.1 and 2.1.2.2, and also from Figure 2.10, where it was shown that an increase in the volume of the calcium oxide will decrease the concrete CTE, it follows that at a water-cement ratio of 0.32, the concrete CTE will be higher than at a water-cement ratio of 0.44, hence the negative slope of the graph.

5.4.4 CONCRETES MADE WITH DOLOMITIC LIMESTONE

In this section, the variation of the concrete CTE with the sand-aggregate ratio and the water-cement ratio is discussed for concretes made of dolomitic limestone.

5.4.4.1 Variation of the Concrete Coefficient of Thermal Expansion with Sand-Aggregate Ratio

The CTEs of concrete made with dolomitic limestone are shown plotted against the water-cement ratios in Figures 5.2 (a), (b), and (c). This is further summarized in Table 5.9. It is observed from Figures 5.2 (a), (b), and (c) that the CTE of concrete made from dolomitic limestone average tends to be highest for the sand-aggregate ratio of 0.40 and lowest for the sand-aggregate ratio of 0.45. This is not as expected. It was expected that the concrete CTE would be highest for the sand-aggregate ratio of 0.50 and least for the sand-aggregate ratio of 0.40 as observed in the case of the granites.

At a sand-aggregate ratio of 0.50, the volume of the siliceous sand is highest, compared with the cases of sand-aggregate ratio of 0.40 and 0.45. Correspondingly, the percentage of silicon dioxide in the concrete mixture is also comparatively highest. Moreover, since the volume of the dolomitic limestone has reduced and so has the volume of calcium oxide, the concrete CTE was expected to be highest at a sand-aggregate ratio of 0.50 than at a sand-aggregate ratio of 0.40 or 0.45.

Table 5.9: Effect of water-cement ratio and sand-aggregate ratio on CTE of concretes made of dolomitic limestone

Water-cement ratio		0.32		0.44	
Sand-aggregate ratio		0.40	0.50	0.40	0.50
Concrete CTE	**(**x 10^{-6}) /^{o}**F**	5.66	5.41	5.52	5.62
	(x 10^{-6}) /^{o}**C**	10.20	9.74	9.94	10.12

5.4.4.2 Variation of the Concrete Coefficient of Thermal Expansion with Water-Cement Ratio

From Figures 5.2 (a), (b), and (c), it is also observed that at a constant sand-aggregate ratio of 0.40, the concrete CTE decreases with increasing water-cement ratio (I.e. the slope of the graph tends to be negative). As the water-cement ratio increases from 0.32 to 0.44, the total volume of the aggregates in the concrete mixture also increases by approximately 4 %. Accordingly, the volume of the dolomitic limestone increases. From Table 4.6, it is noted that the calcium oxide content of the dolomitic limestone is 40.16 % while the calcium oxide content of the siliceous sand is 0.008 %. Hence the total volume of the calcium oxide in the concrete mixture also increases when the dolomitic limestone content increases. In Sections 2.1.2.1 and 2.1.2.2, and also from Figure 2.10, it was noted that an increase in the calcium oxide content will cause a decrease in the concrete CTE. Hence, when the volume of the dolomitic limestone increases, the concrete CTE will decrease accordingly.

However, at sand-aggregate ratios of 0.45 and 0.50, it was observed that the concrete CTE slightly increases with an increase in the water-cement ratio. This was unexpected. It was expected that the concrete CTE would decrease with an increase in the

water-cement ratio just as in the case of the granite. Since as the water-cement ratio increases from 0.32 to 0.44, the total volume of the cement paste in the concrete mixture decreases by 4 % and hence the total volume of the aggregates increases by 4 %. Accordingly, the total volume of the calcium oxide in the concrete mixture will increase. As observed from Figure 2.10, it was expected that the concrete CTE would decrease with the increasing volume of the dolomitic limestone. A possible reason could be that when the water-cement ratio increases, the total volume of the aggregates increases. Hence the volume of the siliceous sand also increases since the sand-aggregate ratio is a constant. The siliceous sand has a higher content of silicon dioxide (Table 4.6) and as noted in Figure 2.9, an increase in the silicon dioxide content of the aggregate will cause a corresponding increase in the concrete CTE. This is believed to be the possible cause of the increase in the concrete CTE as the water-cement ratio increases. Since the case of the sand-aggregate ratio of 0.50 has a higher volume of siliceous sand than the case of the sand-aggregate ratio of 0.45, the slope of the graph for the sand-aggregate ratio of 0.50 is steeper.

In summary, it is noted that the water-cement ratio slightly affects the CTE of concretes. This holds true for the range of water-cement ratios, 0.32, 0.38, and 0.44, and at varying paste contents. Contrary to this, Alungbe et al. (1992) when determining the effect of aggregates and water-cement ratio on concrete CTEs, concluded that the water-cement ratio did not have any effect on the CTE. Their work was carried out on samples with water-cement ratios of 0.33, 0.45, and 0.53 and at varying paste content.

5.5 COMPARISON OF RESULTS WITH LITERATURE

In this section, results from the laboratory-tested samples are compared with results from the Federal Highway Administration (FHWA), and those from a computer program, CHEM 2 by Dossey, Basley and Speer (1994).

5.5.1 FEDERAL HIGHWAY ADMINISTRATION (FHWA) RESULTS

In Figure 5.3, results obtained from this study performed at Auburn University (AU) are compared with those from FHWA's Turner-Fairbank Highway Research Center (TFHRC) in McLean, Virginia. The research at TFHRC was carried out as part of the Long Term Pavement Performance (LTPP) program of the Strategic Highway Research Program (SHRP) where hundreds of cored samples were tested.

It is realized that for concretes made of granitic rocks, the CTEs are quite similar. However for concretes made of gravel the results showed a major difference in the CTE values obtained. Similarly, for concretes made of *dolomitic limestone* (in the case of AU study) and *limestone* and *dolomite* (in the case of FHWA), the result are considerably different.

However, the value of the CTE obtained for concrete made with gravel in the Auburn University study compare well with those reported in literature: 6.8×10^{-6} /^{o}F (Neville and Brooks 1987) and 6.6×10^{-6} /^{o}F (Mehta and Monteiro 2006).

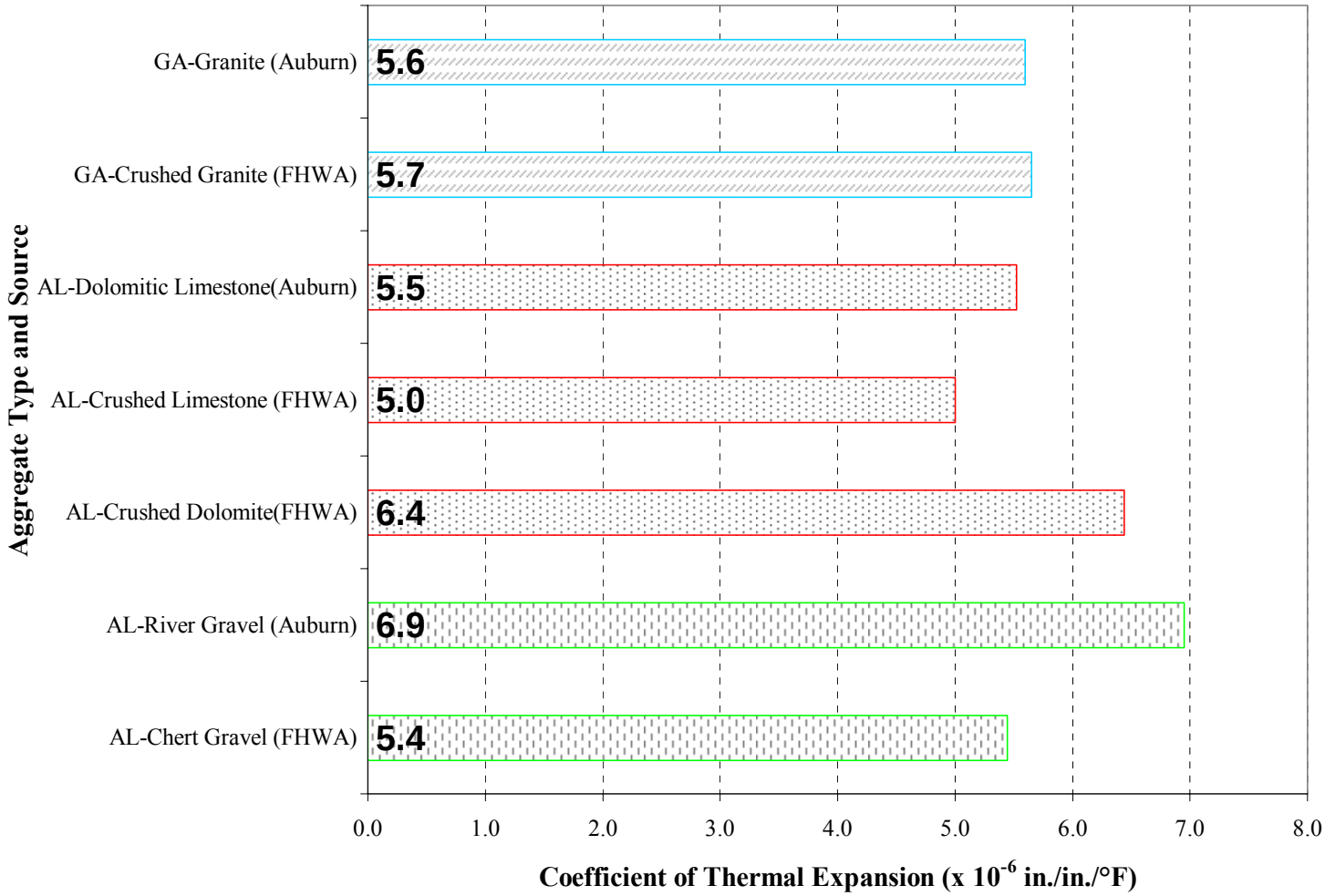

Figure 5.3: Comparism of results from Auburn University with those of FHWA

5.5.2 CHEM 2 PROGRAM

As presented earlier in Chapter 4, chemical analyses of the four aggregates types were undertaken by Wyoming Analytical Laboratories Incorporated, Colorado to determine the main oxide residues present in each of the aggregate samples. The CHEM2 program developed as part of a research work at the University of Texas in Austin was used in determining the mineralogical composition of the aggregates except for siliceous river gravel and siliceous sand. The CHEM 2 program was also used in determining the concrete CTE for concretes made of the various aggregates except for the siliceous river gravel. The program did not run for the cases of siliceous river gravel and siliceous sand. Rather, it consistently gave an error message: *error # 5, an unforeseeable error has occurred*. Hence the model predicted by Dossey et al. (1994) could not be used to estimate the concrete CTE for concretes made of siliceous river gravel.

A CTE of 2.60 x 10^{-6} /^{o}F (4.68 x 10^{-6} /^{o}C) was obtained from running the CHEM2 program on the oxide residue values for *dolomitic limestone*. This CTE value does not compare favorably with the CTE for *limestone* concrete, 3.33 x 10^{-6} /^{o}F (6 x 10^{-6} /^{o}C) found in literature (Merta and Monteiro 2006) or with that from the AU study, which is 5.52 x 10^{-6} in./in./^{o}F (9.90 x 10^{-6} in./in./^{o}C).

A CTE of 24.78 x 10^{-6} /^{o}F (44.60 x 10^{-6} /^{o}C) was obtained after running the CHEM 2 program on the oxide residue values for *granite.* This value of CTE is just too high and impracticable. Also it does not compare well with the CTE of *granite*, 4.44 x 10^{-6} /^{o}F (8 x 10^{-6} /^{o}C) found in literature (Merta and Monteiro 2006) or with that from the AU, which is 5.60 x 10^{-6} in./in./^{o}F (10.08 x 10^{-6} in./in./^{o}C).

5.6 LESSONS LEARNT

- It was noted that when the concrete sample is set in the Invar frame such that the readings on the LVDT readout are within the range of 0.00000 in. to ± 0.00300 in., the LVDT displacement remained well within the linear range during expansion and contraction.
- It appears the LVDT type, even if they are from the same manufacturer affects the net displacement measured on the LVDT.
- Water vapor in the external bath condensed and found its way into the LVDT when the external bath was covered. This caused the LVDT to give bad readings. However, when the external bath was left open, the malfunctioning of the LVDT ceased.
- It was realized that the water level in the external bath should be kept relatively constant at all time. This is to ensure that the expansion of the Invar frame remained the same throughout the experiment, and equal to that noted during the correction factor determination.

CHAPTER 6

CONCLUSIONS AND RECOMMENDATIONS

Early-age cracking in concrete structures is a growing dilemma throughout the United States, structures such as bridge decks, and pavements are all prone to problems related to early-age cracking (Krauss and Rogalla 1996; Whigham 2005; Rao 2008). Self-induced stresses arise when thermal deformations are restrained. Increasing recognition of the potential magnitudes of thermal deformations and stresses induced in integral or tied structures, especially bridges, suggests the need for a realistic coefficient of thermal expansion, rather than assumed values often used for design (Emanuel and Hulsey 1977).

Mitchell (1953) reports that, in the past, several researchers have shown that low durability of concrete could be caused by thermal incompatibility between the cement mortar and the aggregate. This incompatibility has generally been attributed to the wide differences in the coefficients of thermal expansion (CTE) of the various materials. Material selection, especially the coarse aggregate type becomes an important issue. It is obvious that concrete is a composite construction material and that its CTE depends on its components as well as the concrete age and environmental factors (Emanuel and Hulsey 1977; Mindness, Young and Darwin 2002). Therefore for sound design practice, it is imperative to determine the CTE of concretes made with local materials and also select

the materials wisely.

This research, as part of its objective aims at advising on the CTE for concretes made with locally available material for the Alabama concrete industry and also evaluates the AASHTO TP 60 (2004) since it is relatively a new test method.

In order to achieve this, a test setup based on the AASHTO TP 60 (2004) was developed to carry out this experiment. Several concrete samples were made in the laboratory and used for this investigation. The effect on the concrete CTE of the coarse aggregate type was investigated by using three different coarse aggregates, namely siliceous river gravel, granite, and dolomitic limestone. The effect of the aggregate volume on the concrete CTE was also assessed using the sand-aggregate ratios of 0.40, 0.45, and 0.50. The effect of the paste content on the concrete CTE was also investigated using the water-cement ratios 0.32, 0.38, and 0.44. Each concrete mixture was made in the laboratory under a controlled environment, and then cured for 28 days in accordance with ASTM C 192 (2002). The concrete samples were then set up as per AASHTO TP 60 (2004) test for the CTE testing. Three 6 in. x 12 in. cylinders were also made and tested for the corresponding compressive strength of the concrete.

6.1 CONCLUSIONS

The following conclusions are made based on the results of the experimental work performed:

- The CTE values obtained for concretes made with common rock types in Alabama are reported in Table 6.1.

Table 6.1: Coefficient of thermal expansion values for concretes made of common rock types used in the Alabama Concrete Industry

Coarse Aggregates	Concrete CTE Range ($x10^{-6}$ in./in./°F)	Average Concrete CTE ($x10^{-6}$ in./in./°F)
Siliceous River Gravel	6.82 –7.23	6.95
Granite	5.37 – 5.91	5.60
Dolomitic Limestone	5.31 – 5.66	5.52

- The sand-aggregate ratio and water-cement ratio do not have as much influence on the concrete CTE as does the coarse aggregate type. This is evidenced by the coefficient of determination obtained from the statistical analysis.
- An increase in the volume of the coarse aggregate or a decrease in the sand-aggregate ratio increases the CTE for concrete made of river gravel and decreases the CTE for concrete made of granite.
- As the water-cement ratio increases from 0.32 to 0.44, the CTE for concretes made of river gravel increases for all cases except for the case of sand-aggregate ratio of 0.50.
- For the concretes made of granite, the concrete CTE decreases as the water-cement ratio increases from 0.32 to 0.44.

6.2 RECOMMENDATIONS

In order to appreciate fully all the factors affecting the concrete CTE, additional research is recommended. The proposed research may include the effect of fine aggregate type and volume, relative humidity, supplementary cementitious materials type and other coarse aggregate types on the concrete CTE.

The dependence of the correction factor on the type of linear variable differential transformer used, even if they are from the same manufacturer, should also be investigated.

Based on the experience gained through the development and execution of the testing program outlined in this thesis, the following test setup recommendations are provided:

- The concrete sample should be setup in the Invar frame such that the readings on the LVDT readout will be within the range of 0.00000 in. to ± 0.00300 in. This would ensure that during the expansion and contraction of the concrete sample, the LVDT will remain well within the linear range over which it has been calibrated.
- The water level in the external water bath should be kept relatively constant and most preferably, above the top level of the concrete sample but below the cross bar linking the two Invar frames.
- The external water bath should be left open all through out the experimental process. This is to ensure that water vapor does not condense and enter the LVDT.

- As the external water bath is without a lid, water will be lost during the heating (expansion) and cooling (contraction) cycles. To add to this water to ensure that the water level is maintained relatively constant, avoid adding water directly to the external water bath as this could disturb the concrete samples and cause bad readings to be recorded, but rather add water to the external water bath by means of the circulator's water tank.

REFERENCES

AASHTO TP 60-00. 2004. *Standard Method of Test for Coefficient of Thermal Expansion of Hydraulic Cement Concrete*. Washington D.C: American Association of State Highway and Transportation Officials.

AASHTO T 126-1-7. 2001. *Standard Method of Test for Making and Curing Concrete Test Specimens in the Laboratory*. Washington D.C: American Association of State Highway and Transportation Officials.

AASHTO. 2007. *AASHTO LRFD Bridge Design Specifications. Customary U.S. Units* 4th ed. Washington D.C: American Association of State Highway and Transportation Officials.

Adams, G. I., C. Butts, L. W. Stephenson, and W. Cooke. 1926. *Geology of Alabama*, Geological Survey of Alabama. Special report no. 14.

ASTM C 33. 2003. *Standard Specification for Concrete Aggregates*. West Conshohocken, PA: American Society for Testing and Materials.

ASTM C 39. 2003. *Standard Test Method for Compressive Strength of Cylindrical Concrete Specimens*. West Conshohocken, PA: American Society for Testing and Materials.

ASTM C 138. 2001. *Standard Test Method for Density (Unit Weight), Yield, and Air Content (Gravimetric) of Concrete*. West Conshohocken, PA: American Society for Testing and Materials.

ASTM C 143. 2003. *Standard Test Method for Slump of Hydraulic-Cement Concrete*. West Conshohocken, PA: American Society for Testing and Materials.

ASTM C 192. 2002. *Standard Practice for Making and Curing Concrete Test Specimens in the Laboratory*. West Conshohocken, PA: American Society for Testing and Materials.

ASTM C 231. 2004. *Standard Test Method for Air Content of Freshly Mixed Concrete by the Pressure Method*. West Conshohocken, PA: American Society for Testing and Materials.

ASTM C 1064. 2004. *Standard Test Method for Temperature of Freshly Mixed Hydraulic-Cement Concrete*. West Conshohocken, PA: American Society for Testing and Materials.

ASTM E 867-06. 2008. *Road and Paving Materials; Vehicle-Pavement Systems*. Section four. Construction. Vol. 04.03. West Conshohocken, PA: American Society for Testing and Materials.

Ai, H., J. F. Young, and G. W. Scherer. 2001. Thermal Expansion Kinetics: Methods to Measure Permeability of Cementitious Materials: II, Application to Hardened Cement Pastes, *Journal of the American Ceramic Society.* 84, no.2:385-391.

Alungbe, G. D., M. Tia, and D. G. Bloomquist. 1992. Effect of aggregate, water-cement ratio, and curing on the coefficient of linear thermal expansion of concrete. *Journal of the Transportation Research Record* 1335:44 – 51.

Berwanger, C. and A. F. Sarkar. 1976. Thermal expansion of concrete and reinforced concrete. *ACI Journal* no. 73-52:618 – 621.

Daniel, T. W., T. L. Neathery, and T. A. Simpson. 1966. *Rocks and Minerals of Alabama: A guide book for Alabama rock hounds*. Geological Survey of Alabama, Circular 38.

Darwin, D., and J. Browning. 2008. Construction of low cracking high performance concrete (LC-HPC) bridge decks: field experience. Proceedings of the Concrete Bridge Conference, May 4-7, St. Louis, MO CD-Rom.

Diestelkamp W. S., 2001. A short introduction to SAS. University of Dayton. http://homepages.udayton.edu/~diestews/sasintro.htm

Dossey, T., J. V. Salinas, and B. F. McCullough. 1994. Methodology for improvement of oxide residue models for estimation of aggregate performance using stoichiometric analysis. *Transportation Research Record* 1437:59 – 64.

Dossey, T., B.F. McCullough, and A. Dumas. 1994. *Effects of aggregate blends on the properties of Portland cement concrete pavements*. Center for Transportation Research Report 1244-8. Project 0-1244.

Emanuel, J. H. and J. L. Hulsey. 1977. Prediction of the thermal coefficient of expansion of concrete. *Journal of the American Concrete Institute* 74, no. 4:149–155.

Hobbs, D.W. 1971. The dependence of the bulk modulus, Young's Modulus, creep, shrinkage and thermal expansion of concrete upon aggregate volume concentration. *Materials and Construction* 4, no. 20:107–114.

Hossain, M., T. Khanum, J. Tanessi, G. Sceiber, and R.A.Montney. 2006. The PCC coefficient of thermal expansion input for the Mechanistic Empirical Pavement Design Guide. CD ROM of *The 85th Annual meeting of the Transportation Research Board*: 1–21.

Kada, H., M. Lachemi, N. Petrov, O. Bonneau, and P.-C. Aitcin. 2002. Determination of the coefficient of thermal expansion of high performance concrete from initial setting. *Materials and Structures* 35: 35–41.

Kannekanti, V., and J. Harvey. 2006. Sensitivity analysis of 2002 design guide distress prediction models for jointed plain concrete pavement. *Journal of the Transportation Research Board*, no. 1947: 91-100.

Kohler, E., R.F.Alvarado, D. Jones. 2007. Measurement and variability of coefficient of thermal expansion for concrete pavements. CD ROM of *The 86th annual meeting of the Transportation Research Board*: 1–12.

Krauss, P. D., and E. A.Rogalla. 1996. *National Highway Cooperative Research Program (NCHRP) Report 380. Transverse Cracking in Newly Constructed Bridge Decks*. Washington D.C: Transportation Research Board.

Loubser, P. J. and J. G.Bryden. 1972. An apparatus for determining the coefficient of

thermal expansion of rocks, mortars and concretes. *Magazine of Concrete Research* 24, No 79:97–100.

Mallela, J., A. Abbas, T. Harman, C. Rao, R. Liu, and M. Darter. 2005. Measurement and significance of the coefficient of thermal expansion of concrete in rigid pavement design. *Journal of the Transportation Research Board*, no. 1919:38–46.

McCullough, B. F., D. Zollinger, and T. Dossey. 1999. Evaluation of the Performance of Texas Pavements Made with Different Coarse Aggregates. *Center for Transportation Research Report* 3925-1:113–117.

Mehta, P. K., and P. J. M. Monteiro. 2006. *Concrete, Microstructure, Properties, and Materials.* New York: McGraw Hill: 3rd ed.:114–116.

Meyers, S. L. 1940. Thermal coefficient of expansion of portland cement long time tests. *Industrial and Engineering Chemistry*, 32, no. 8:1107–1112.

Mindess, S., J. F.Young, D. Darwin. 2002. *Concrete*. 2nd ed. Prentice Hall, Upper Saddle River New Jersey.

Mitchell, L. J. 1953. Thermal expansion tests on aggregates, neat cements and concretes. Proceedings of the ASTM: 963–977.

Pirsson, L. V. 1908. *Rocks and Rock Minerals, a manual of the elements of petrology without the use of the microscope*. New York. John Wiley and Sons Inc.

Ndon, U. J. and K. L. Bergerson. 1995. Thermal expansion of concretes: case study in

Iowa. J*ournal of Materials in Civil Engineering* 7 no. 4:246–251.

Neville, A. M. 1981. *Properties of Concrete.* 3rd ed. Essex, UK: Longman Scientific and Technical.

Neville, A. M., and J. J.Brooks. 1987. *Concrete Technology*. Essex, UK: Longman Scientific and Technical.

Parsons, W. H., and W.H. Johnson. 1944. Factors affecting the thermal expansion of concrete aggregate materials. *Journal of the American Concrete Institute* 40: 457–466.

Radjy, F., E. J. Sellevold., and K. K. Hansen. 2003. Isosteric Vapor Pressure-Temperature Data for Water sorption in Hardened Cement Paste: Enthalpy, Entropy and sorption Isotherms at Different Temperatures, *Report BYG-DTU R-057*, Lyngby: Technical University of Denmark. Available at *http://www.byg.dtu.dk/upload/institutter/byg/publications/rapporter/byg-r057.pdf*

Sellevold, E. J., and O. Bjontegaard. 2006. Thermal expansion coefficient of cement paste and concrete: effect of moisture content. *Advances in Cement and Concrete*: 27 – 35.

Scherer, G. W. 2000. Measuring permeability of rigid materials by a beam-bending method: I, Theory, *Journal of the American Ceramic Society*. 83, no.9:2231-2239.

Schindler A. K., B. F. McCullough. 2002. The importance of concrete temperature control during concrete pavement construction in hot weather conditions. *Journal*

of the Transportation Research Board, TRR No. 1813: 3-10.

Schumann,W. 1993. *Handbook of Rocks, Minerals, and Gemstones*. Houghton Mifflin.

Suhr D. D. 2002. Proc GLM of Proc CALIS. Paper 260-26. Statistics, data analysis, and data mining. University of Northern Colorado. http://www2.sas.com/proceedings/sugi26/p260-26.pdf

Szabo, M. W. 1967. Sand and Gravel in Alabama, a Summary Report. *Geological Survey of Alabama*, Circular 44.

Tanesi, J., M. E. Kutay, A. Abbas, and R. Meininger. 2007. Effect of CTE variability on concrete pavement performance as predicted using the mechanistic empirical pavement design guide. CD ROM of *the 86th annual meeting of the Transportation Research Board*: 1 – 14.

Tazawa, E. and S. Miyazawa. 1996. Influence of autogeneous shrinkage on cracking in high strength concrete. Fourth International Symposium on the Utilization of High Strength and High Performance Concrete, Paris, France: 321-330.

Whigham J. A. 2005. Evaluation of restraint stresses and cracking in early age concrete with the rigid cracking frame. Masters Thesis, Auburn University, AL, 150.

Wittmann, F. H., and J. Lukas. 1974. Experimental study of thermal expansion of hardened cement paste. *Materials and Structures*. 7, no. 40: 247–252.

Won, M. 2005. Improvements of testing procedures for concrete coefficient of thermal expansion. *Journal of the Transportation Research Board*, no. 1919:23–28.

Yamakawa, H., H. Nakauchi, T. Kita, and H. Onuma. 1986. A study of the coefficient of thermal expansion of concrete. *Transactions of the Japan Concrete Institute.* 8:111–118.

Ziegeldorf, S.W., K. Kleiser, and H. K. Hilsdorf. 1978. Effect of thermal expansion of aggregate on thermal expansion of concrete. Budapest: Omkdt-technoinform. *Colloque Internationale sur les materiaux granulaire*/*International symposium on aggregates and filler*: 452–464.

APPENDIX A

CONCRETE MIXTURE PROPERTIES AND CTE TEST RESULTS

The objective of this appendix is to present the concrete mixture proportions used, and the raw CTE test results obtained. In Figures A1 and A2, the difference between the CTEs for Frames A and B, and those between the rise and fall are also presented.

Table A-1 (a): Concrete mixture proportions prior to correcting for moisture

Concrete Mixture Identification	Water (lb)	Type I Cement (lb)	Coarse Aggregate (lb)	Fine Aggregate (lb)	Air (%)	Admixture	
						Water Reducer (oz)	Air (oz)
GR-40-32	29.2	91.3	194.6	126.8	0.4	12.8	0.1
GR-40-38	29.8	78.3	200.4	130.6	0.4	11.0	0.1
GR-40-44	30.3	68.9	205.0	133.6	0.4	5.5	0.1
GR-45-32	29.2	91.3	178.3	142.6	0.4	12.8	0.1
GR-45-38	29.8	78.3	183.6	146.8	0.4	12.8	0.1
GR-45-44	30.3	68.9	187.9	150.3	0.4	5.5	0.1
GR-50-32	29.2	91.3	162.1	158.4	0.4	12.8	0.1
GR-50-38	29.8	78.3	167.1	163.3	0.4	11.0	0.1
GR-50-44	30.3	68.9	170.8	166.9	0.4	5.5	0.1
RG-40-32	29.2	91.3	190.8	126.8	0.4	12.8	0.1
RG-40-38	29.8	78.3	196.8	130.8	0.4	9.4	0.1
RG-40-44	30.3	68.9	201.0	133.6	0.4	5.5	0.1

Table A-1 (b): Concrete mixture proportions prior to correcting for moisture

Concrete Mixture Identification	Water (lb)	Type I Cement (lb)	Coarse Aggregate (lb)	Fine Aggregate (lb)	Air (%)	Admixture	
						Water Reducer (oz)	Air (oz)
RG-45-32	29.2	91.3	175.1	142.8	0.4	11.0	0.1
RG-45-38	29.8	78.3	180.2	147.0	0.4	11.0	0.1
RG-45-44	30.3	68.9	184.2	150.2	0.4	5.5	0.1
RG-50-32	29.2	91.3	159.0	158.4	0.4	12.8	0.1
RG-50-38	29.8	78.3	163.9	163.3	0.4	11.0	0.1
RG-50-44	30.3	68.9	167.3	166.8	0.4	8.3	0.1
DL-40-32	29.2	91.3	199.3	126.8	0.4	12.8	0.1
DL-40-38	29.8	78.3	205.4	130.7	0.4	11.0	0.1
DL-40-44	30.3	68.9	210.0	133.6	0.4	5.5	0.1
DL-45-32	29.2	91.3	182.9	142.8	0.4	11.0	0.1
DL-45-38	29.8	78.3	188.3	147.0	0.4	11.0	0.1
DL-45-44	30.3	68.9	192.2	150.0	0.4	8.3	0.1
DL-50-32	29.2	91.3	166.1	158.4	0.4	12.8	0.1
DL-50-38	29.8	78.3	171.2	163.3	0.4	11.0	0.1
DL-50-44	30.3	68.9	174.7	166.7	0.4	9.6	0.1

Table A-2 (a): Concrete CTE test results

Concrete Sample Identification	Frame A				Frame B				ΔCTE (A-B)	Average CTE (A+B)/2
	Thermal Cycle		ΔCTE (Rise-Fall)	Avg. CTE	Thermal Cycle		ΔCTE (Rise-Fall)	Avg. CTE		
	Rise	Fall			Rise	Fall				
	Concrete CTE (x 10^{-6} /^{o}F)									
RGN-40-32	6.87	6.75	0.12	6.81	7.25	7.18	0.07	7.22	-0.40	7.01
RGN-40-38	6.85	6.79	0.06	6.82	7.36	7.28	0.08	7.32	-0.50	7.07
RGN-40-44	6.98	6.98	0.00	6.98	7.41	7.54	-0.13	7.48	-0.49	7.23
RGN-45-32	6.65	6.52	0.13	6.59	7.06	7.06	0.00	7.06	-0.48	6.82
RGN-45-38	6.77	6.71	0.06	6.74	7.19	7.03	0.16	7.11	-0.37	6.93
RGN-45-44	6.67	6.67	0.00	6.67	7.06	7.03	0.03	7.05	-0.38	6.86
RGN-50-32	6.73	6.69	0.04	6.71	7.18	7.17	0.01	7.18	-0.46	6.94
RGN-50-38	6.7	6.56	0.14	6.63	7.05	6.97	0.08	7.01	-0.38	6.82
RGN-50-44	6.74	6.8	-0.06	6.77	6.99	6.94	0.05	6.97	-0.20	6.87
DLN-40-32	5.71	5.57	0.14	5.64	5.68	5.67	0.01	5.68	-0.03	5.66

Table A-2 (b): Concrete CTE test results

Concrete Sample Identification	Frame A				Frame B				ΔCTE (A-B)	Average CTE (A+B)/2
	Thermal Cycle		ΔCTE (Rise-Fall)	Avg CTE	Thermal Cycle		ΔCTE (Rise-Fall)	Avg CTE		
	Rise	Fall			Rise	Fall				
	Concrete CTE (x 10^{-6} /^{o}F)									
DLN-40-38	5.4	5.6	-0.20	5.50	5.71	5.64	0.07	5.68	-0.18	5.59
DLN-40-44	5.93	5.82	0.11	5.88	5.17	5.17	0.00	5.17	0.71	5.52
DLN-45-32	5.56	5.45	0.11	5.51	5.2	5.03	0.17	5.12	0.39	5.31
DLN-45-38	5.4	5.37	0.03	5.39	5.86	5.81	0.05	5.84	-0.45	5.61
DLN-45-44	5.16	5.44	-0.28	5.30	5.64	5.57	0.07	5.61	-0.31	5.45
DLN-50-32	5.17	4.87	0.30	5.02	5.84	5.74	0.10	5.79	-0.77	5.41
DLN-50-38	5.16	5.44	-0.28	5.30	5.7	5.86	-0.16	5.78	-0.48	5.54
DLN-50-44	5.51	5.61	-0.10	5.56	5.68	4.94	0.74	5.68	-0.12	5.62
GRN-40-32	5.85	5.77	0.08	5.81	5.51	5.41	0.10	5.46	0.35	5.64
GRN-40-38	5.72	5.63	0.09	5.68	5.35	5.23	0.12	5.29	0.39	5.48
GRN-40-44	5.63	5.59	0.04	5.61	5.23	5.01	0.22	5.12	0.49	5.37

Table A-2 (c): Concrete CTE test results

Concrete Sample Identification	Frame A				Frame B				ΔCTE (A-B)	Average CTE (A+B)/2
	Thermal Cycle		ΔCTE (Rise-Fall)	Avg CTE	Thermal Cycle		ΔCTE (Rise-Fall)	Avg CTE		
	Rise	Fall			Rise	Fall				
	Concrete CTE (x 10^{-6} /^{o}F)									
GRN-45-32	5.92	5.83	0.09	5.88	5.62	5.38	0.24	5.50	0.38	5.69
GRN-45-38	5.39	5.33	0.06	5.36	5.68	5.67	0.01	5.68	-0.32	5.52
GRN-45-44	5.68	5.5	0.18	5.59	5.61	5.47	0.14	5.54	0.05	5.57
GRN-50-32	5.99	5.99	0.00	5.99	5.94	5.73	0.21	5.84	0.15	5.91
GRN-50-38	5.80	5.74	0.06	5.77	5.83	5.64	0.19	5.74	0.04	5.75
GRN-50-44	5.51	5.39	0.12	5.45	5.54	5.43	0.11	5.49	-0.04	5.47

Table A-3 : Difference between the CTEs for Frames A and B

Bin $=CTE_{(Frame\ A)} - CTE_{(Frame\ B)}$	**Frequency**	**Cumulative Percentage**
-0.8	0	0.00%
-0.7	1	3.70%
-0.6	0	3.70%
-0.5	1	7.41%
-0.4	6	29.63%
-0.3	5	48.15%
-0.2	0	48.15%
-0.1	3	59.26%
0	2	66.67%
0.1	2	74.07%
0.2	1	77.78%
0.3	0	77.78%
0.4	4	92.59%
0.5	1	96.30%
0.6	0	96.30%
0.7	0	96.30%
0.8	1	100.00%
More	0	100.00%

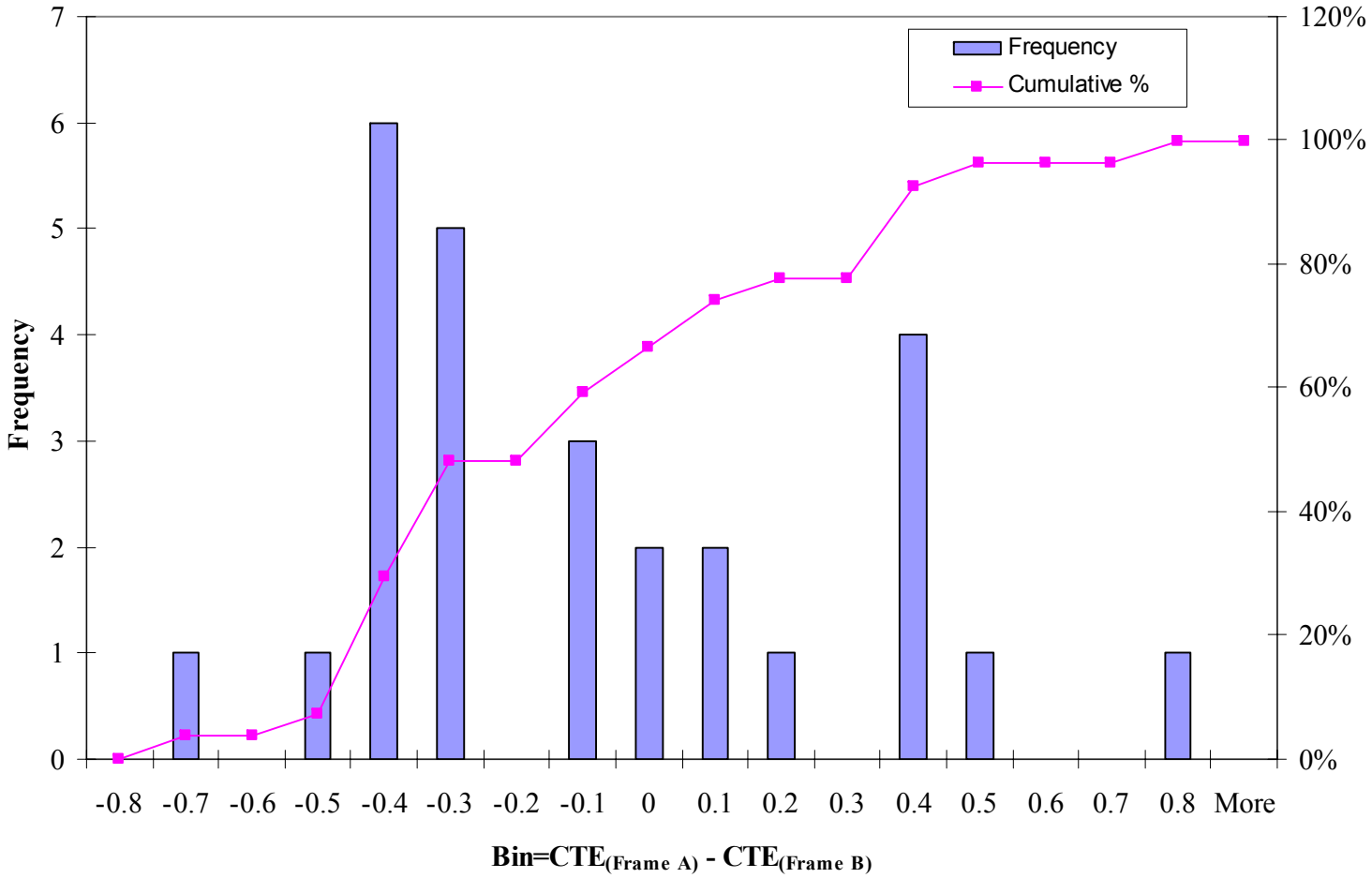

Figure A 1: Histogram and Cumulative percentage plot for the difference in the values of the CTE for frames A and B

Table A-4 : Difference between the CTEs for the rise and fall test segments

Bin $=CTE_{(rise)} - CTE_{(fall)}$	**Frequency**	**Cumulative Pecentage**
-0.4	0	0.00%
-0.3	0	0.00%
-0.2	2	3.70%
-0.1	4	11.11%
0	6	22.22%
0.1	23	64.81%
0.2	14	90.74%
0.3	4	98.15%
0.4	0	98.15%
0.5	0	98.15%
More	1	100.00%

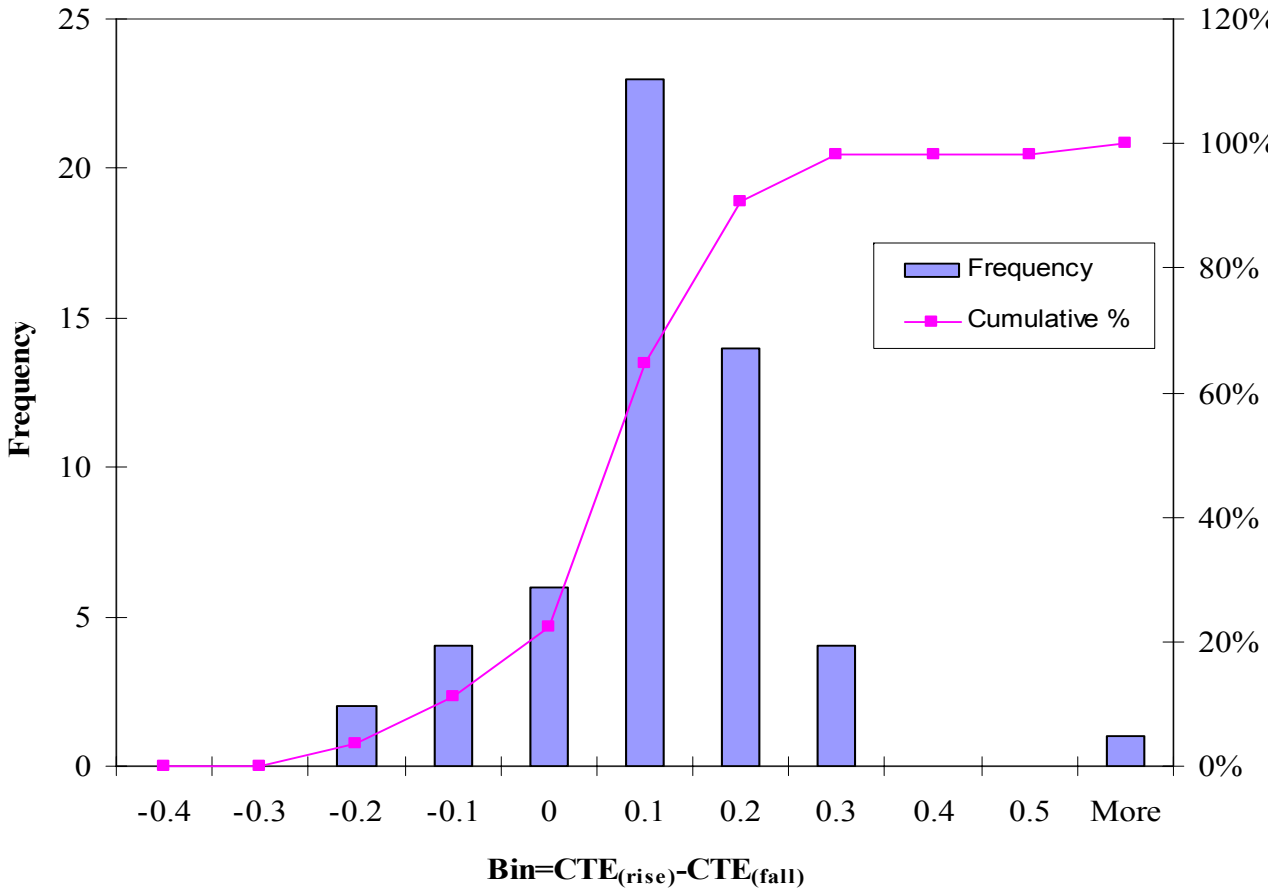

Figure A 2: Histogram and Cumulative percentage plot for the difference in the values of the CTE for the rise and fall segments

APPENDIX B

STATISTICAL ANALYSIS RESULTS

Table B-1: Statistics of the CTE test results from frame A

Variable	Cycle	Number of Concrete Samples	Mean	Stand. Dev.	Stand. Error	Min.	Max.
CTE	**Fall**	27	5.94	0.60	0.12	4.87	6.98
CTE	**Rise**	27	5.98	0.61	0.12	5.16	6.98
CTE	**Diff(1-2)**		-0.04	0.61	0.17		

Table B-2: Results of the t-test for CTE test results from frame A

Variable	Method	Variances	Degrees of Freedom	t Value	Pr > |t|
CTE	**Pooled**	Equal	52	-0.230	0.817
CTE	**Satterthwaite**	Unequal	52	-0.230	0.817

Table B-3: Equality of variances for the rise and fall CTE values from frame A

Variable	Method	Numerator Degrees of Freedom	Denominator Degrees of Freedom	F Value	Pr > F
CTE	**Folded F**	26	26	1.050	0.908

Table B-4: Statistics of the CTE test results from frame A

Variable	Cycle	Number of Concrete Samples	Mean	Lower CL Stand. Dev.	Stand. Dev.	Upper CL Stand. Dev.	Stand. Error	Min.	Max.
CTE	**Fall**	27	6.022	0.662	0.840	1.151	0.162	4.940	7.540
CTE	**Rise**	27	6.124	0.616	0.782	1.072	0.151	5.170	7.410
CTE	**Diff (1-2)**		-0.101	0.681	0.812	1.004	0.221		

Table B-5: Results of the t-test for CTE test results from frame B

Variable	Method	Variances	DF	t Value	Pr > |t|
CTE	**Pooled**	Equal	52	-0.46	0.6479
CTE	**Satterthwaite**	Unequal	51.7	-0.46	0.6479

Table B-6: Equality of variances of the rise and fall values for frame B

Variable	Method	Numerator Degrees of Freedom	Denominator Degrees of Freedom	F Value	Pr > F
CTE	**Folded F**	26	26	1.15	0.718

Table B-7: Statistics of the combined CTE test results for frames A and B

Variable	Frame	Number of Concrete Samples	Mean	Lower CL Stand. Dev.	Stand. Dev.	Upper CL Stand. Dev.	Stand. Error	Min.	Max.
CTE	**A**	27	5.960	0.475	0.604	0.827	0.116	5.020	6.980
CTE	**B**	27	6.087	0.628	0.797	1.093	0.154	5.115	7.475
CTE	**Diff (1-2)**		-0.126	0.594	0.707	0.875	0.193		

Table B-8: Results of the t-test for the combined CTE values from frames A and B

Variable	Method	Variances	Degrees of Freedom	t Value	Pr > |t|
CTE	**Pooled**	Equal	52	-0.66	0.5146
CTE	**Satterthwaite**	Unequal	48.4	-0.66	0.5148

Table B-9: Equality of variances of the combined CTE values from frames A and B

Variable	Method	Numerator Degrees of Freedom	Denominator Degrees of Freedom	F Value	Pr > F
CTE	**Folded F**	26	26	1.75	0.162

Table B-10: Results of ANOVA procedure to determine the difference in CTE values of concretes made with the different rock types

Source	Degrees of Freedom	Sum of Squares	Mean Square	F Value	Pr > F
Model	2	11.599	5.799	294.490	<.0001
Error	24	0.473	0.020		
Corrected Total	26	12.072			

Table B-11: Other Statistical results using the ANOVA procedure to determine the difference in CTE values of concretes made with the different rock types

R-Square	Coefficient Variable	Root MSE	CTE Mean
0.961	2.330	0.140	6.024

Table B-12: Statistical results using the GLM procedure to determine the difference in CTE values of concretes made with the different rock types using the t Tests

Alpha	0.05
Error Degrees of Freedom	24
Error Mean Square	0.0197
Critical Value of t	2.064
Least Significant Difference	0.1365

Tabel B-13: t-test grouping of the concrete CTE means for the different coarse aggregate types used with the GLM procedure

t Grouping	Mean	Number of Concrete Samples	Rock Type
A	6.949	9	River Gravel
B	5.598	9	Granite
B	5.523	9	Dolomitic Limestone

NB: Means with the same letter are not significantly different**.**

Table B-14: Statistical results using the GLM procedure to determine the difference in CTE values of concretes made with the different rock types using the Tukey's Studentized Range (HSD) Test

Alpha	0.05
Error Degrees of Freedom	24
Error Mean Square	0.0197
Critical Value of Studentized Range	3.532
Minimum Significant Difference	0.165

Table B-15: Turkey grouping of the concrete CTE means for the different coarse aggregate types used using the GLM procedure

Tukey Grouping	Mean	Number of Concrete Samples	Rock Type
A	6.949	9	River Gravel
B	5.598	9	Granite
B	5.523	9	Dolomitic Limestone

NB: Means with the same letter are not significantly different**.**

Table B-16: Results of the GLM procedure to determine the effect of water-cement ratio on the CTE values of the concrete samples

Source	Degrees of Freedom	Sum of Squares	Mean Square	F Value	Pr > F
Model	2	0.0098	0.005	0.01	0.991
Error	24	12.823	0.534		
Corrected Total	26	12.833			

Table B-17: Other Statistical results using the GLM procedure to determine the effect of water-cement ratio on the CTE values of the concrete samples

R-Square	Coefficient Variable	Root MSE	CTE Mean
0.000764	12.161	0.731	6.011

Table B-18: Statistical results using the GLM procedure to determine the effect of water-cement ratio on the CTE values of the concrete samples using the t Tests

Alpha	0.05
Error Degrees of Freedom	24
Error Mean Square	0.534
Critical Value of t	2.064
Least Significant Difference	0.711

Table B-19: t grouping of the concrete CTE means for the different water-cement ratios used using the GLM procedure

t Grouping	Mean	Number of Concrete Samples	Water-cement ratio
A	6.034	9	0.38
A	6.012	9	0.44
A	5.987	9	0.32

NB: Means with the same letter are not significantly different**.**

Table B-20: Statistical results obtained using the GLM procedure with the Tukey's Studentized Range (HSD) Test option to determine the effect of water-cement ratio on the CTE values of the concrete samples

Alpha	0.05
Error Degrees of Freedom	24
Error Mean Square	0.534
Critical Value of Studentized Range	3.532
Minimum Significant Difference	0.861

Table B-21: Turkey grouping of the concrete CTE means for the effect of water-cement ratio on CTE using the GLM procedure

Tukey Grouping	Mean	Number of Concrete Samples	Water-cement ratio
A	6.034	9	0.38
A	6.012	9	0.44
A	5.987	9	0.32

NB: Means with the same letter are not significantly different**.**

Table B-22: Results of the GLM procedure to determine the effect of sand-aggregate ratio on the CTE values of the concrete samples

Source	Degrees of Freedom	Sum of Squares	Mean Square	F Value	Pr > F
Model	2	0.0387	0.0193	0.040	0.964
Error	24	12.794	0.533		
Corrected Total	26	12.833			

Table B-23: Other Statistical results using the GLM procedure to determine the effect of sand-aggregate ratio on the CTE values of the concrete samples

R-Square	Coefficient Variable	Root MSE	CTE Mean
0.00302	12.147	0.730	6.011

Table B-24: Statistical results using the GLM procedure with the t test option to determine the effect of sand-aggregate ratio on the concrete CTE values

Alpha	0.05
Error Degrees of Freedom	24
Error Mean Square	0.533
Critical Value of t	2.064
Least Significant Difference	0.710

Table B-25: t grouping of the concrete CTE means for the different sand-aggregate ratios used, using the GLM procedure

t Grouping	Mean	Number of Concrete Samples	Sand-aggregate ratio
A	6.062	9	0.40
A	5.999	9	0.50
A	5.972	9	0.45

NB: Means with the same letter are not significantly different

Table B-26: Statistical results using the GLM procedure with the Tukey's Studentized Range option to determine the effect of sand-aggregate ratio on the concrete CTE values

Alpha	0.05
Error Degrees of Freedom	24
Error Mean Square	0.533
Critical Value of Studentized Range	3.532
Minimum Significant Difference	0.859

Table B-27: Turkey grouping of the concrete CTE means for the effect of sand-aggregate ratio on CTE using the GLM procedure

Tukey Grouping	Mean	Number of Concrete Samples	Sand-aggregate ratio
A	6.062	9	0.40
A	5.999	9	0.50
A	5.972	9	0.45

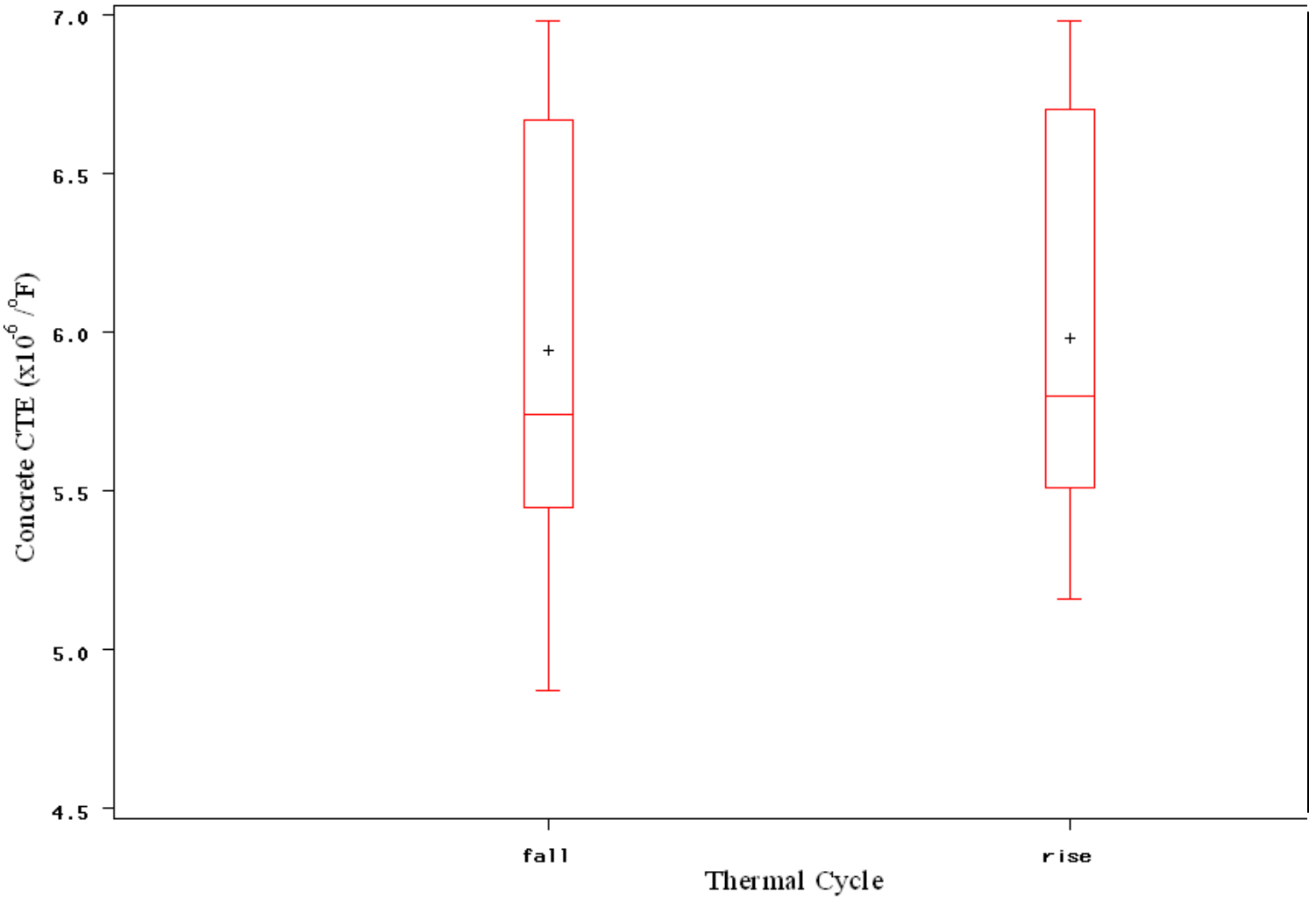

Figure B-1: Side by side box plots comparing the distribution of the concrete CTEs for the different thermal cycles using frame A

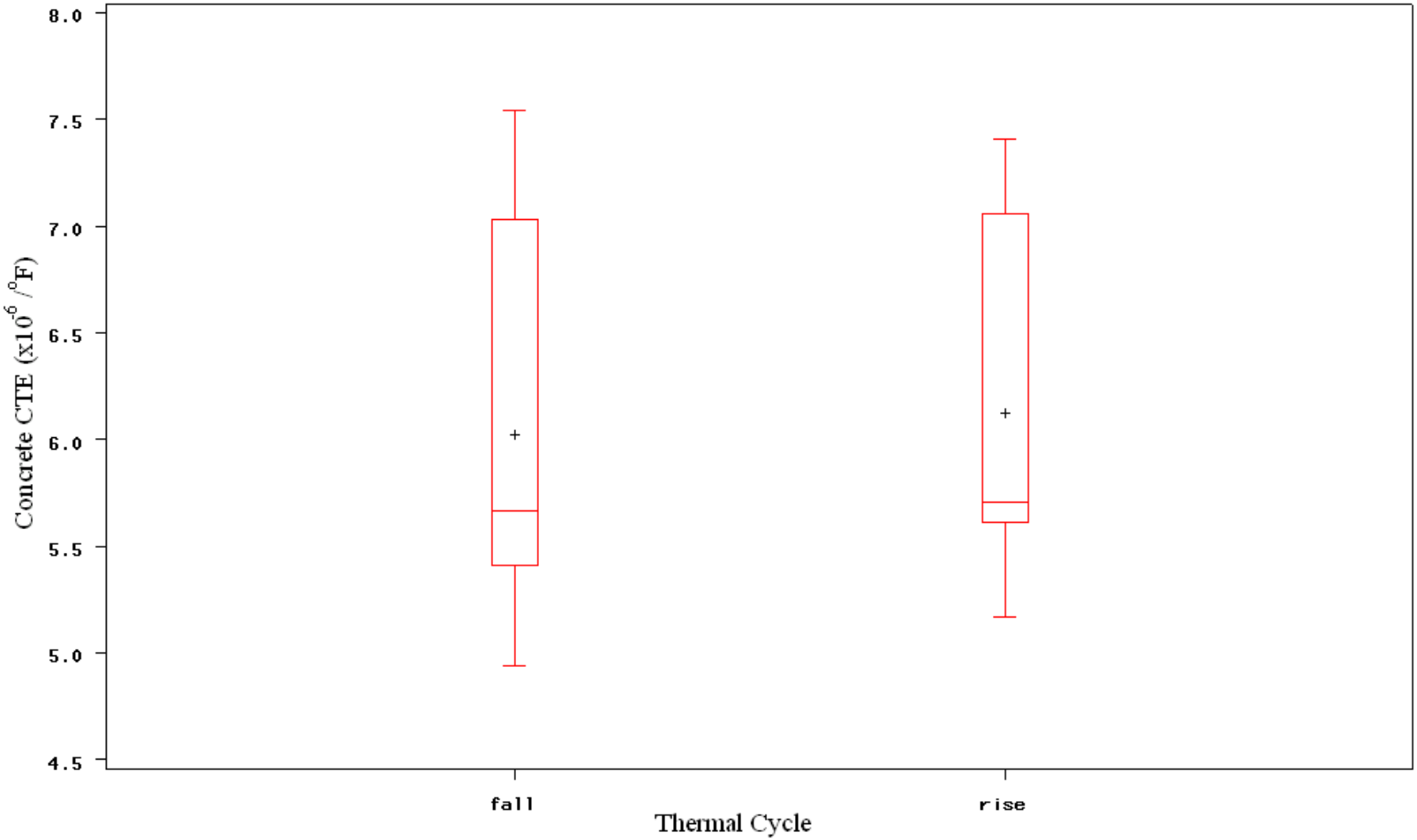

Figure B-2: Box plots comparing the distribution of the concrete CTEs for the different thermal cycles using frame B

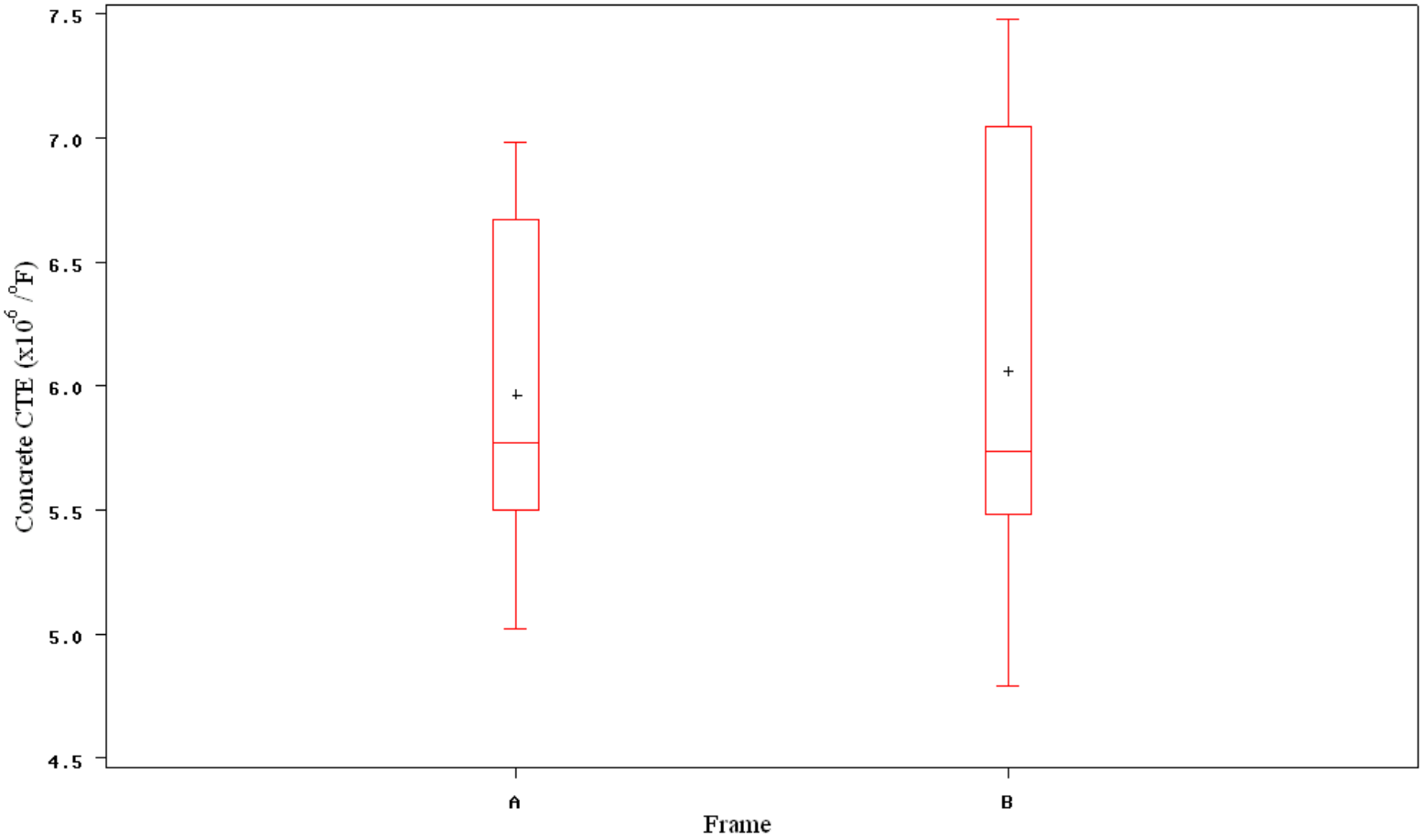

Figure B-3: Box plots comparing the distribution of the average concrete CTEs for frames A and B

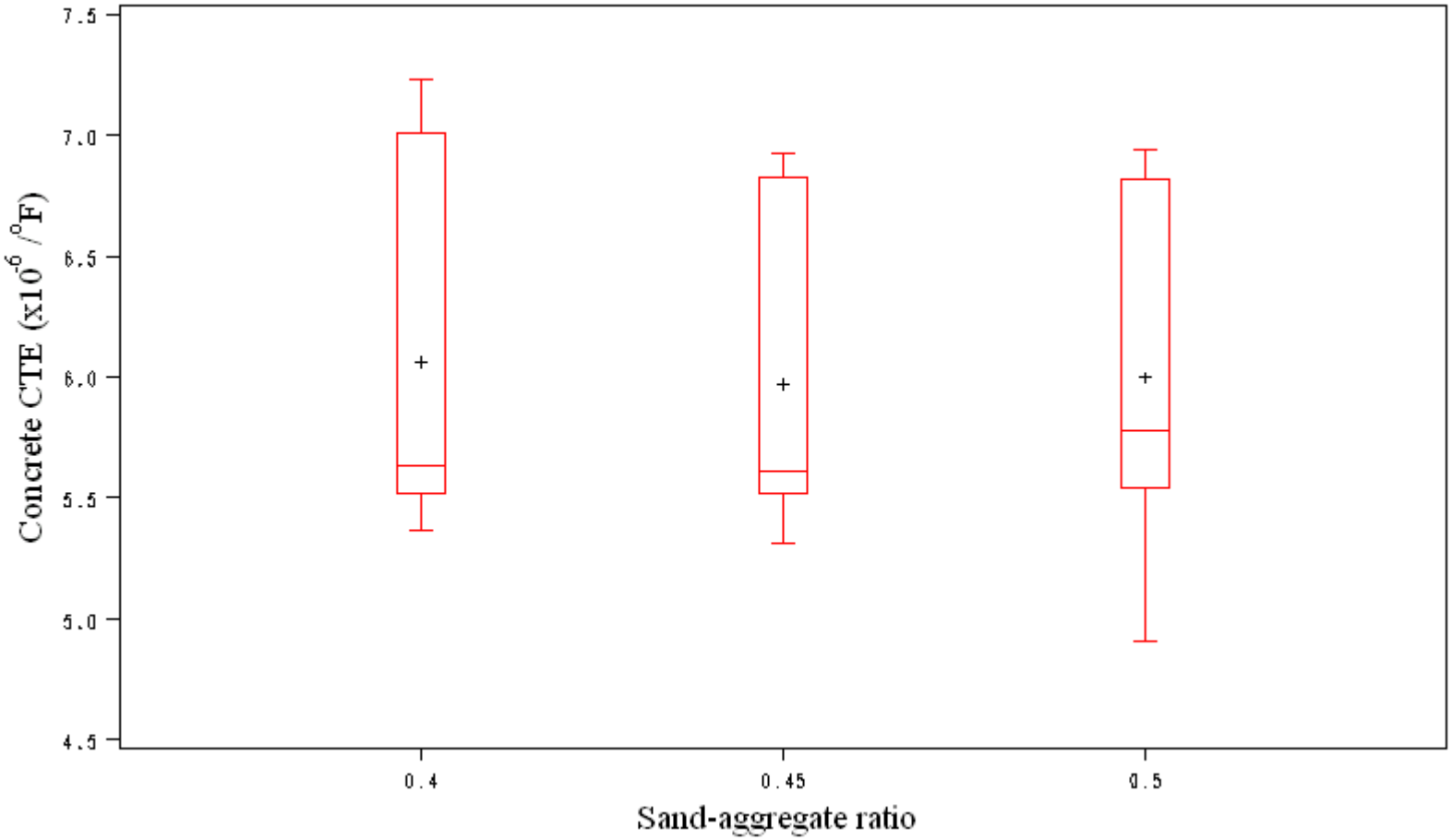

Figure B-4: Box plots comparing the distribution of the concrete CTEs for the different sand-aggregate ratios

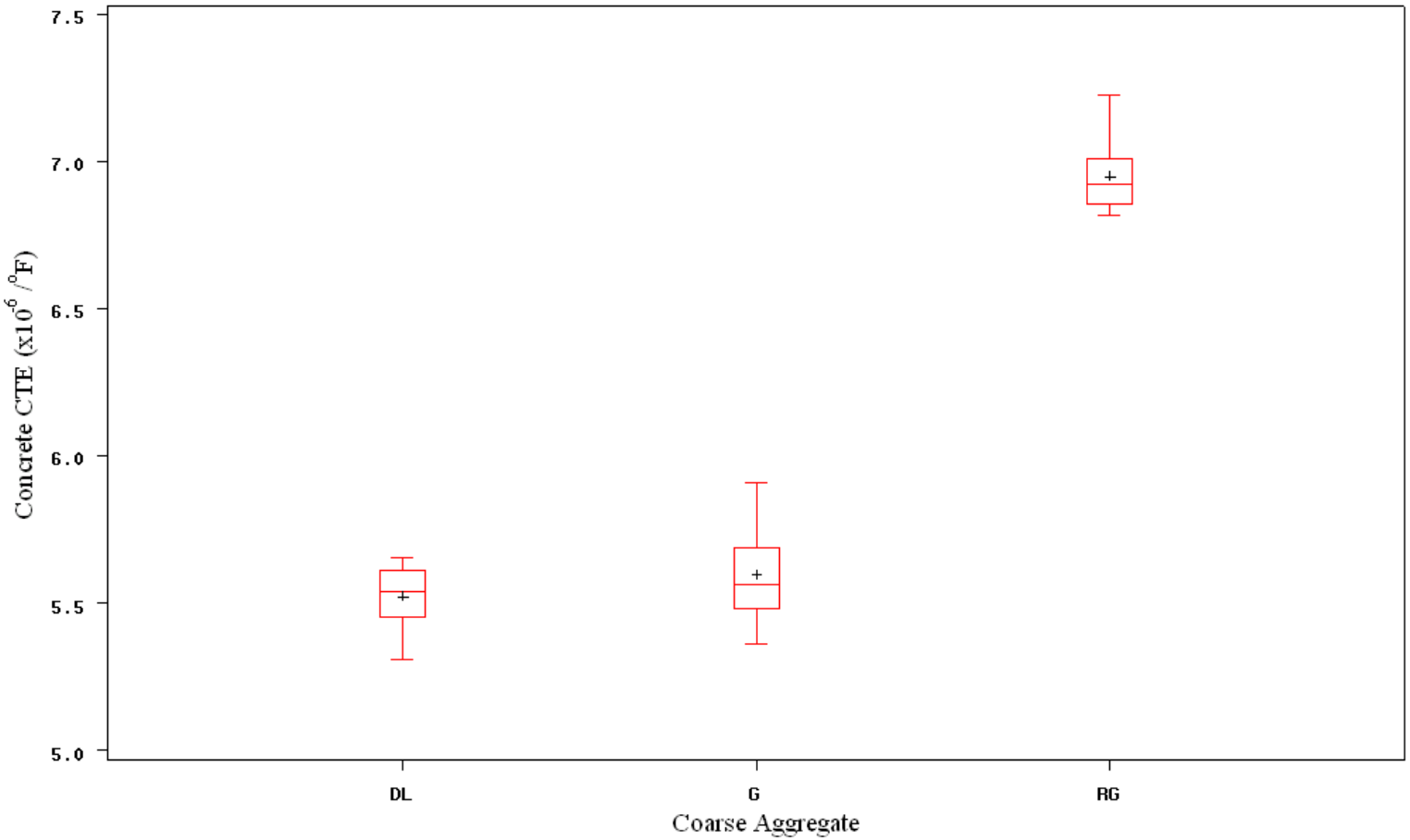

Figure B-5: Box plots comparing the distribution of the CTEs of concrete made of different coarse aggregate types

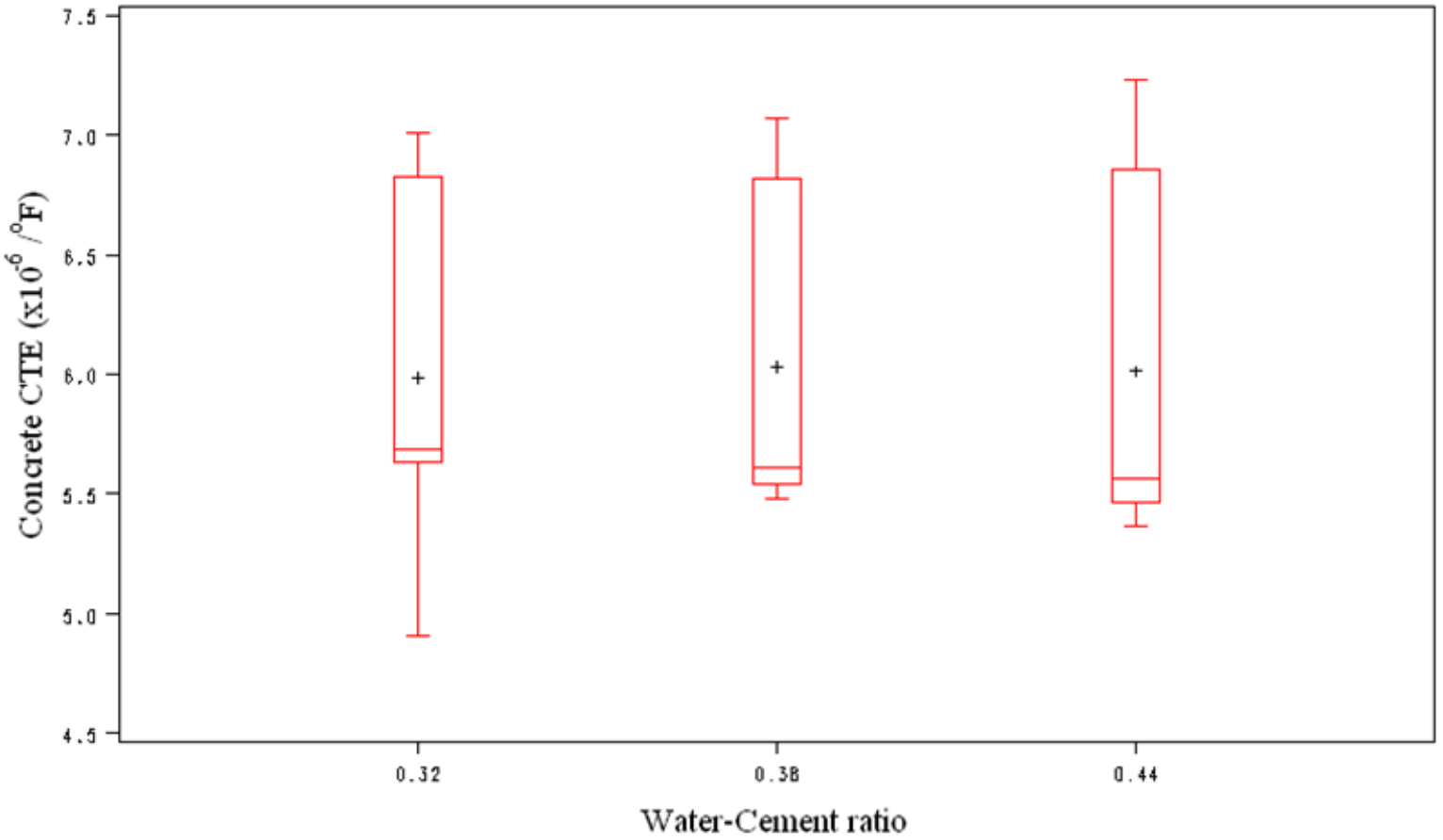

Figure B-6: Side by side box plots comparing the distribution of the average concrete CTEs for the different water-cement ratios

APPENDIX C

SAMPLE RECORDING SHEETS

Table C 1: Typical compressive strength data entry sheet

Concrete Mixing Date:			
Date of Test:			
Sample Characteristics			
Sample Identification:			
Age (days) :	28	28	28
Sample Size:	6 in. x 12 in.	6 in. x 12 in.	6 in. x 12 in.
Area (in^2):	28.28	28.28	28.28
Load (Ibf):			
Stress (psi):			
Comments			

Table C 2: Typical compressive strength calculation sheet

Concrete Mixing Date:			
Date of Test:			
Sample Characteristics			
Sample Identification:			
Age (days) :	28	28	28
Sample Size:	6 in. x 12 in.	6 in. x 12 in.	6 in. x 12 in.
Area (in^2):	28.28	28.28	28.28
Load (Ibf):			
Stress (psi):			
Observed range of test cylinder strength			%
Acceptable range of cylinder strength (AASHTO T 22 2003)		7.8	%
Check- One Outlier? (Y/N):			
Average of Three Tests:			psi
Average Results:			psi
Compressive Strength:			psi
Comments			

Table C 3: Typical CTE data entry sheet

Concrete Sample Properties

Sample Identification Number: _____

Sample Type: _____

Sample Age: _____

Concrete Sample Conditioning at 73 °F

Initial weight after 24hrs: _____ *lb*

Final weight after 48hrs: _____ *lb*

Change in weight _____ %

Date of CTE Test: _____

Frame Identification No.: _____

Concrete Mixing Date: _____

LVDT Identification No.: _____

Sample Dimensions:

	Readings					
	1st	*2nd*	*3rd*	*4th*	*Average*	
Length						*in.*
Diameter						*in.*

First Cycle

Temperature-External Probe Readings (°F)							LVDT Readings (in.)		
Target	Probe 1	Probe 2	Probe 3	Probe 4	Average	ΔT	1st	2nd	3rd
50 °F									
122 °F									
50 °F									

Second Cycle

Temperature-External Probe Readings (°F)							LVDT Readings (in.)		
Target	Probe 1	Probe 2	Probe 3	Probe 4	Average	ΔT	1st	2nd	3rd
50 °F									
122 °F									
50 °F									

Third Cycle

Temperature-External Probe Readings (°F)							LVDT Readings (in.)		
Target	Probe 1	Probe 2	Probe 3	Probe 4	Average	ΔT	1st	2nd	3rd
50 °F									
122 °F									
50 °F									

Comments:

Table C 4: Typical CTE calculation sheet one

Concrete Sample Properties

Sample Identification Number: _____

Sample Type: _____

Sample Age: _____

Concrete Sample Conditioning at 73 °F

Initial wt after 24hrs: _____ *lb*

Final wt after 48hrs: _____ *lb*

Change in weight: _____ %

Date of CTE Test: _____

Frame Identification No.: _____

Concrete Mixing Date: _____

LVDT Identification No: _____

Concrete Sample Dimensions:

	Readings				
	1st	*2nd*	*3rd*	*4th*	*Average*
Length					*in.*
Diameter					*in.*

First Cycle

Temperature-External Probe Readings (°F)						**LVDT Readings (in.)**				
Tar-get	Probe1	Probe2	Probe3	Probe4	Ave-rage	ΔT	1st	2nd	3rd	ΔL_m
50 °F										
122 °F										
50 °F										

Second Cycle

Temperature-External Probe Readings (°F)						**LVDT Readings (in.)**				
Tar-get	Probe1	Probe2	Probe3	Probe4	Ave-rage	ΔT	1st	2nd	3rd	ΔL_m
50 °F										
122 °F										
50 °F										

Third Cycle

Temperature-External Probe Readings (°F)						**LVDT Readings (in.)**				
Tar-get	Probe1	Probe2	Probe3	Probe4	Ave-rage	ΔT	1st	2nd	3rd	ΔL_m
50 °F										
122 °F										
50 °F										

Table C 5: Typical CTE calculation sheet two

Date of Test:					
Sample Identification Number:					
Frame Identification Number:					
LVDT Identification Number:					
Correction Factor (C_f) = $\left[\Delta L_f / L_{CS} \right] / \Delta T$				/ °F	
Calculations		**Cycle**			
		First	**Second**	**Third**	**Units**
$\Delta L_f = C_f x L_o x \Delta T$	*Expansion Segment*				in.
	Contraction Segment				in.
$\Delta L_a = \Delta L_m + \Delta L_f$	*Expansion Segment*				in.
	Contraction Segment				in.
CTE (α) = $\left[\Delta L_a / L_o \right] / \Delta T$	*Expansion Segment*				/°F
	Contraction Segment				/°F
Summary					
Average CTE					
Expansion					/°F
Contraction					/°F
Total					/°F